TAMPEREEN TEKNILLINEN YLIOPISTO
TAMPERE UNIVERSITY OF TECHNOLOGY

Fanni Mylläri

From Boiler to Atmosphere: Effect of Fuel Choices on Particle Emissions from Real-Scale Power Plants

Julkaisu 1570 • Publication 1570

Tampere 2018

Tampereen teknillinen yliopisto. Julkaisu 1570
Tampere University of Technology. Publication 1570

Fanni Mylläri

From Boiler to Atmosphere: Effect of Fuel Choices on Particle Emissions from Real-Scale Power Plants

Thesis for the degree of Doctor of Science in Technology to be presented with due permission for public examination and criticism in Sähkötalo Building, Auditorium SA203, at Tampere University of Technology, on the 5th of October 2018, at 12 noon.

Tampereen teknillinen yliopisto - Tampere University of Technology
Tampere 2018

Doctoral candidate: Fanni Mylläri, M. Sc.
Aerosol Physics, Laboratory of Physics
Faculty of Natural Sciences
Tampere University of Technology
Finland

Supervisor: Topi Rönkkö, Associate Professor
Aerosol Physics, Laboratory of Physics
Faculty of Natural Sciences
Tampere University of Technology
Finland

Pre-examiners: Zoran Ristovski, Professor
Chemistry, Physics, Mechanical Engineering,
Nanotechnology and Molecular Science
Science and Engineering Faculty
Queensland University of Technology
Australia

Esa Vakkilainen, Professor
Energy Technology
Lappeenranta University of Technology
Finland

Opponent: Ari Leskinen, Adjunct Professor
Finnish Meteorological Institute
Finland

ISBN 978-952-15-4193-3 (printed)
ISBN 978-952-15-4214-5 (PDF)
ISSN 1459-2045

Abstract

Fossil fuels, coal and oil are used for energy production around the world. Combustion of these fossil fuels produces gases and particles that affect air quality and climate. The CO_2 emissions can be decreased by substituting fossil fuels with biomass and this substitution can further affect the particle emissions of the power plants. This thesis focuses on characterising particles of real-scale power plants with various fuels, from combustion to atmospheric dilution. The studied power plants were a combined heat-and-power (CHP) plant (combusting coal and a coal–wood pellet mixture) and a heating plant with three fuel mixtures. The particles were characterised mainly based on particle number size distribution and number concentration, using aerosol sampling from the superheater area of the boiler of the CHP plant, the stack of the CHP and the heating plant and the atmosphere surrounding the CHP plant.

Measurements for the aerosol samples taken from the boiler indicated that the particles from the combustion of coal and the mixture of coal and industrial pellets had already formed in the boiler. The formation of the particles was studied by changing the dilution of the aerosol sample and by comparing the electrical charges of the particles in the boiler. The coal-combustion particles were around 25 nm in diameter. The addition of 10.5% industrial pellets to the coal caused the formation of a second particle mode, the soot mode (120 nm in diameter), in the boiler. In the heating plant, the addition of light fuel oil to heavy fuel oil had a similar effect on the oil-combustion particles. The particles from the combined coal-and-pellet combustion agglomerated and coagulated before reaching the sampling point in the stack. These processes, combined with the effect of an electrostatic precipitator, resulted the mean diameter of the particles to be 80 nm. Further, the flue-gas desulphurisation and fabric filters lowered the particle number concentrations. The particles measured inside the stack were also observed from the atmosphere before they were diluted to background concentrations. The flue-gas plume was measured in four occasions, in three wind directions and with four flue-gas cleaning and fuel combinations. These measurements resulted in the observation of a new particle formation in the diluting plume. In the atmospheric measurements, the concentrations of SO_2 and CO_2 played an important role in measuring the dilution process. In the heating-plant experiment, the characterization of oil-combustion particles showed that the lower fuel sulphur content decreased the particles' hygroscopic growth factors.

The atmospheric primary emissions of coal-fired power plants can be effectively lowered through flue-gas cleaning technologies. In this study, flue-gas cleaning was shown to affect the flue gas's particle number and the mass concentration as well as its black carbon concentration. The cleaning did not prevent new particle formation in the flue-gas plume in the atmosphere, but it did reduce the potential for particle formation.

Tiivistelmä

Fossiilisia polttoaineita kuten kivihiili ja öljyä käytetään maailmanlaajuisesti energiantuotannossa. Näiden fossiilisten polttoaineiden käyttäminen tuottaa kaasuja ja hiukkasia, joilla on vaikutusta ilmanlaatuun ja ilmastoon. CO_2-päästöjen vähentämiseksi fossiilisia polttoaineita korvataan biomassalla. Tällä voi olla vaikutusta voimalaitoksen hiukkaspäästöihin. Tässä väitöskirjassa on määritetty voimalaitoksien hiukkaspäästöjen ominaisuuksia erilaisilla polttoaineilla aina kattilasta ilmakehään. Tutkitut voimalaitokset olivat yhdistetty sähkön ja lämmöntuotannon voimalaitos (combined heat and power plant (CHP), poltti hiiltä sekä hiilen ja puupellettien seosta) ja kaukolämpölaitos, jossa poltettiin kolmea öljyseosta. Hiukkasten lukumääräkokojakauma ja lukumääräkonsentraatio määritettiin näytteestä, joka otettiin CHP-laitoksen kattilasta, CHP-laitoksen piipusta, kaukolämpölaitoksen piipusta ja CHP-laitosta ympäröivästä ilmakehästä.

Kattilaolosuhteista otetuille aerosolinäytteille suoritetut mittaukset indikoivat, että hiilen poltosta sekä hiili-pellettiseoksen poltosta syntyneet hiukkaset olivat syntyneet jo kattilassa, eivät näytteenoton yhteydessä. Hiukkasten muodostumista tutkittiin primäärilaimennussuhdetta muuttamalla ja vertailemalla hiukkasissa olevien varausten määrää. Hiilipoltossa muodostuneiden hiukkasten keskimääräinen halkaisija oli 25 nm. Hiilestä 10.5% korvattiin pelletillä, jonka seurauksena kattilasta otetun näytteen hiukkaskokojakaumaan muodostui toinen moodi, nokimoodi (keskimääräinen halkaisija 120 nm). Kaukolämpökattilaa tutkittaessa kevyen polttoöljyn seostaminen raskaaseen polttoöljyyn aiheutti myös nokimoodin muodostumisen. Hiili-pellettiseospoltossa muodostuneet hiukkaset agglomeroituivat ja koaguloituivat ennen piipun näytteenottoa. Nämä prosessit yhdistettynä sähkösuodattimen käyttöön aiheuttivat hiukkasten keskimääräisen koon muutoksen 80 nm:iin. Edelleen savukaasun rikinpoistolaitos ja letkusuodattimet madalsivat hiukkasten lukumääräpitoisuutta. Piipussa mitatut hiukkaset pystyttiin havaitsemaan ilmakehästä tehdyissä mittauksissa ennen savukaasun laimenemista ilmakehän taustapitoisuuksiin. Savukaasuvanan laimenemista mitattiin neljä kertaa, kolmeen eri tuulen suuntaan ja neljällä eri savukaasunpuhdistus- ja polttoaineyhdistelmällä. Nämä mittaukset osoittivat että laimentuvassa savukaasuvanassa muodostuu uusia hiukkasia. Ilmakehämittauksissa SO_2 ja CO_2 olivat tärkeässä roolissa laimenemisen tutkimisessa. Kaukolämpölaitoksessa tehdyissä mittauksissa havaittiin myös, että polttoaineen madaltuva rikkipitoisuus pienensi hiukkasten hygroskooppisuuskasvukertoimia.

Voimalaitosten ilmakehäpäästöjä voidaan vähentää tehokkaasti savukaasun puhdistusmenetelmillä. Tässä työssä osoittettiin, että savukaasupuhdistimilla voitiin vaikuttaa hiukkasten lukumäärä- ja massapitoisuuksiin sekä mustan hiilen pitoisuuksiin. Savukaasun puhdistus ei kuitenkaan pystynyt estämään hiukkasmuodostusta laimentuvassa savukaasuvanassa vaikka se vähensi hiukkasmuodostuspotentiaalia.

Preface

This study was carried out at Tampere University of Technology (TUT) during the years 2014−2018 at the Aerosol physics unit in the Physics laboratory, Faculty of Natural Sciences. I would like to express my sincere gratitude to my supervisor Ass. prof. Topi Rönkkö and prof. Jorma Keskinen. Topi was pointed as my supervisor after one year of studies. At the same time, I got a position in the TUT graduate school. It enabled me to continue with this topic after the MMEA project ended in 2014. Later on, parts of the thesis have been written during the EL-TRAN project, funded by the Academy of Finland. I would also thank the Aimo Puromäki fund from the KAUTE foundation and Finnish Foundation for Technology Promotion for personal grants during my studies. I also want to thank professors Esa Vakkilainen and Zoran Ristovski for their valuable pre-examination comments.

I want to thank all of my co-authors for your valuable feedback while writing the papers for this thesis. Even to this day, you all still continue to answer my measurement-related questions – like they have not gotten old by now. Furthermore, I have to thank Anna Häyrinen and Jani Rautiainen for enabling the measurement campaign at Hanasaari, and D. Sc. Erkka Saukko and D. Sc. Panu Karjalainen for making the measurement campaign at Helen Oy a success.

In between the measurement campaigns, I have spent most of time with the people of the OQ group and have enjoyed the time with you. You all form the positive atmosphere in the lab and in the coffee room. I think our strength is in the community, allowing effortless asking and receiving of help when needed.

I have been blessed with wonderful old and new friends. You all have gotten your share of the thesis process, and thus thank you for tolerating me talking about my research. Of course we have not just talked, we have cooked food, played boardgames, knitted and escaped together during the years – to mention a few. During these last few years I feel I have gotten a Tampere family. Thank you for your friendship Kirsi, Matti, Suvi, Jouni and all of the kids. Thank you Matti and Kirsi for the honour of being Laura's godmother. I think she continues to be a great "alibilapsi".

Kiitos vanhemmilleni siitä, että olette olleet kiinnostuneet tekemisistäni vuosien kuluessa ja kannustaneet jatkamaan. Kiitos veljelleni Mikolle siitä, että olet tarjonnut haasteita lautapelien muodossa. Sinua vastaan pelatessa olen voinut voittaa vain ensimmäisellä kerralla. Veljeni Artun olen valjastanut testaamaan erilaisia keittiökemian ihmeitä vuosien aikana erittäin onnistunein tuloksin. Kiitos ja anteeksi. The last four years I have been doing research at the office, in the TUT aerosol lab and various combustion facilities in Finland and abroad. After each measurement campaign, it has been wonderful to get back home. I want to thank my husband Markku for his understanding and support during the years. Especially the last year has shown that we are strong. I love you.

Contents

Abstract i

Tiivistelmä iii

Preface v

Acronyms and symbols ix

List of included publications xi

Authors' contributions to the publications xiii

1 Introduction 1
1.1 Research objectives and scope of the thesis 2

2 Power-plant emission studies 5

3 Experimentation 11
3.1 Coal-fired power plant 11
3.2 Oil-fired power plant 14

4 Results and discussion 21
4.1 Characterisation of particles from the combustion of coal and a mixture of coal and industrial wood pellets 21
4.2 Particle emission of power plants 24
4.3 Flue-gas plume in the atmosphere 31

5 Conclusions 35
5.1 Future outcomes 37

Bibliography 41

Publications 51

Acronyms and symbols

BC	black carbon
CHP	combined heat-and-power
CPC	condensation particle counter
CS	condensation sink
DMA	differential mobility analyser
E	ejector diluter
EAA	electrical aerosol analyser
EDS	energy dispersive X-ray spectrometer
EEPS	Engine exhaust particle sizer
ELPI	electrical low-pressure impactor
em.	water emulsion
ESP	electrostatic precipitator
FF	fabric filters
FGD	flue-gas desulphurisation
FPS	fine-particle sampler
FTIR	Fourier transform infra-red spectrometer
GPS	Global positioning system
HFO	heavy fuel oil
HTDMA	hygroscopic tandem differential mobility analyser
HTNR	high-temperature NO_x reduction
LFO	light fuel oil
MOUDI	micro orifice uniform-deposit impactor
PM	particulate matter
PN	particle number concentration

PTD porous tube diluter

RH relative humidity

SCR selective catalytic reduction

SMPS scanning mobility particle sizer

SNCR selective non-catalytic reduction

SP-AMS soot-particle aerosol mass spectrometer

TD thermodenuder

TEM transmission electron microscope

VOC volatile organic compound

wFGD wet flue-gas desulphurisation

List of included publications

This thesis is a compilation style thesis and consists of an introduction part and the following four publications. The publications are cited in the introduction according to their numbering.

I Fanni Mylläri, Panu Karjalainen, Raili Taipale, Pami Aalto, Anna Häyrinen, Jani Rautiainen, Liisa Pirjola, Risto Hillamo, Jorma Keskinen, Topi Rönkkö. "Physical and chemical characteristics of flue-gas particles in a large pulverized fuel-fired power plant boiler during co-combustion of coal and wood pellets" *Combustion and Flame* 2017, vol 176, pp. 554-566, Feb. 2017

II Fanni Mylläri, Eija Asmi, Tatu Anttila, Erkka Saukko, Ville Vakkari, Liisa Pirjola, Risto Hillamo, Tuomas Laurila, Anna Häyrinen, Jani Rautiainen, Heikki Lihavainen, Ewan O'Connor, Ville Niemelä, Jorma Keskinen, Miikka Dal Maso, Topi Rönkkö, "New particle formation in the fresh flue gas plume from a coal-fired power plant: effect of flue gas cleaning" *Atmospheric Chemistry and Physics*, vol 16, pp. 7485–7496, Jan. 2016.

III Fanni Mylläri, Liisa Pirjola, Heikki Lihavainen, Eija Asmi, Erkka Saukko, Tuomas Laurila, Ville Vakkari, Ewan O'Connor, Jani Rautiainen, Anna Häyrinen, Ville Niemelä, Joni Maunula, Risto Hillamo, Jorma Keskinen, Topi Rönkkö, "Characteristics of particle emissions and their atmospheric dilution during co-combustion of coal and wood pellets in large combined heat and power plant" *Accepted to Journal of the Air & Waste Management Association*

IV Matti Happonen, Fanni Mylläri, Panu Karjalainen, Anna Frey, Sanna Saarikoski, Samara Carbone, Risto Hillamo, Liisa Pirjola, Anna Häyrinen, Jorma Kytömäki, Jarkko V. Niemi, Jorma Keskinen, Topi Rönkkö, "Size distribution, chemical composition, and hygroscopicity of fine particles emitted from an oil-fired heating plant" *Environmental Science & Technology*, vol 47, pp. 14468–14475, Nov. 2013.

Authors' contributions to the publications

Measurements in **papers I, II and III** were made at once during a single measurement campaign but in three measurement locations. Due to the multiple measurement sites, I was not able to make all of the measurements myself. Nevertheless, I participated in planning of the measurement campaign and the experimental setups from the beginning. I also had a major role in organizing the measurements. I was also responsible for the timing of the helicopter flights.

I conducted the stack measurements and Ville Niemelä helped me with the flue-gas sampling. Anna Häyrinen and Jani Rautiainen provided data regarding the regulated measurements, fuel characteristics and details about the power plants' operation. I was responsible for the entirety of the review processes.

Paper I:

I coordinated the measurements between the locations. Panu Karjalainen analysed the data, and together, we interpreted the results. I wrote most of the manuscript's first draft and drew all of the figures in the manuscript. The politics of biomass combustion was written by Pami Aalto.

Paper II:

I analysed the data related to the stack and helicopter measurements. I participated in data interpretation and originated the idea to model sulphuric-acid nucleation in the flue-gas plume to test, whether such nucleation could explain the results. I wrote most of the manuscript's first draft, except the modelling parts, which were written by Tatu Anttila, who also performed the modelling. Eija Asmi was in charge of ensuring the success of the helicopter measurements.

Paper III:

I analysed the data related to stack, aethalometer and helicopter measurements. I also participated in data interpretation and wrote most of the manuscript's first draft. Liisa Pirjola made the black carbon measurements possible. Heikki Lihavainen was crucial to ensuring the success of the helicopter measurements.

Paper IV:

I conducted the particle number size distribution and hygroscopicity measurements with Matti Happonen and Panu Karjalainen. I participated in improving the hygroscopic tandem differential mobility analyser for the measurements. I was involved in the data interpretation and made a minor contribution to the manuscript text. I drew the figures for the manuscript.

1 Introduction

Werner von Siemens created one of the first working generators in 1866, and 16 years later, the first central power stations were opened in New York and London (Termuehlen and Emsperger (2003), Thomas (2017)). The coal production and consumption statistics since 1980 are shown in Fig. 1.1 (BP2, 2017). Since 2014, coal production and consumption have followed a decreasing trend worldwide. Coal consumption was roughly 32 PWh in 1965, which is roughly half of the coal consumption in 2016. In Finland in 2016, coal consumption was 66.7 TWh, which was 0.10% of the global total (BP2, 2017).

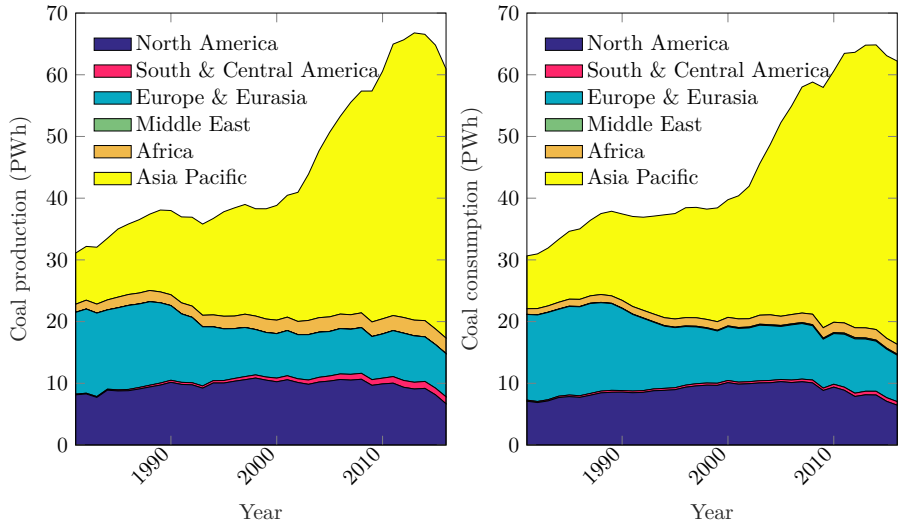

Figure 1.1: The total coal production (left) and consumption (right) in various regions plotted as a function of the year. Reproduced from BP2 (2017) with permissions.

Power-plant planning starts with choises regarding the fuel and the power capacity (electricity, heat, or both). These two factors with the financial costs guide the combustion method and the amount of fuel needed for energy production. Depending on its quality the fuel can be burned in burners, over a grate, in a fluidised bed or in an internal-combustion engine. The combustion of the fuel releases energy, which heats the circulating water within the walls of the boiler. The energy in the water or steam is used to produce heat, electricity or both. The energy that is not tranferred to the circulating water remains in the flue gas. The heat in the flue gas can be further used to heat the steam or the water in the tubes i.e., in a superheater or, later on to heat the water in an economizer or the

combustion air in a reheater. The efficiency of the boiler can vary between 80 and 95% depending on the plant type. The electricity generating efficiency from the combustion of fuel is 30 – 48% which depends on the heat exchangers, steam pressure and temperature. In a combined heat-and-power (CHP) plant, rest of the heat is captured to district heat.

Once most of the heat has been transferred to the power plants' steam – water circulation, the flue gas can be cleaned. This cleaning is needed for environmental reasons. Power plants have emission limits to protect enviroment. These emission limits are defined for gaseous compounds and for particles, both of which are released during combustion. Some of the gaseous compounds can be removed from the flue gas using scrubbers and catalysts, such as NO_x and SO_2. Particles in the flue gas can be filtered using the impaction, diffusion of intersection mechanisms on filters or using the electrical charge of the particles to collect them on electrostatic precipitator (ESP) plates.

In the beginning, centralised energy production using coal caused environmental problems. Likens and Bormann (1974) wrote, '...these trends in fuel consumption, fuel preference, and pollution control technology (increasing height of smokestacks and installing particle precipitators) have transformed local "soot problems" into a regional "acid rain problem" '. The acid rain problem triggered efforts to control the SO_2 emissions of power plants. Currently, the emission problems is global as humans have disturbed the Earth's climatic system (IPCC, 2013). The atmospheric levels of greenhouse gases are increasing. According to IPCC (2013), CO_2 concentration determines the extent of climatic warming. Thus, the most effective method to slow down global warming might be decreasing the CO_2 emissions.

Fossil-fuel combustion is one of the largest sources of CO_2 emission. However, the CO_2 is not the only pollutant from combustion, which also produces particles and other gaseous compounds. The combustion-generated particles are not the only ones that affect the climate. Some particles form in the atmosphere from vapours emitted by natural sources, and some are emitted directly from other sources (e.g. sea salt). All the different particles and vapours mix in the atmosphere, and both their properties and processes that they undergo in the atmosphere affect the climate. According to Boucher et al. (2013, p. 617, Fig. 7.18), the total radiative forcing of aerosol particles has a negative effect, although the uncertainty is high. To know the real effects that aerosols have through radiative forcing, the primary emissions of particles and gases must be evaluated based on calculations, from models and/or measurements.

1.1 Research objectives and scope of the thesis

The aim of this thesis is to provide information about the emissions of fossil-fuel-fired power plants, particularly those that use coal or a mixture of coal and industrial pellets and three oil fuel mixtures. The characteristics of the emissions provide detailed information for use in climate models. The characterisation of these emissions provides answers to the following questions:

- How do power plants' fuel choices affect flue-gas particles' properties?
- What are the primary emissions of power plants?
- How do aerosol particles from combustion behave in the atmosphere?

Chapter 1 highlighted the fuels used in energy production and introduced basic information about energy production and emissions. The second chapter 2 is about previous power-plant emission studies. The results from these previous studies are compared with

the results presented in this thesis. The following chapters expand upon the flue-gas lifespan. Chapter 3 gives detailed information about the power plants, the fuels and the measurement instruments used in each measurement setup. Chapter 4 presents the results related to a CHP plant's particle emissions, from the boiler to the atmosphere. The particles originating from combustion of coal and of the mixture of coal and industrial pellets were characterised from a hot aerosol sample from the boiler. The particles were also characterised from a sample taken from the flue-gas duct. Measurements were also made regarding two flue-gas cleaning situations. The results are then shown for the primary particle emissions of an oil-fired heating plant. The volatility and hygroscopicity of the particles from the oil-fired heating plant are discussed with the results form the stack measurements of the CHP plant. The results are presented here because some of the particles' atmospheric properties can be also measured from the flue-gas sample before the gas is emitted into the atmosphere. Lastly, the results for a CHP plant are discussed in terms of gas concentrations and the particle number concentration in the atmosphere. Chapter 5 provides a summary of the results and a discussion about this study's impacts regarding aspects related to the power-plant emissions.

2 Power-plant emission studies

This chapter focuses on previous power-plant emission studies and features details about measurement techniques and particle characteristics. This chapter also provides information about how the papers included in this thesis relate to the previous literature. The internal structure of this chapter follows the lifespan of the flue gas: from the boiler to the atmosphere.

Primary particle emissions due to combustion can be studied in multiple ways, and this thesis uses two methods. In the first method, particles in the hot flue gas were characterised, when the flue gas was sampled from the boiler. The second method was to study the particle emissions from the stack. The hot flue gas measurement from the boiler provided information about the effect that the fuel had on the particles during the combustion process. Particle sampling from hot flue gas requires a specific sampler because the temperatures inside the boilers range from 500 to 1 300 °C. The temperature of the flue gas is not the only problem; there can be high concentrations of particles and water, which can condense inside a sampling probe. Some of the previous researches (Aho et al., 2008; Jiménez and Ballester, 2005) have used a diluting probe that tolerates temperature over 1 000 °C. These hot temperature diluters were designed to decrease the sample's temperature and its water vapour and particle concentrations before the measurement. The other option for taking particle sample from a hot environment is to use a non-diluting sampling probe, which only lowers the sample temperature. Such non-diluting probes have been applied to temperatures of roughly 800 °C. Further, the sample can be diluted for example with ejector diluters (Broström et al., 2007; Davidsson et al., 2007). Due to the high temperature of the sampling, cooling of the sample can produce particles (Abdul-Khalek et al., 1999; Sippula et al., 2012) from compounds with low vapour pressure. On the other hand, diluters can be designed to promote nucleation of gaseous compounds to the particle phase during dilution (Jiménez and Ballester, 2005). Dilution affects the measurement results; therefore, the characterization of the dilution is important.

After the dilution of the flue-gas sample, the particles in the sample can be characterised based on their properties, such as mass and number concentrations, particle mass and particle number size distributions and particle diameters. Particle formation, particle mass and particle number size distributions have been studied both on the real and laboratory scales with regard to power plants (Joutsensaari et al., 1992; Kauppinen and Pakkanen, 1994; McElroy et al., 1982; Nielsen et al., 2002; Schmidt et al., 1976; Ylätalo and Hautanen, 1998). The real-scale power-plant measurements have been conducted using a sample dilution and aerosol instrumentation such as electrical low-pressure impactors (ELPIs) (Keskinen et al., 1992), scanning mobility particle sizers (SMPSs) (Wang and Flagan, 1990), low pressure impactors and electrical aerosol analyser (Liu and Pui, 1975). These previous measurements for real-scale power plants were made from the ESP inlet.

There is limited information related to measurements where the flue-gas sample is taken directly from a real-scale power plant boiler and the particles are characterised with similar instrumentation and methods than in **paper I**. Kuuluvainen et al. (2015) made particle measurements from a bubbling fluidized bed boiler using similar diluter as in **paper I**. They made combustion test with fuel mixtures of various fuels: bark, sludge, peat and solid recovered fuel. They found out that the particle number size distribution was bimodal. The first mode (20 nm in diameter) was formed in the dilution by condensation of gaseous species over core particles and this mode was sensitive to measurement location, fuel mixture and additive feeding. The second mode (80 nm in diameter) was formed in the combustion and it was more stable than the first mode. In addition to particle number size distribution measurements, Kuuluvainen et al. (2015) studied the morphology of the particle from TEM images, the effective density of the particles and the electric charge of the particles. One key finding was that the effective density of the particles was nearly constant in the first mode and varied as a function of size in the second mode. The electric charge of the particles varied between the modes; the first mode had a negative net charge whereas the second mode had negative and positive net charge depending on the diameter of the particle. The physical properties of particles (e.g. size, electrical charge, effective density) provide information about the formation process of the particles.

After boiler, the heat in the hot flue gas is transferred to water. The cooled flue gas can be cleaned of particles with various flue-gas cleaning devices before the gas is released into the atmosphere. For example, the CHP plant in **papers I, II and III** has a six-section unit ESP, a two-chamber semi-dry flue-gas desulphurisation (FGD) (discussed in Korpela et al. (2015)) and fabric filters (FF). Regarding the flue-gas cleaning, the previous studies have been focused on filtration efficiency of the various flue-gas components, such as trace metals (Helble, 2000) and particulate matter (PM), after undergoing flue-gas cleaning with the devices. The filtration efficiency of an ESP for various trace metal elements was found to be around 99% (Helble, 2000). Ylätalo and Hautanen (1998), on the other hand, studied PM before and after ESP. The collection efficiency of the ESP depended on the boiler load, the ESP voltages, the operation of the coal mill and the particle size (Ylätalo and Hautanen, 1998). The most difficult particle diameter range to collect using an ESP was 0.1-3 μm (Ylätalo and Hautanen, 1998). The operation of the ESP was sensitive to the particle's diameter (Ylätalo and Hautanen, 1998). The ESP influenced the incoming particle number size distribution by removing the larger particles; some of the smaller particles went through the ESP. The information about the particle number size distribution after use of the ESP provides information about the collection efficiency of that ESP. The collection efficiency of an ESP determines the particle number size distribution of the flue gas that is released into the atmosphere or that is passed to other flue-gas cleaning devices.

Some previous studies have focused on PM (Córdoba et al., 2012; Frey et al., 2014; Ma et al., 2016; Saarnio et al., 2014; Yi et al., 2008), but a few have also considered particle number concentrations (PN) (Frey et al., 2014; Yi et al., 2008). The characterisation of fine particles after applying ESP is the focus of **papers II and III**; further, the particles have been characterised after flue-gas desulphurisation (FGD) and FF using the same measurement setup. The main differences between the measurements are often the diluter, the dilution temperature (hot/cold) and the instrumentation choices. Therefore, the comparability of the measurement results from power plants is difficult. This can slow down the processes of understanding the properties of particles from similar power plants. In **papers II and III**, the power plant under the study is the same as that in Frey et al. (2014). The biggest difference between the measurements was in the dilution temperature,

which caused some differences in the particle number size distribution results, as discussed later.

The desulphurisation has been designed to decrease SO_2 concentration in the flue gas. However, the SO_2 removal efficiency depend on the technique (semi-dry or wet) applied in the desulphurisation plant. More than 90% of the desulphurisation plants use Ca^{2+} method world wide and over 85% of them are wet-FGD (Jamil et al., 2013). The wFGD removes more than 95% of the SO_2 whereas the removal efficiency is 85-90% for a semi-dry FGD (Jamil et al., 2013). The semi-dry FGD is normally combined with fabric filters, whereas after wet-FGD, the emission is directly released to the atmosphere without any additional filters. Córdoba et al. (2012) studied the operation of FGD, when mixture of petroleum coke and coal was combusted in a pulverized coal combustion plant. The analysis was mainly based on offline samples collected from various parts of the flue-gas cleaning systems and PM samples collected on filters. Their results showed that FGD removes PM from the flue-gases. On the otherhand, Saarnio et al. (2014) studied mainly PM_1 samples collected before and after semi-dry FGD from a coal-fired power plant. The analysis made for the PM_1 samples showed that the particles after ESP, before FGD, consisted mainly of inorganic impurities of coal. They also found out that the usage of FGD changed the chemical composition of the particles. After FGD, the particles consisted mainly of chemical species from reagents used in the FGD process. Based on the TEM images in Saarnio et al. (2014), the particles were mainly internally mixed after the FGD but some primary emission particles were also observed separately from the internally mixed particles. Córdoba et al. (2012) and Saarnio et al. (2014) both state that FGD decreases PM emissions and alters the chemical composition of the particles by removing the primary particles and replacing them with particles released from FGD. In comparison to Saarnio et al. (2014), the PM measurements were made using online instrument in **papers II and III**. Further, the transmission electron microscope (TEM) images from particles were used to identify the chemical composition of the particles as well as mixing state (**paper III**).

Yi et al. (2008) made the measurements at a coal-fired power plant equipped with bag-house filters. They studied online particle mass and number size distribution with ELPI and conducted an offline PM analysis from collected samples before and after bag-house filters. In addition, they studied morphology of the particles by an electron microscope and energy dispersive X-ray spectrometer (EDS) analysis. The particle number size distribution showed a bimodal number size distribution with mean diameters of 100 nm and 2000 nm. Based on the electron microscope images most of the particles were spherical. Frey et al. (2014) have also studied a coal-fired power plant but it was equipped with ESP, FGD and FF. They made volatile particle number size distribution measurements with SMPS and calculated emission factors for particle mass and particle number. In addition, they studied the chemical composition of the particles in both flue-gas cleaning situations. Frey et al. (2014) reported also results for co-combustion of 4.5% of pellets mixed with coal. However, the main result in Frey et al. (2014) was that the particles from coal-fired power plant after flue-gas desulphurisation and fabric filters had a negative radiative forcing (over a dark surface) mainly due to sulphate particles released from FGD. **Paper II and III** present similarly to Frey et al. (2014), the particle number size distributions for non-volatile particles from coal and mixture of coal and 10.5% pellet combustion situations. **Paper III** contains calculated emission factors for dust, black carbon and particle number concentration with both fuels and two flue-gas cleaning situations.

Power plant emissions to atmosphere have been studied on 1970-1980's when the flue-gas

cleaning was not widely used. Meagher et al. (1981) studied two power plants combusting coal containing approximately 3.8% of sulphur. One of the power plants did not have any flue-gas cleaning systems and the other had a wet flue-gas desulphurisation plant. The measurements made with instruments installed to an aircraft showed that the atmospheric oxidation rates were the same and were not affected by the flue-gas cleaning. Liebsch and De Pena (1982) studied a coal-fired power plant with electrostatic precipitators by measuring conversion from SO_2 to ${SO_4}^{2-}$ in a flue-gas plume. The results were similarly shown in plume travel time as in **papers II and III** and in Dittenhoefer and De Pena (1978). In Liebsch and De Pena (1982), the measurements were made after the plume had diluted 5 minutes whereas in **papers II and III** the measurements were done right after emission. The largest differences were in cut-point diameter of the particle counter and the particle number size distribution measurement. The smallest detected particles were 6 nm in Liebsch and De Pena (1982) and the particle number size distribution was measured with electrical aerosol analyser (EAA) (cyclic measurement) with the lowest cut-point of 10 nm. Since then, the flue-gas cleaning devices have become more common and the aerosol instrumentation has developed so that the smallest detectable particle diameters are around 2.5 nm when using condensation particle counters (**papers II and III**) and the particle number size distribution can be measured 1 Hz time resolution down to 5.6 nm particles in diameter (**papers II and III**).

Emission-controlling devices have been installed in power plants to achieve the emission limits set by governments and other authorities. The emission limits of a power plant vary depending on its age, fuel, power/size, yearly operation hours and location. Emission limits are mainly set for PM, NO_x (as NO_2) and SO_2 or SO_3. In addition, the concentration of heavy metals in particles and in gases can be regulated; for instance, in coal-fired power plants, it is mandatory to measure the total Hg concentration of the flue gas once per year. Finnish and EU laws regulate the emission limits for power plants (Ministry of the Environment, 2014). Continuous measurements of SO_2, NO_x, PM, O_2, temperature, pressure and H_2O are required for all power plants that exceed 100 MW in power. The H_2O concentration measurement is not mandatory if the regulated measurements are made on dry flue gas. The law allows exceptions to these emission measurements based on operation hours or fuel. These regulations and emission limits have affected the gaseous and particulate concentrations in the flue gas emitted to the atmosphere.

Once flue-gas flow enters the atmosphere, it starts mixing with the surrounding air. Diffusion, convection and turbulent mixing of flue gas and air cause this natural dilution. The rate at which the flue gas dilutes depends on the source strength, the background concentration and meteorology (Stevens et al., 2012). The dilution can be studied through in-flight measurements taken from an aircraft (Brock et al., 2002; Keil et al., 2002; Lonsdale et al., 2012; Stevens et al., 2012) such as an ultralight aircraft (Junkermann et al., 2011a) or a helicopter (**papers II and III**). To understand this dilution, these flights should be made crosswind, upwind and downwind from the source. Stevens et al. (2012) and Lonsdale et al. (2012) have studied long-distance crosswind profiles of the plumes' gas and particle concentrations as a function of the distance from the stack. In Junkermann et al. (2011a), the focus of the measurements was mainly in the upwind and downwind directions, but some crosswind profiles were also measured.

The dilution of a fresh flue-gas plume can be traced using a trajectory calculation or with gaseous tracers. The gaseous tracers for the fresh flue gas included CO_2, H_2O and O_3 (Junkermann et al., 2011b); and SO_2 and NO_x (Lonsdale et al., 2012); SO_2, CO, HNO_3, total reactive gas phase nitrogen (NO_y=NO+NO_2+HNO_3+PANs+$RONO_2$...), NO and

NO_2 (Brock et al., 2002). These gases can be classified into two groups: non-reactive (CO_2, H_2O) and reactive tracers (all others). In addition to gases, primary particles can be used to trace a flue-gas plume in the atmosphere. The primary emissions in the flue-gas plume have been measured through particle number size distribution (Junkermann et al., 2011b; Lonsdale et al., 2012; Stevens et al., 2012) and number concentration. Measurements have been conducted with a condensation particle counter (CPC) battery (Brock et al., 2002) and an optical particle counter (Brock et al., 2002). In some cases, the measurement instruments have observed new particle formation in diluted plumes (Junkermann et al., 2011a; Stevens and Pierce, 2014; Stevens et al., 2012) within a few and tens of kilometres from a power plant. Stevens and Pierce (2013) made a parameterisation for particle formation in sulphur-rich plumes. The equations regarding sulphuric acid formation and nucleation in **paper II** were taken from Stevens and Pierce (2013) and used to produce a simplified model to compare the experimental results with those from a sulphuric-acid nucleation model. A more detailed model have been published by Lazaridis et al. (2001) which for example includes more detailed chemical reaction models of gaseous compounds, deposition and condensation.

The dilution of atmospheric flue-gas plume and atmospheric oxidation processes are difficult to study due to multiple variables. The variables can be weather, flue-gas cleaning devices and precursors. Brock et al. (2003) made atmospheric measurements with aircraft near Houston, Texas. One of the studied sources was a coal-fired power plant. The main gaseous emission components of the power plant were NO_x and SO_2 and the power plant did not emit high concentrations of volatile organic compounds (VOCs) or PM. Brock et al. (2003) found out that the SO_2 mixing ratio correlated well with the particle volume concentration. However, they also found out that nitrates and organics were the main contributors for particle growth in the flue-gas plume. Similar results have been reported by Pirjola et al. (2015) for internal combustion engines and by Kulmala et al. (2013) for atmospheric nucleation processes. Results presented in **paper II** suggests similar results related to the observed particle formation yet measuring also the dilution process before the particle formation in the atmosphere.

Further, the particles emitted from the stack or the particles formed in the atmosphere are exposed to various atmospheric conditions such as humidity, radiation and temperature. The particle properties such as hygroscopicity is discussed in **paper IV** for combustion originated particles. If the particle has hygroscopic tendencies, it will absorb water from the surrounding gas. In **paper IV**, the hygroscopic growth factors were determined for three fuel mixtures combusted in a real-scale power plant. In the study of Henning et al. (2012) the soot particles were generated with soot generator and in Happonen et al. (2013) the particles were in the engine exhaust. The hygroscopicity was estimated based on a growth factor; the ratio between the particle diameter in the humid environment and the particle diameter in the dry environment. Soot particles were found to have growth factors close to one, so no clear indication of hygroscopic growth. The hygroscopicity of the particles is also affected by the chemical composition of the particles and one of the most important components is sulphate (Henning et al., 2012).

Hygroscopicity of the particles is linked with the volatile compounds on the particles. For example, nucleation mode particles originated from sulphuric acid are volatile (Rönkkö et al., 2013), the volatility can be measured using thermodenuder (TD) heated up to 265 °C. The volatile fraction consists of compounds that are in gaseous phase in high temperature exhaust but condense on particle surfaces in cooling dilution of exhaust. The amount of volatiles varies depending on the fuel sulphur content and engine load (Rönkkö

et al., 2013). Actually, similar information about the condensation of volatile species on particles can be obtained with dilution ratio tests as in **paper I** or with fuel changes (Kuuluvainen et al., 2015). In **paper IV**, the TD method was used to the particles from an oil-fired heating plant, where the volatility was linked with hygroscopic properties of the particles.

In this thesis, particle emissions of a real-scale power plant were characterised simultaneously with the state-of-the-art instrumentation and dilution. Physical properties of the particles were used to characterise the formation mechanisms in the boiler conditions, after flue-gas cleaning devices and in the atmospheric conditions. The characterisation of the particles in the boiler was made combusting two fuels: coal and a mixture of coal and 10.5% wood pellets. The effect of flue-gas cleaning on the particles was studied in two flue-gas cleaning situations after electrostatic precipitators – with and without flue-gas desulphurisation and fabric filters. The atmospheric measurements were made in each of the previous cases by following the diluting plume with a helicopter. The helicopter enabled one second sampling resolution for particle number concentration, for particle number size distribution and for selected gaseous components. In addition, particle number size distribution, hygroscopicity and volatility were measured for particles from an oil-fired heating plant. Moreover to particle emission characterisation, the connecting factor in the fuel choices of the power plants was the mixing of widely used fossil fuels, such as heavy fuel oil and coal, with more refined and presumably more environmentally friendly fuels, namely industrial pellets and light fuel oil.

3 Experimentation

This chapter focuses on describing the power plants, fuels and measurement locations, and it also gives an overview of the measurement instruments and setups used in **papers I, II, III and IV**. First, the CHP plant and its fuel characteristics are introduced. Second, the measurement methods applied in the boiler (**paper I**), stack (**papers II and III**) and atmospheric (**papers II and III**) measurements are discussed. Third, the oil-fired power plant, fuel mixtures and measurements are described (**paper IV**).

3.1 Coal-fired power plant

The studied power plant was a base-load CHP plant situated in Helsinki, Finland (see Fig. 3.1). The power plant had two boilers (each 362 MW_{th}) that entered use in 1974 and 1977, respectively. The boilers were equipped with reheaters and utilised a natural circulation of flue gas. Each boiler had 12 pulverised fuel burners situated on its front wall. The burners had been upgraded to high-temperature NO_x reduction (HTNR) burners (Tampella/Babcock-Hitachi) (Ochi, 2009) in 1992 and 1993, respectively to achieve lower NO_x emissions. The combustion air, which was also the carrier air for the pulverised fuel, was heated up to 350 °C before reaching the fuel grinders. The fuel was then ground using ball-ring grinders (nine rolling balls) before being blown through a sieve to the burners.

The low-NO_x burners were used to achieve reduced NO_x concentrations by staging the combustion air to secondary and tertiary air. The air staging lowered the combustion temperature to around 1 100 °C. A pellet-feeding system was installed in the power plant prior to the measurements. This system fed wood pellets to two of the four ball-ring grinders. The wood pellets and coal were then ground together. The combined grinding affected the fuel particles' diameters. The sieve returned any particles that were still too large to the grinders, which had been designed for coal grinding. The normal size range for coal particles is 47–62 µm (58–69% below 74 µm and 100% below 600 µm). The wood pellets' properties affected the grindability, so the fuel-particle size changed depending on the amount and the quality of the wood pellets.

3.1.1 Coal- and wood-pellet characteristics

The studied wood pellets were industrial quality wood mixed with coal; the pellets provided from 6% to 10.5% of the boiler's thermal power. Industrial pellets (or wood pellets of industrial quality) fulfill the EN 14961-1 standard, which states that such pellets have lower quality than do domestic pellets. A low-quality wood pellet is defined one that includes bark. Normally, wood for these pellets is produced by grinding logs or stem wood to a powder and then drying that powder before pelletizing it. This manufacturing

Figure 3.1: Hanasaari CHP power plant situated in Helsinki, Finland. The measurements in **papers I, II and III** were conducted at this power plant.

method makes the industrial pellets more brittle than domestic pellets. A mixture of coal and industrial pellets results in a fuel-particle diameter ranging from 54 to 174 µm (28–59% below 74 µm and 79–99% below 600 µm). A comparison of the fuel particles' mean diameters shows that the coal–industrial pellet mixture is ground to larger particles than coal alone is.

Table 3.1: Properties of coal and the pellets used in the combustion tests made in a CHP plant. Adapted from **papers I, II, III**.

		Industrial pellet	Coal
Moisture	%	6.7	11.0–11.3
Ash	%	0.8	10.5–11.4
Volatiles	%	78.1	32.8–33.1
Heating value	GJ/t	17.7	24.6–24.9
C	%	47.4	62.3–63.1
H	%	5.6	4.1–4.2
N	%	0.1	1.8–2
O	%	39.4	0
S	mg/kg dry	180	3 100–4 600
Cl	mg/kg dry	39	236
Ca	mg/kg dry	2 300	4 300–4 800
Mg	mg/kg dry	280	1 700–1 900
Na	mg/kg dry	69	1 400–1 600
K	mg/kg dry	760	2 500–2 900
Al	mg/kg dry	130	14 200–15 000

The source wood's chemical composition and the pelletizing method affect the pellet's chemical composition. The properties of coal and industrial pellets are listed in Table 3.1. Coal had higher moisture and ash content. The O and volatile content were higher in the pellet than in the coal. The concentrations of S and Cl, however, were lower in pellet than in coal. In fact, the alkali metals (K and Na) had lower concentrations in the pellet than in the coal as well. The heating value of the pellet was lower than that of the coal.

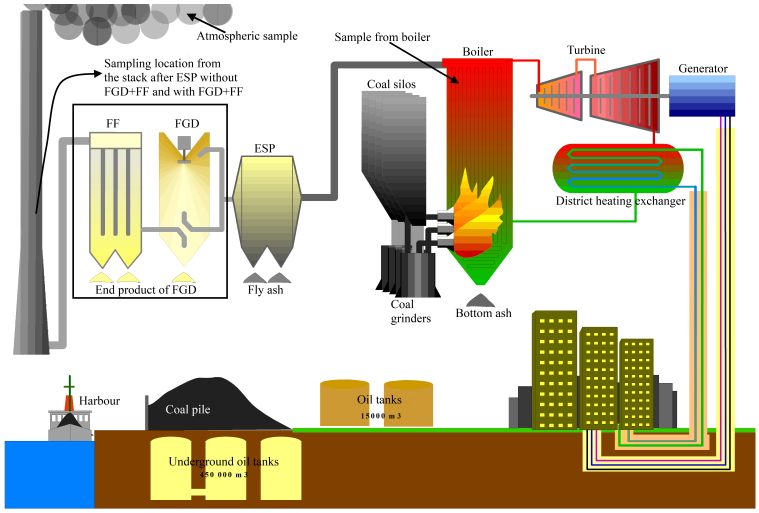

Figure 3.2: A schematic picture of the Hanasaari CHP plant, which utilises both coal and coal−pellet-mixture combustion. The measurement locations in **papers I, II and III** are indicated with arrows: the boiler, the stack and the atmosphere. Figure courtesy of Helen Oy.

3.1.2 Measurement instruments and flue-gas treatment devices

The flue-gas aerosol of the coal-fired power plant was studied in three locations: boiler, stack and atmosphere; the locations are shown in Figure 3.2. In the power plant, each of the boilers had its own flue-gas duct. One of the boilers and the corresponding duct inside the stack were used in the experiments. The flue-gas sample was measured after two flue-gas cleaning situations: first, after an ESP, and second, after the ESP and semi-dry FGD unit and FFs. These situations are later referred as *FGD+FF off* and *FGD+FF on*, respectively. The flue-gas ducts had their own ESPs, FGDs and FFs so, the flue gases were not mixed before reaching the stack measurement location. However, the flue gases were mixed when they entered the atmosphere.

The atmospheric measurements were made with instruments installed in a helicopter. The flue gas from the two boilers that had their own flue gas ducts became mixed when released into the atmosphere. The mixing of the flue gases in the atmosphere meant that the measurement instruments inside the helicopter were measuring mixed flue gases. In the *FGD+FF on* situation, both of the flue-gas cleaning devices were operating, whereas in the *FGD+FF off* situation only the studied flue gas was bypassing the FGD and FF; the gas in the other flue was cleaned with FGD and FFs. An image related to the helicopter measurements is shown in Figure 3.3. Figure 3.3 shows that the flue-gas plume could be detected with the eye. The helicopter flew both upwind and downwind of the plume and also made some crosswind flights. More details about the helicopter flight paths are in **paper II** (Figure 1) and **paper III** (Figure SI1).

Combustion aerosol contains high concentrations of gases and particles. Sample dilution is needed, as flue gas contains high concentrations of water, and the aerosol instruments work at room temperature and are designed to measure relatively low particle number concentrations. On the other hand, gas analysers need particle-free air and low concentrations to maintain their detection accuracy. Table 3.2 is a brief list of the locations

Figure 3.3: A picture of the measurement of atmospheric dilution of flue gas from pulverized-fuel combustion. Measurements were made by aerosol instruments installed in a helicopter. The figure demonstrates that the flue-gas plume can be visually observed while conducting measurements.

of the measurement instruments and gas analysers applied in **papers I, II and III**. More detailed measurement setups are presented in Figure 3.4, which provides additional information about the sampling line lengths and the arrangement of the instruments.

Flue gas can contain volatile gaseous species that can condense on the surfaces of primary particles (Lyyränen et al., 2004). The condensation of these volatile species can be observed from the particle number size distribution (e.g. as a change in the mean particle diameter). The primary diluter used in the boiler measurements had three primary dilution ratios. The dilution-ratio tests were used to evaluate the places where the particles formed. If particles formed in the dilution, the primary dilution ratio changes should have changed the nature of the particle number size distribution because of the volatile species. To support the primary dilution-ratio tests, the electric-charging probability of the particles was determined based on neutral and charged particle concentrations. These concentrations were measured with a mini-ESP and a SMPS consisted of a differential mobility analyser (DMA) and a CPC. The electric-charging probability values were compared with the particle-equilibrium charge distribution (by Boltzmann; see Hinds (1982, eqs. 15.30 and 15.31)) to obtain information on the particles' formation temperature. The calculation of the Boltzmann particle-equilibrium charge distribution relied on the combustion temperatures in the boiler and on the particle size.

The dilution process was not tested in the stack measurements, as the temperatures of the sampling probe and dilution gas were higher than that of the flue-gas. Moreover, a TD (Heikkilä et al., 2009) was used in the stack measurements to ensure the measurement of nonvolatile particles. However, the flue gas taken with the helicopter needed no additional dilution because of the natural dilution in the atmosphere. The atmospheric sample was diluted naturally in the atmosphere and was captured with measurement instruments (Table 3.2) installed in the helicopter.

3.2 Oil-fired power plant

The other studied power plant was a peak-load power plant; it was also situated in Helsinki, Finland. The studied boiler (47 MW_{th}) was an oil-fired water-tube boiler (Foster

Table 3.2: Sampling techniques, measurement instruments and gas analysers used at various locations within the power plant in **papers I–III**.

location	device	manufacturer
Boiler	PTD[1]+E[2]	self-made and Dekati Ltd.
	ELPI[3]	Dekati Ltd.
	SMPS[4]	TSI Inc.
	CO_2 analyser FTIR[5] DX-4000	Gasmet
	CO_2 analyser SIDOR	SICK Maihak
Stack	FPS[6]+E[2]	Dekati Ltd.
	ELPI[3]	Dekati Ltd.
	SMPS[7]	TSI Inc.
	CPC[8]	TSI Inc.
	Aethalometer AE33[9]	Magee Scientific
	CO_2 analyser VA3100	Horiba
	CO_2 analyser GM 35-type	SICK
	SO_2 analyser GM 32-type	SICK
Atmosphere	CPC[8]	TSI Inc.
	EEPS[10]	TSI Inc.
	CO_2 analyser G1301-m	Picarro
	SO_2 analyser 43i	Thermo Scientific
	RH[11]analyser	

[1] porous tube diluter, Vesala (2007), Aho et al. (2008)
[2] ejector, Giechaskiel et al. (2004)
[3] electrical low-pressure impactor, Keskinen et al. (1992), Marjamäki et al. (2002), Yli-Ojanperä et al. (2010)
[4] scanning mobility particle analyser, DMA3071 (differential mobility analyser) and CPC3025 (condensation particle counter), 0.6 slpm/6 slpm, Wang and Flagan (1990)
[5] Fourier transform infrared spectrometer
[6] Fine-particle sampler (FPS), Mikkanen and Moisio (2001)
[7] scanning mobility particle analyser, DMA3071 and CPC3775, 0.6 slpm/6 slpm, Wang and Flagan (1990)
[8] condensation particle counter, CPC3776, 1.5 slpm, Stolzenburg and McMurry (1991)
[9] Drinovec et al. (2015)
[10] Engine-exhaust particle sizer, Mirme (1994), Johnson et al. (2004)
[11] Relative humidity

Wheeler) with a rotary cup-type burner. The boiler entered operation in 1995. In **paper IV**, the boiler operated at 30 MW. The usage hours of the plant alternated on yearly basis, from 1 458 hours in one year to 2 164 hours in the next year. The boiler typically operated with two fuels: natural gas and oil. The power plant had one stack (108 metres tall) with two inner ducts, and it lacked flue-gas cleaning devices.

3.2.1 Oil characteristics

The oils (Table 3.3) were stored in their own containers and blended before combustion. The purpose of the blending was to lower the viscosity of the heavy fuel oil (HFO), as the viscosity of HFO is almost 50 times higher than that of light fuel oil (LFO). Still, the fuel blend had to be heated both before and during blending and before combustion. In **paper IV**, three oil blends were combusted during the measurements:

- HFO
- water emulsion (em.) of HFO (HFO+em.)
- 66 mol-% HFO and 34 mol-% LFO blend with em. (HFO+LFO+em.)

The water emulsion was obtained by mixing district heating water with the oil blend. The amount of added water varied from 3 to 4 L min^{-1} (i.e. it was less than 10% of the total fuel consumption).

Table 3.3: Properties of heavy and light fuel oils used in measurement at a peak-load power plant. The water content of the fuel was determined either with the Karl Fischer method or by distillation. Adapted from **paper IV**.

		Heavy fuel oil	Light fuel oil
Water (by distillation)	mol-%	<0.05	-
Water (Karl Fischer)	mg/kg	-	35
Density	g cm^{-3}	0.956 (at 60 °C)	0.8183 (at 20 °C)
Viscosity	mm^2 s^{-1}	99.52 (at 60 °C)	2.60 (at 20 °C)
Heating value (calculated)	GJ/t	40.9716	43.3548
Ash	m-%	0.04	-
C	mol-%	87.2	85
S	mol-%	0.89	0.01
N	m-%	0.31	-

3.2.2 Measurements

The flue-gas sampling and dilution system used in the stack measurements for the heating plant in **paper IV** (Fig. 3.5) was similar to the dilution system used in **papers II and III**. In the fine-particle sampler (FPS), the dilution air was heated to 39 °C. The total dilution ratio was around 60 during the measurements. After the dilution, the flue-gas sample was captured by the instruments with an approximately 10-metre-long copper line. The diluted flue-gas sample was divided into four branches, each with measurement instruments. The first branch consisted of a PM1-cyclone and a CPC3010 (TSI Inc.), plus a soot-particle aerosol mass spectrometer (SP-AMS) (Aerodyne Research Inc.). The second branch had a nano-micro orifice uniform-deposit impactor (MOUDI) (model 125B, MSP Corporation, Shoreview, MN, USA). This device was used for size fractioned PM collection to obtain mass samples for elemental analysis. The third branch led to NO_x and

CO_2 analysers. The CO_2 concentration was used to calculate the total dilution ratio for the flue-gas sample. The last branch had a TD before reaching the site of the particle size distribution measurements. The particle number size distributions were measured with an ELPI (Dekati Inc.), a nano-SMPS (TSI Inc.) and a SMPS (TSI Inc.). The fourth branch also had a hygroscopic tandem differential mobility analyser (HTDMA) (introduced in **paper IV** and in Happonen et al. (2013)) to measure the particles' hygroscopicity. The TD was used to study the volatility of the particles.

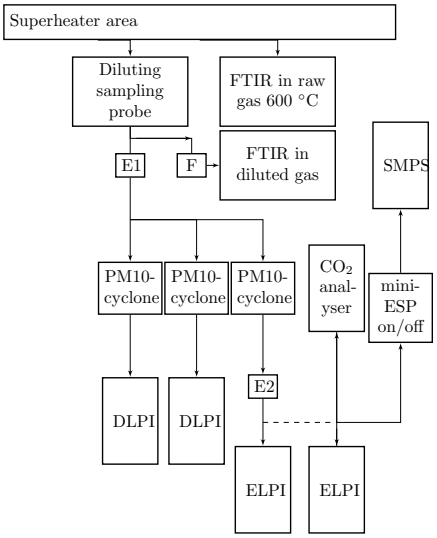

(a) Measurement setup used to characterise particles in hot flue gas sampled from superheater area of the boiler. Adapted from **paper I**.

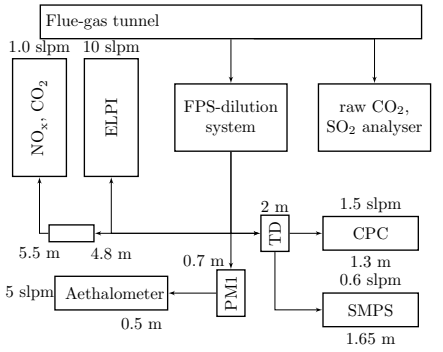

(b) Measurement setup applied in flue-gas measurements in the stack. Adapted from **papers II and III**.

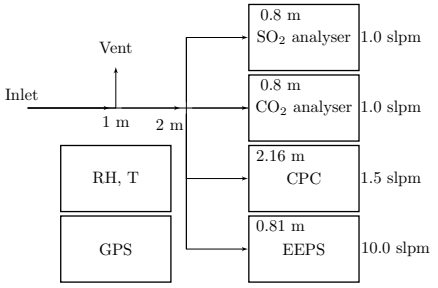

(c) Measurement setup installed in the helicopter to study the flue-gas plume in the atmosphere. Adapted from **papers II and III**.

Figure 3.4: Measurement setups used at the various measurement locations within the CHP plant: (a) boiler, (b) stack and (c) atmosphere. Instuments used in the measurement setups are presented in Table 3.2. The E1 and E2 corresponds to ejector diluters, F stands for filter, PM1 means cyclone with 1 µm cut-off diameter and TD is the thermodenuder. The dashed line in (a) represents 11-m long sampling line.

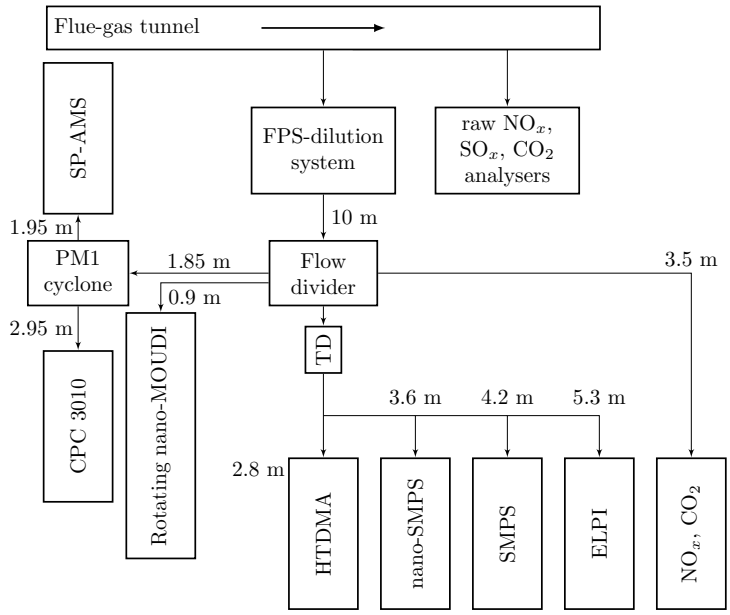

Figure 3.5: The measurement setup used to characterise particle emissions and properties of the particles resulting from the oil-mixture combustion in a peak-load heating plant. The studied particle properties were hygroscopicity, volatility and chemical composition. Adapted from **paper IV**.

4 Results and discussion

The results of **papers I, II and III** are presented here in the order following the path of the flue gas from the boiler to the atmosphere. These results are mainly related to the CHP plant, and the results for the heating plant (**paper IV**) are clearly indicated. The first section focuses on the particles in the boiler, and specifically those in the superheater area. The second section focuses on the particles after the flue-gas cleaning. This section also includes measurements of the particle characteristics that have atmospheric relevance (hygroscopicity and volatility) from the flue-gas duct of the oil-fired power plant. Lastly, the results of the atmospheric dilution of the flue-gas plume are presented. The results regarding both the dilution process and the new particle formation are discussed in the final section.

4.1 Characterisation of particles from the combustion of coal and a mixture of coal and industrial wood pellets

In **paper I**, the dilution of the sample was conducted at a higher temperature than in the previous studies concerning pulverised coal combustion. Additionally, the fine-particle characterisation in **paper I** was more detailed than that in the previous studies by Joutsensaari et al. (1992), Kauppinen and Pakkanen (1994), McElroy et al. (1982), Ylätalo and Hautanen (1998), Schmidt et al. (1976) and Nielsen et al. (2002) in terms of the fine-particle number and mass size distributions, as well as particles' effective density and charging state (as described in Sec. 3.1.2).

In **paper I**, the dilution ratio of the primary diluter was changed to study the effect that the diluter would have on particle formation. Figure 4.1a shows that the change in the primary dilution ratio did not affect the shape of the particle number size distribution. The particles' mean diameter was 25 nm for all the dilution ratios, which indicated that the particles formed in the power plant's boiler rather than in the diluter. This result also indicated that the gas phase did not contain low-vapour-pressure gases that could condense on the particles' surfaces.

To further characterise the particles, the particle-charging probability was calculated from the SMPS measurements, which were made with and without a mini-ESP (Figure 4.1b). This probability was linked with the particle-equilibrium charge distribution (by Boltzmann; see Hinds (1982, eqs. 7-31 and 7-32)), which depends on the particles' formation temperature and the particle number concentration (Burtscher et al., 1986). Wiedensohler (1988) made a parameterisation for the particle-equilibrium charge distribution. The Wiedensohler parameterisation is valid at room temperature. The charge probability has also been used as an indication of the particles' formation temperatures (Alanen et al., 2015; Lähde et al., 2009; Maricq, 2006; Sgro et al., 2011). Here, it was used for supporting

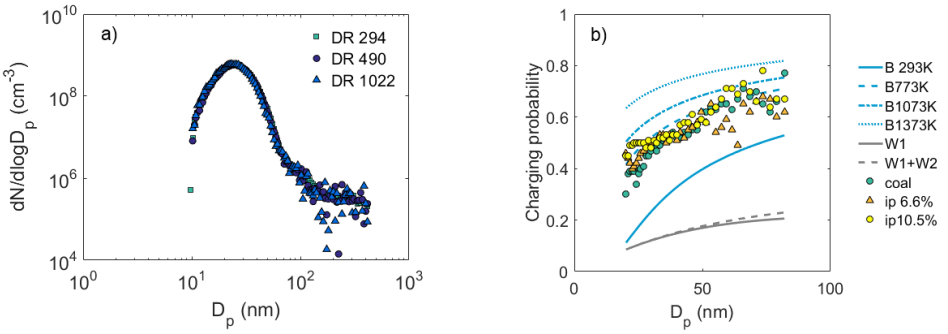

Figure 4.1: Particle number size distributions measured with SMPS for (a) total dilution ratios of 294, 490 and 1022 by changing the primary dilution ratio and (b) the fraction of charged particles in the size range of 20 – 70 nm with three fuel mixtures. In (b), B293K, B773K, B1073K and B1373K refer to Boltzmann particle-equilibrium charge distribution at the given temperature (in Kelvins). The labels W1 and W1+W2 refer to the Wiedensohler parameterisation for 1 and 2 elemental charges in a particle, respectively. The charging probabilities were then calculated for combustion coal, coal + 6.6% industrial pellets, and coal + 10.5% industrial pellets. These measurements were conducted for flue-gas sample from the superheater area of CHP plant. Modified from **paper I**.

information, along with the primary dilution-ratio tests, to show that the 25 nm particles formed in the boiler and not in the diluter. Figure 4.1b shows that the particles in the boiler had three to four times as much charge as the ones formed at room temperature. The Boltzmann equilibrium charge probability at 800 K is the closest one to the measured charge probability.

Based on a previous study (Nzihou and Stanmore, 2015), the joint-combustion of coal and wood pellets should increase the PM. However, the PM formation was affected by the amount of pellets and the pellet quality in **paper I**. The difference was observed in the particle number concentration with industrial-pellet – coal mixtures (see Figure 4.2). The addition of industrial wood pellet decreased the particle number concentration based on the peak height of the particle number distribution. The results for particle number concentration in the boiler are also listed in Table 3 in **paper I**. The mean particle diameter of the mode was 25 nm for most of the coal – wood pellet mixtures. The coal and 10.5% industrial-pellet mixture was an exception, as this addition caused another mode in the particle number size distribution with a mean diameter of 125 nm. The particles in second mode have higher impact to the volume concentration compared to the particles in first mode (see Figure 4.2b).

The particle number size distribution of coal with the 10.5% addition of industrial pellets was found to be bimodal, whereas the other particle number size distributions were unimodal. The difference in modality could be explained by the fuels' individual properties. Transmission electron microscope (TEM) analyses of the particle samples collected from the boiler were made after the online measurements. The TEM analysis confirmed the bimodality of the particle size distribution (see Figure 4.3). The qualitative EDS analysis for 10-25 nm (Figure 4.3b) particles showed that the particles contained Si, Al, P, Fe, Ca and Ti; moreover, the 120-130 nm (Figure 4.3c) particles contained Si, Al, P, Fe, Ca, Ti and Mg. These chemical compositions supported the elemental composition

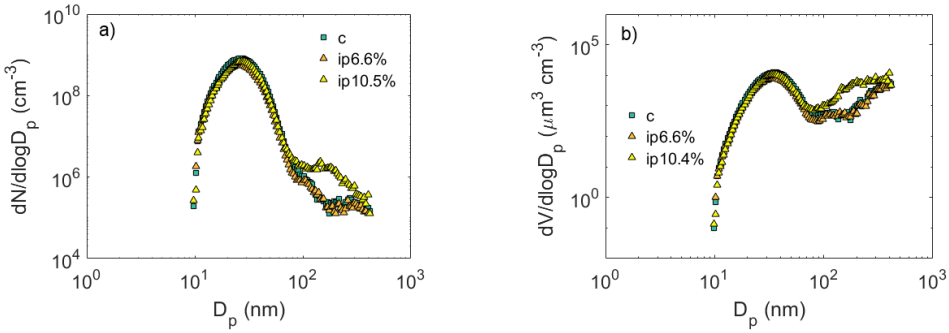

Figure 4.2: (a) The particle number size distribution and (b) the particle volume size distribution (measured with SMPS) from the superheater area aerosols of CHP plant. Coal and mixture of coal and 6.6% of industrial pellets resulted nearly unimodal particle size distribution with a mean diameter of 25 nm. Two particle modes (mean diameters of 25 nm and 125 nm) can be seen in the size distributions with the mixture of coal and 10.5% industrial pellets. Modified from **paper I**.

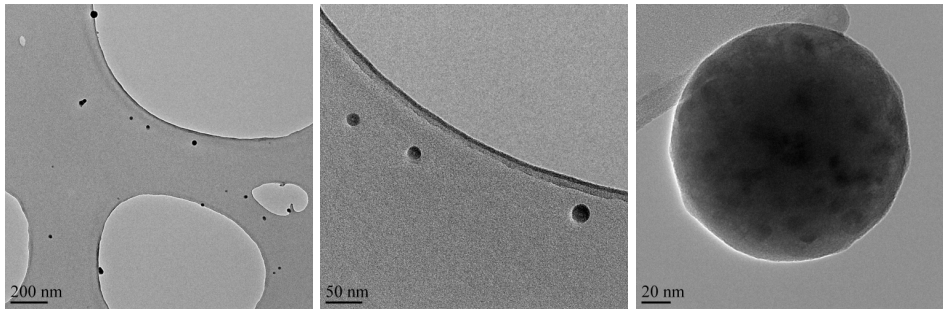

(a) Overview of particles. **(b)** 10-25 nm particles. **(c)** 120-130 nm particles.

Figure 4.3: Particle types observed in the power-plant boiler with coal and 10.5% industrial pellet mixture, collected onto TEM grids during the experiments at CHP plant. Based on the EDS analysis, the particles consisted mainly of inorganic material. Adapted from **paper I**.

that were reported in previous coal-combustion studies (Damle et al., 1981; Flagan and Friedlander, 1978; Linak et al., 2000; McElroy et al., 1982; Ninomiya et al., 2004; Xu et al., 2011). In TEM, the 25 nm particles lost some material under the electron beam. This disappeared material was seen as comprising hollow spherical particles such as red blood cells. The hollowness of the particles could be related to low-vapour-pressure chemical compounds exiting the particle under the electron beam.

The effective density calculations made in **paper I** showed that the effective density of the particles was approximately 2.05 g cm^{-3}. Thus, the calculated effective density was higher than 1.3 g cm^{-3}, which was the previously identified lower limit for mineral particles (Flagan and Friedlander, 1978). This calculated effective density supported the EDS analysis of the particles in the TEM. This EDS analysis showed that the particles consisted mainly of inorganic substances that can be found in minerals.

The absence or undetectable concentrations of K, Na and Cl in particles indicated that the addition of 10.5% wood pellets might not increase the corrosion risk of the boiler, which was in line with the results of studies by Pisa and Lazaroiu (2012) and Montgomery et al. (2008). The lack of alkalis and chloride was explained by the chemical composition of the fuels. The 100% coal version had higher total alkali and chloride concentrations than for the mixture of coal and industrial wood pellets, as the industrial wood pellets had a lower total alkali and chloride concentrations compared with coal. Consequently, pellet substitution lowered the total alkali and chloride concentrations in the boiler. The most important compound to prevent alkali chloride formation has been found to be sulphur (Broström et al., 2007; Montgomery et al., 2008). Sulphur can prevent the formation of alkali chlorides by reacting with the alkalis by forming alkali sulphates by consuming the alkalis from the gas phase. The alkali sulphite compounds form at higher temperatures and are stable after formation. Thus, the alkali sulphate formation could be used to prevent the formation of alkali chlorides. In **paper I**, coal contained higher S concentration than pellets, which decreased the corrosion risk caused by the fuel mixture. However, it is possible that at some point, the alkali chloride formation can become more dominant in the flue gas, such as that reported by Pisa and Lazaroiu (2012).

Particles from the wood pellet – coal mixture combustion were on average more electrically charged than the coal combustion-originated particles. Taking into account that the pellet – coal mixture produced lower nanoparticle concentrations and higher electrical charge on nanoparticles, the pellet – coal combustion could lead a slightly more efficient ESP operation.

4.2 Particle emission of power plants

4.2.1 The combustion of coal and the mixture of coal and industrial wood pellets

The following paragraphs concentrate more on the differences in the particle emissions caused by the co-combustion of industrial pellets and coal. A comparison between the particle number size distributions after the ESP in Figure 4.4 shows that the peak concentration of wood pellet – coal combustion was slightly lower than the peak concentration in the coal combustion. The particle diameter for the coal combustion after the ESP was 80 nm, which was measured with the SMPS. The wood pellet addition in the boiler did not change the mean particle diameter after the ESP. The more efficient performance of the ESP in co-combustion could be due to the higher-charged fraction of particles below 70 nm in diameter or the second particle mode in the particle number size distribution. The particle number size distribution from the wood pellet – coal combustion after the ESP, the FGD and the FF was similar in shape to that after the ESP. The peak concentration was also lower after the FGD and FF than after the ESP. With the coal combustion, the situation was different in terms of the number size distribution shape. The mean diameter was shifted to smaller sizes: less than 60 nm in the SMPS compared to co-combustion.

The chemical composition of the particles was obtained using a TEM and an aethalometer, which measured the absorbed and reflected portion of the light through the particle collection filter paper. The black carbon (BC) concentration for emission factor calculation was obtained from the aethalometer 880 nm wavelength (Drinovec et al., 2015). The black carbon concentration was obtained from the aethalometer signal, which was converted to mass concentration using mass absorption coefficients. The BC concentration was three-times higher for mixture of industrial wood pellet and coal combustion (see **paper**

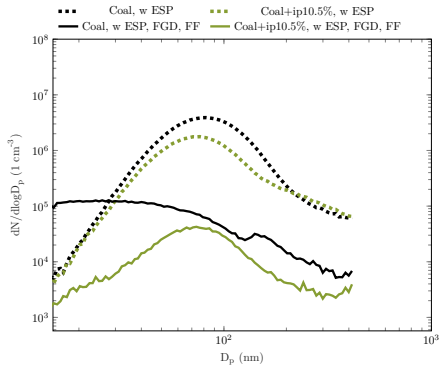

Figure 4.4: The non-volatile particle number size distribution of the flue-gas sampled from stack of the CHP plant. The measurement was made with the SMPS. The studied flue-gas cleaning situations were with the ESP and with the ESP, FGD, FF. The mean particle diameter for the particles measured was approximately 80 nm, except the coal-combustion situation with ESP, FGD, FF. Modified from **papers II and III**.

III) than pure coal combustion (unpublished BC concentrations for coal combustion). The BC concentrations measured after the FGD and the FF were close to zero, which was seen as a high standard deviation in the measurement values. Some error in the results could be obtained from the conversion of absorption signal to a BC mass because the mass absorption coefficients used to convert the signal of the aethalometer to the BC mass should have chosen based on the fuel and combustion method (Olson et al., 2015). Another explaining factor for the BC formation in co-combustion situation could be the increased amount of fuel and the lack of excess oxygen (Wang et al., 2016). However, the co-combustion particles contained more BC (Drinovec et al., 2015), causing a warming effect on the atmosphere. In addition, it was observed that the FGD and FF cancelled the effect of fuel on BC formation in the combustion.

The TEM images of the particles from the co-combustion (in Figure 4.5) showed three types of primary particles in the stack after the ESP: inorganic 25 nm (Figure 4.5b) in diameter (EDS: Si, Al, Ca, P, Fe and Mg), inorganic 400 – 500 nm (Figure 4.5a) in diameter (EDS: Si, Al, Fe, K, Ca, Mg and Ti) and soot (Figure 4.5c) particles. The small inorganic primary particles (Figure 4.3b) had agglomerated with each other and had coagulated with the large primary particles (Figure 4.3c) after leaving the boiler. In addition, the soot particles had formed their own agglomerates, but some small inorganic particles were also found from the soot agglomerates (EDS: C and small amounts of Si, Al, P and Ca).

After the flue-gas cleaning (ESP, FGD and FF), the agglomerated particles disappeared due to the FGD and FF. However, the FGD produced new particles (Figure 4.5d, EDS: Ca, S and small amount of Ti, Si and Mg) that were not observed after the ESP. The chemical composition of particles after the FGD (S and Ca rich particles) supported the previous observations made by Saarnio et al. (2014). According to Saarnio et al. (2014), the FGD plant modified the chemical composition of the particles. After FGD, the particles contained reagents from the desulphurisation process (e.g. $CaSO_4$ and NaCl). Some of the larger primary particles were covered with agglomerates (Figure 4.5e), which consisted of primary particles, were also seen in TEM images after the FGD and FF.

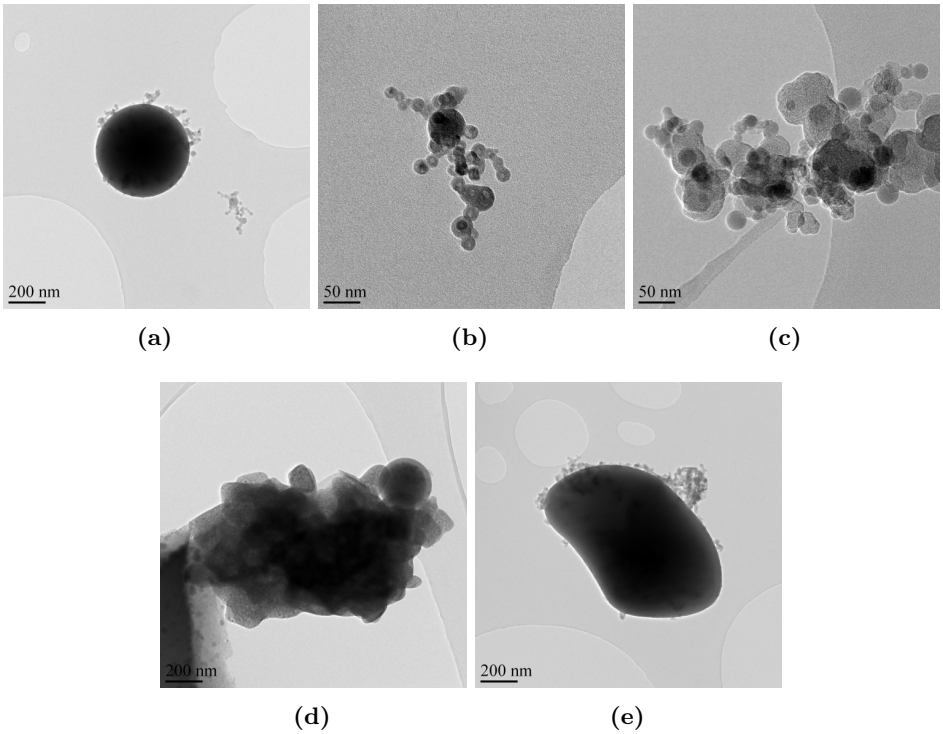

Figure 4.5: TEM images of particles collected from the flue gas on the TEM grids with (upper row) ESP and with ESP, FGD, FF (lower row) in the flue gas of the CHP plant. The flue-gas after ESP contained three types of particles (upper part, a-c). First, particles (a) which were 400 – 500 nm in diameter and spherical in shape. Those particles had collected agglomerates (shown in b) on their surfaces. The chemical composition of the spherical particles was mainly inorganic. Second, particles (b) that have agglomerated to 50 – 300 nm sizes, depending on the fractal dimension. The agglomerate consisted of small spherical particles which contained inorganic compounds based on EDS analysis. Third, another type of agglomerate (c) was over 250 nm in diameter and had a nanostructure of soot. When the flue-gas was cleaned using ESP, FGD and FF, there was two types of particles. First, particles in a size range of 800 – 1 600 nm. These particles were irregular in shape and had a porous surface structure. The particles consisted mainly of Ca^{2+} and $SO_4{}^{2-}$ (measured with EDS). The second type after FGD, FF was the large 800 – 1 200 nm particles, that were irregular in shape and had collected agglomerates on its surface. Adapted from **paper III**.

Co-combustion additionally affects the filtration efficiency of the FGD and FF. In **papers II and III**, the filtration efficiency was evaluated after the flue-gas cleaning, since bypassing them was fairly simple and did not require any changes to measurement set-up. The effect of the FGD and FF on the particle number and mass concentration was remarkable, since the filtration efficiency was 99.9% for the nanoparticle number concentration and 95 – 98% for the PM. The filtration efficiency was not affected drastically by the 10.5% addition of industrial pellets to the coal (see Table 4.1). The FGD and FF also had an effect on the SO_2 concentration in the flue gas. The combination of FGD and FF lowered the SO_2 concentrations by a factor of four (coal + industrial pellet) or five (coal).

Table 4.1: Flue-gas concentrations of CO_2, SO_2, NO_x, O_2, total particle number (N_{tot}), dust, emission factors of PM (EF_{PM}), BC (EF_{BC}) and PN (EF_{PN}), and flue-gas flow rate and temperature measured in the stack. Mean values (+ standard deviation) are presented for both flue-gas cleanings with both fuels. Adapted from **papers II and III**.

	after ESP		after FGD and FF	
	coal	coal+10.5% industrial pellet	coal	coal+10.5% industrial pellet
CO_2 (%)	9.92±2.2	10.6±0.13	10.3±0.96	10.3±0.16
SO_2 (ppbv)	243000±71300	256000±61400	55200±14600	59900±7200
NO_x (ppmv)	252±74	260±8.1	258±65	260±8.1
O_2 (%)	6.16±0.11	5.9±0.2	6.11±0.10	5.9±0.12
N_{tot} (cm^{-3})	$(1.8\pm0.2)\cdot10^6$	$(0.738\pm0.070)\cdot10^6$	420±640	354±623
EF_{PN} (MJ^{-1})	$8.74\cdot10^{12}$	$3.37\cdot10^{11}$	$1.96\cdot10^8$	$1.66\cdot10^8$
Dust (mg/Nm^3)	188±82	110±13	4±1	5±2
EF_{PM} (mg MJ^{-1})	91	50	2	2
EF_{BC} (ng MJ^{-1})	3600	11 740	14	14
Flow (Nm^3/h)	$(4.86\pm0.20)\cdot10^5$	$(4.61\pm0.42)\cdot10^5$	$(4.65\pm0.064)\cdot10^5$	$(4.57\pm0.096)\cdot10^5$
Temperature (°C)	130±13	129±5	78±2	77±7

Power plant emissions can be presented as concentrations or as emission factors. The particle number and mass concentrations are shown in Table 4.1. Table 4.1 also contains the calculated emission factors for particle number (EF_{PN}), mass (EF_{PM}) and black carbon in PM_1 size fraction (EF_{BC}). The emission factors were calculated using CO_2 concentration and the fuel-specific default emission factor for CO_2 (t CO_2 TJ^{-1}). The BC concentration for coal combustion is unpublished data from the same measurement as **papers II and III**. The emission factors were almost the same between the fuel mixtures after the flue-gas cleaning. The EF_{PN} was around 10^8 MJ^{-1}, the EF_{BC} was 14 ng MJ^{-1} and the EF_{PM} was 2 mg MJ^{-1} for both of the fuels after flue-gas cleaning. Without the flue-gas cleaning devices (FGD and FF), the coal combustion situation of the EF_{PN} was $8.74 \cdot 10^{12}$ MJ^{-1} and the EF_{PM} was 91 mg MJ^{-1}, compared to the wood pellet-coal mixture combustion of the EF_{PN} was $3.37 \cdot 10^{11}$ MJ^{-1}, and the EF_{PM} 50 mg MJ^{-1}. The biggest difference was observed between the EF_{BC}, because for the mixture of coal and 10.5% industrial pellet, the EF_{BC} was 11.7 μg MJ^{-1}, and for coal combustion, it was 3.6 μg MJ^{-1} after the ESP.

The emission factors can be used to estimate, for example yearly emissions caused by coal combustion by taking into account the energy produced by coal combustion and the emission factors (in Table 4.1). If only the flue-gas cleaning situation with the ESP was looked at, the global particle number emissions were $2 \cdot 10^{27}$ particles $year^{-1}$, 43 000 kt $year^{-1}$ and 830 t of BC in a year calculated with the emission factors in **paper III**. The yearly particle number emission was close to the yearly particle number emission for power production ($2.5 \cdot 10^{27}$, 2010) estimated by Paasonen et al. (2016) with a different method. Paasonen et al. (2016) also calculated an estimate for yearly particle mass emission for power production (40 000 kt $year^{-1}$, PM2.5), which was at the same order of magnitude as the particle mass emissions from a coal-fired power plant based on the yearly consumption of coal and usage of the ESP in flue-gas cleaning.

Estimation for Finland's coal combustion emissions was made using the coal consumption (66.7 TWh from 2016) and the information about flue-gas cleaning (e.g. all power plants equipped with ESP, FGD and FF). The estimation was made using emission factors for particle number concentration (PN) and PM calculated for coal combustion. The yearly particle mass emissions were 960 t $year^{-1}$ and the particle number emissions $4.7 \cdot 10^{19}$ particles $year^{-1}$. For comparison, the $PM_{2.5}$ emissions from traffic were 6 750 t $year^{-1}$ in 2015 and were 13 151 t $year^{-1}$ for energy production (Ymparisto.fi, 2015). Unfortunately, the data for comparison could not be found from 2016, since the statistics for 2016 will be released in autumn 2018.

4.2.2 Atmosphere-relevant characteristics of oil-combustion particles

The non-volatile and volatile particle number size distribution of oil combustion is shown in Figure 4.6. A large number of particles below 400 nm was observed in the flue gas of an oil-heating plant. The mean particle diameter was around 47 nm for all oil mixtures. The LFO addition to the HFO – water emulsion mixture caused an additional mode of around 120 nm, which was close to the size of soot. The addition of water to the HFO did not change the shape of the particle number size distribution.

The formation of the second mode was observed in the boiler with the lowest sulphur content of the fuel and with the oil mixture that had the lowest sulphur content. The lower sulphur content of the fuel has been found to correlate (Ntziachristos et al., 2016; Sippula et al., 2014) and uncorrelate (Anderson et al., 2015) with soot particles in marine engines designed for HFO combustion. The BC (measured with SP-AMS) explained

6 – 20.3% of the PM_1 of the oil-combustion emissions. For HFO combustion, the BC concentration was 0.986 mg m^{-3}, emulsion addition decreased the BC concentration to 0.864 mg m^{-3} and the LFO addition increased the BC concentration to 3.65 mg m^{-3}. The BC results followed the trend set by the co-combustion and the sulphur content of the fuel.

In Figure 4.6, the particle number size distribution was unimodal with HFO and HFO emulsion with and without the TD. The non-volatile particle number size distribution was measured using a thermodenuder heated up to 265 °C. The non-volatile particle number size distribution peak for the HFO combustion particles was higher than the peak concentration for the non-volatile HFO and water emulsion particles. The water emulsion mixed with the HFO lowered the volatility of the particles compared to the HFO combustion. The difference in the volatility could be due to the higher share of unknown substances (unanalysed mass in Figure 5, **paper IV**) or a slightly higher share of particulate organic matter in the HFO combustion particles (**paper IV**, Figure 5).

The LFO addition to the HFO emulsion increased the share of particulate organic matter and unanalysed mass, as well as the amount of volatile compounds in the particles. The particle concentration in the first mode was increased with the TD, whereas the concentration in the second mode was decreased. This behaviour indicated that the particles have grown by condensation of volatile components from the first mode to the second mode. Because of the TD, the particles in the second mode shrank to sizes that correspond the diameter of the particles in the first mode. Depending on the atmospheric conditions, these volatile components on particle surfaces could either evaporate or oxidise, affecting the particle size and the chemical composition of the particles, and even further, affect their hygroscopicity.

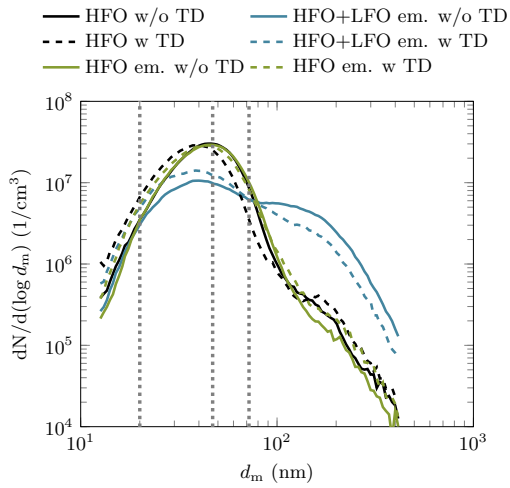

Figure 4.6: A particle number size distribution measured with and without a thermodenuder (TD) from the oil-fired heating plant with three fuels. The fuels were heavy fuel oil (HFO), heavy fuel oil emulsified with water (HFO+ em.) and mixture of heavy fuel oil and light fuel oil emulsified with water (HFO+LFO em.). The vertical lines present the particle sizes selected for the hygroscopicity studies. Adapted from **paper IV**.

A simple method used to estimate the hygroscopicity of the particles was to calculate the

growth factor. The growth factor was calculated by dividing the humidified particle diameter with the dry diameter. The growth factor can also provide information about shape of the particles (e.g. agglomerates). If the particles are agglomerates, the agglomerate structure can collapse when exposed to high humidity (Pagels et al., 2009).

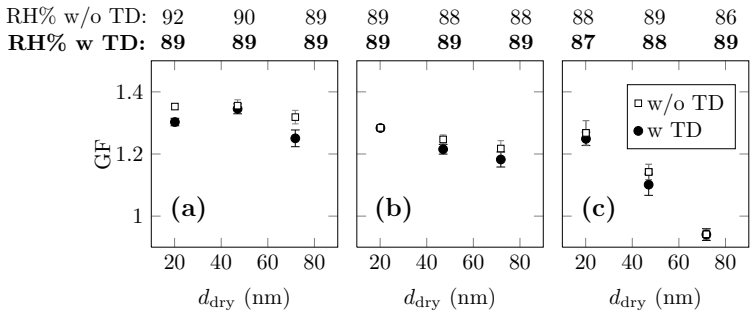

Figure 4.7: The hygroscopic growth factors (GF in the y-axis) of particles from the oil-fired heating plant measured with and without the thermodenuder (TD) when combusting (a) the HFO, (b) the HFO emulsion and (c) the HFO+LFO emulsion. The measurements were made at a relative humidities (RH) indicated in the upper part of the Figure. The d_{dry} diameters, i.e. particle diameters before the humidification, are also marked with grey lines in Fig. 4.6. Adapted from **paper IV**.

Figure 4.7 shows the growth factors for each of the studied oil mixtures and three dry particle diameters (20 nm, 47 nm and 72 nm). The dry particle diameters were also shown in Figure 4.6 with the vertical dashed lines. The GFs were measured for the volatile and non-volatile particles at relative humidity, from 86 – 92%. The HFO combustion produced particles with growth factors of between 1.2 and 1.4. The HFO emulsion combustion particles had growth factors from 1.2 to 1.3 with a decreasing linear trend as a function of increasing dry particle diameter. The HFO, LFO emulsion combustion particles had growth factors from 0.9 to 1.25 with a steep linear decrease as function of dry particle diameter.

The TD was used to remove the volatile components from the particles, which means that the non-volatile particles can still contain inorganic non-volatile species and soot. The difference in the growth factors of volatile particles and non-volatile particles shows the difference in the hygroscopic properties of the volatile species. Here, clear differences were not observed between the growth factors of non-volatile and volatile particles, which can mean that the volatile species in the particles do not increase the hygroscopicity of the particles. However, most of the non-volatile particles grew larger in the humid environment, which means that the inorganic compounds in the particles caused the hygroscopic growth. This is because the 100% soot does not grow under humid conditions (Henning et al., 2012). Soot particles mainly contain carbon, whereas the oil combustion nanoparticles consisted of 10 – 20% of elements, 25 – 50% of ions, 6 – 20.3% of BC and 25 – 35% of unanalysed matter.

The HFO had the highest sulphur content of the fuels. The more blended the oil mixture was, the lower the sulphur content was in the oil mixture. The sulphur content of the fuel was reflected by the sulphate ($SO_4{}^{2-}$) fraction in the nanoparticles. The HFO combustion caused the highest fraction of sulphate for the 20 nm particles in diameter, whereas the other oil mixtures decreased the amount of sulphate in the 20 nm particles. However,

the 47 nm and 72 nm particles from HFO emulsion and HFO+LFO emulsion combustion contained a higher amount of sulphate than the 20 nm particles (**paper IV**, Figure 4). The sulphur concentration of the fuel (the highest with HFO) did not affect the growth factors of particles 20 nm in diameter (see Figure 4.7). Although, the lower of sulphur content of the fuel (HFO emulsion and HFO+LFO emulsion) could have decreased the growth factors of the 47 nm and 72 nm particles. Previous study by Henning et al. (2012) showed that the sulphur content of the coating affects the hygroscopic growth factor. The sulphur dependence of the growth factor was also observed with the oil-blend combustion in marine engines (Kuittinen, 2016).

The 72 nm particles from the HFO and LFO emulsion combustion shrank slightly when exposed to the humidity in the HTDMA. The behaviour indicated an agglomerate or a porous surface structure. The chemical composition of the HFO and LFO emulsion combustion particles was somewhat different than with the other fuels since the ionic mass fraction was the lowest.

4.3 Flue-gas plume in the atmosphere

Background particle number concentrations in the atmosphere can be higher than the flue-gas plume nanoparticle concentrations. The flue-gas nanoparticle concentrations depended on the power plants's flue-gas cleaning (**papers II and III**). In **paper II**, the flue-gas plume from the coal-fired power plant was studied upwind and downwind from the stack. The major difference from the previous studies was analysing the measured data based on the plume age on a second time scale. The time scale was more dense than in Brock et al. (2002), where the in-flight measured data were from discrete plume age intervals from 0 to 13 hours. Plume age in **paper II and III** was calculated based on the distance from the stack (Global positioning system (GPS) coordinates) and wind speed at the flight altitude. The agescale was divided to 5-second intervals, which were used to classify the measurement data. Within each 5-second interval, the median value was calculated from the measurement data of CO_2, SO_2 and ΔN_{tot}. The ΔN_{tot} was calculated using the background concentrations obtained from the upwindside of the stack. The age-based approach was used in **papers II and III**, because Brownian diffusion, coagulation, gas-to-particle conversion and condensation are time dependent (Hinds, 1982) and can take place in the diluting flue-gas plume.

Figure 4.8 shows the dilution profiles as a function of plume age. The concentrations of CO_2 and SO_2 were plotted on the left axis, whereas the ΔN_{tot} was plotted on the right axis. Regarding to the $[CO_2]$ and $[SO_2]$, the dilution profiles have a high peak between 0 and 100 seconds. This peak was caused by the flue gas exiting from the duct. The concentrations observed before the peak mainly represent the background concentrations. The exiting flue-gas flow was turbulent, meaning that some of the flue gas might have diffused to the upwind side of the stack. In **papers II and III**, the dilution started between the fresh and 100-second-old flue-gas plume from the highest concentration value. All of the measured components behaved similarly in the dilution, and they followed the dilution profile defined by the Gaussian dilution model. The atmospheric measurement of the flue gas also showed the same differences in SO_2 and N_{tot} concentrations that were observed in the stack measurement with the FGD and FF; the concentrations were lower compared to the situation without FGD and FF.

In **paper II**, the dilution of CO_2 and SO_2 in the background concentrations was complete in 200 – 300 seconds (0.74 – 1.5 km) after emission (see 4.8a). In addition, the dilution

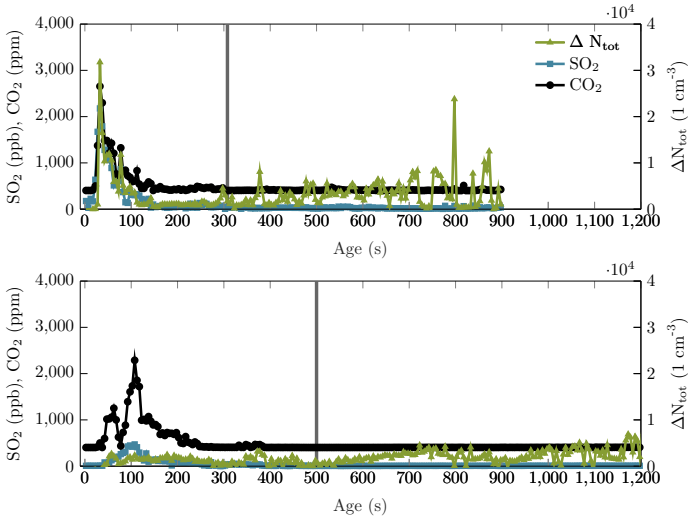

(a)

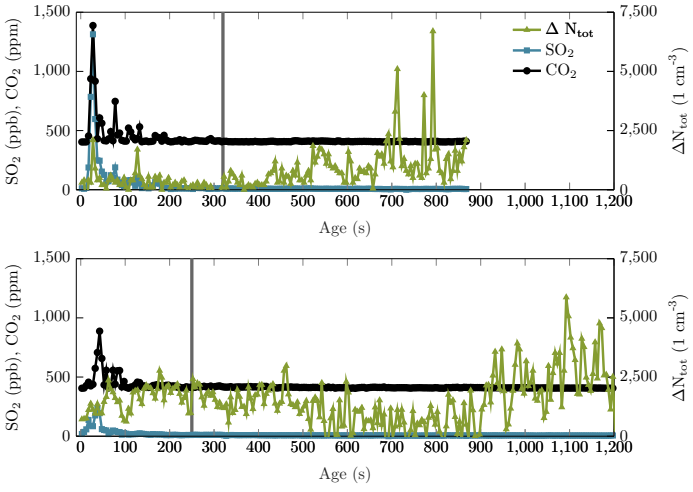

(b)

Figure 4.8: Flue-gas dilution profiles of CO_2, SO_2 and ΔN_{tot} in the plumes of CHP plant in (a) coal-combustion situation and (b) coal and industrial pellets 10.5% combustion situation. The upper panels of (a) and (b) were measured in *FGD+FF off* and the lower panels in *FGD+FF on* situations. The ΔN_{tot} is the difference between the concentrations measured from the plume and the atmospheric background. The concentration values are mean values for 5 second intervals. The measurements were made from the atmosphere with instruments installed in a helicopter. Adapted from **paper II and III**

time scales were similar in **paper III**, corresponding to approximately 2 km from the stack. The peak concentrations for CO_2 were 950 – 2 900 ppm, depending how well the fresh flue-gas plume was caught with the helicopter. The SO_2 peak concentrations varied from 250 ppb to 2 100 ppb, depending on the flue-gas cleaning and the fuel in the flue-gas plume in the atmosphere. After dilution, the concentrations of SO_2 and CO_2 were at the background concentration level and did not provide a trace for the plume. Since the dilution time scale was some hundreds of seconds, the validity of the dilution profile in **paper II** was analysed using the Gaussian plume model. The Gaussian plume model is a solution to an advection – diffusion equation. The equation describes the changes in the flue-gas plume concentrations due to wind advection and turbulent mixing with the surrounding air (Stockie, 2011). The Gaussian plume model describes the dilution in three dimensions. The model uses also the height of the stack, the mean wind speed, the emission rate and the dispersion coefficients as inputs. The dispersion coefficients were calculated using the parameterisation and the atmospheric stability class by Klug (1969). The wind speed and a solar radiative flux at the surface were obtained from measurements (see **paper II** for more details) to calculate the atmospheric stability class. The Gaussian dilution model was used to calculate the dilution profile of the concentration in the plume centre line.

Inputs for the model from the stack measurements were first manipulated with an atmospheric dilution ratio to match the peak concentrations measured close to the stack. After that, the manipulated input concentrations were diluted with the Gaussian plume model and compared to the in-flight results. A comparison was made between the Gaussian plume modelled CO_2 concentration and the measured CO_2 concentration for both of the flue-gas cleaning situations (see **paper II**, Table 2). The comparison showed that the Gaussian plume model explained the flue-gas dilution profile, which was measured from the atmosphere (**paper II**). The Gaussian plume model was also used to calculate the theoretical maximum for SO_2 concentration in the plume centre line based on the SO_2 concentration measured from the flue-gas duct. The theoretical maximum was 131 – 413% higher than the measured SO_2 concentration. The observed difference could be due to the oxidation of SO_2.

The increase in the total particle number concentration was observed when the plume aged in the atmosphere. The increase was observed in three wind/flight directions during two separate days and fuel combinations and in two flue-gas cleaning situations. The measurement results of the total particle number concentration (ΔN_{tot}) in **papers II and III** are shown in Figure 4.8. After the ΔN_{tot} reached zero (200 seconds, 300 seconds, 300 seconds and 600 seconds, in Figure 4.8a upper and lower, b upper and lower, respectively), a moderate increase in the ΔN_{tot} was observed after 400 seconds, 500 seconds, 400 seconds and 800 seconds. In both of the *FGD+FF off* cases, the ΔN_{tot} behaved similarly, the SO_2 concentration was approximately the same however, the N_{tot} in the stack was different. In the *FGD+FF on* cases, the SO_2 and N_{tot} in the stack were same; but the time scales for increasing ΔN_{tot} were different by 500 seconds and 800 seconds. There was no clear relationship between the increasing ΔN_{tot}, and the concentrations of measured components in the flue gas was found to explain the plume behaviour.

The particles in the flue gas were 80 nm in diameter (**paper II** Figure S5 and **paper III** Figure 3) based on the SMPS measurements in the stack. In the industrial pellet – coal mixture combustion, the signal in the Engine exhaust particle sizer (EEPS) was clearly linked to the 80-nm particles in the flue-gas plume diluting in the atmosphere in the *FGD+FF off* case. In the *FGD+FF on* case with industrial pellet – coal mixture

combustion, the signal from the 80-nm particles was weak, although visible. In the coal-combustion situation (**paper II**), the signal in the EEPS from the flue gas-originated particles was not that clear because the background aerosol concentrations or the noise in the electrometers was too high.

In **paper II**, a simple sulphuric acid nucleation model was applied in the diluting plume to see if the nucleation of a sulphuric acid could explain the increase in the total particle number concentration. The model inputs were gained directly from the stack and atmospheric measurement data (**paper II**). The nucleation model assumed that the formation of H_2SO_4 only depended on the measured SO_2 and the calculated OH^- concentration as well as a condensation sink $(CS)^{-1}$ (Kulmala et al., 2006; Stevens and Pierce, 2013; Stevens et al., 2012). The model also assumed that the H_2SO_4 was only lost on the particle surfaces. The total CS was calculated based on the CS calculated from stack measurements in **paper II**. Then, the CS_{stack} was diluted to the background CS with the atmospheric dilution ratio calculated based on the CO_2 in the stack and from the peak concentration of the atmospheric measurements. The background CS was calculated from the SMEAR III station measurement data (Junninen et al., 2009). The concentration of the OH^- was calculated based on the parametrization from Stevens et al. (2012), which included a downward short wave radiative flux at the surface and $[NO_x]$ from the measurements. The NO_x concentration in relation to the parameterisation was calculated based on the atmospheric time-dependent dilution ratio and the NO_x concentration in the stack. A background $[NO_x]$ was assumed to be negligible based on Pirjola et al. (2014). The nucleation rate (J_{nuc}) depended only on the $[H_2SO_4]$ and a coefficient A (Kulmala et al., 2006). Different values of A were tested in a sensitivity analysis. The nucleation rate was further applied to the particle appearance rate (Lehtinen et al., 2007) for particles over 2.5 nm in diameter. The diameter of 2.5 nm was chosen based on the lowest detection limit of CPC3776, which was used in measurements.

Based on the model, the sulphuric acid concentration in the flue-gas plume was at the same level as in the atmosphere: $1-10{\cdot}10^6$ cm^{-3}. The result was in a range that had been previously reported by Mikkonen et al. (2011) and Sarnela et al. (2015) for Finnish non-industrial and industrial areas. The sulphuric acid formation in the atmosphere was limited by the OH^- production and the $[SO_2]$. The OH^- and the SO_2 had opposing trends in their concentrations during the plume dilution. The $[SO_2]$ was decreased in the diluting plume, while $[OH^-]$ production was restrained by $[NO_x]$ in the beginning. The opposing trends caused fairly constant sulphuric acid concentrations after the steepest descent in dilution of SO_2 and NO_x concentrations. The sulphuric acid concentration was too low to produce high appearance rates to explain the particle number concentration measured with the CPC. The sensitivity of the model for A and $[H_2SO_4]$ was tested by taking 10-fold A and varying $[H_2SO_4]$ from 1 to 10-fold. Based on the sensitivity analysis, the $[H_2SO_4]$ should have been 5-fold to 10-fold higher than calculated here, based on the atmospheric measurements. If assuming only the sulphuric acid nucleation, the result indicated that $[OH^-]$ and SO_2 were underestimated or that CS had been overestimated. The underestimation of $[OH^-]$ could be explained with high $[NO_x]$, which had also been the case in Lonsdale et al. (2012, Fig. 1). The underestimation of SO_2 was possible because the measurement values from the atmosphere were 3–4 times lower than the SO_2 would have been based on the atmospheric time-dependent dilution ratio and SO_2 concentration in the stack. In fact, the unknown concentration of SO_3 and low-VOCs were not taken into account in the model. According to an atmospheric study from Kulmala et al. (2013) and an engine exhaust study from Pirjola et al. (2015), the organic compounds have a high impact on the atmospheric nucleation, and these compounds can actually be one major error source in the model.

5 Conclusions

The main objective of this thesis was to characterise the fine particles of a power plant, from the boiler to the atmosphere. The characterisation was made with two solid fuels, coal and a mixture of coal and industrial pellets, and with three oil-mixtures. Figure 5.1 summarises the effect of the fuel on the particles of the studied power plants, from the boiler into the atmosphere. In the coal-combustion tests, the primary dilution ratio was varied to study the location of particle formation. The primary dilution ratio tests showed that the particles were formed in the power plant boiler and not in the dilution probe. The coal combustion produced a unimodal particle size distribution with a count median diameter of 25 nm, whereas 10.5% of the industrial pellet – coal mixture combustion produced a bimodal particle number size distribution. The first mode corresponded to the mode that originated from the coal combustion and the second mode was linked with the industrial pellet addition. The count median diameter of the second mode was 125 nm. In addition to the changes in the shape of particle number size distribution, the 10.5% industrial pellet addition increased the electrical charge of the particles in the boiler. The TEM images showed that the particles were mainly spherical and consisted of inorganic matter.

The power plant flue gases were cleaned with the ESP, FGD and FFs. The ESPs removed over 99% of the particle number concentration. The particle number size distribution after the ESPs was unimodal with a count median diameter of 70 – 80 nm. The black carbon concentration after the ESP was higher with the 10.5% industrial pellet – coal mixture compared to the coal combustion. The FGD and FFs cleaned the flue gas from particles with over 99% efficiency when calculated from the particle number concentration. The particle number size distribution was unimodal after the FGD and FFs with a count median diameter of 30 – 72 nm. The TEM images of particle samples revealed that the primary particles formed agglomerate structures before the sampling location. The desulphurisation and FFs affected not only the particle number concentration but the black carbon and SO_2 concentrations. Actually, the black carbon concentrations were very low after the last flue-gas cleaning devices were used.

The particle number concentrations in the urban background and in the city centre were taken for comparison against the power plant emissions (Figure 5.1). The particle number concentrations of the studied power plant were lower than the urban background particle number concentrations, and the result showed that this particular power plant does not worsen the air quality in Helsinki in terms of the particle number concentration. On the contrary, the flue gas from the power plant could dilute the particle number concentration. The other emission components, such as gases, however, can influence the air quality.

The flue-gas behaviour in the atmosphere was studied with measurement instruments installed in a helicopter. The measurement showed that it was possible to distinguish

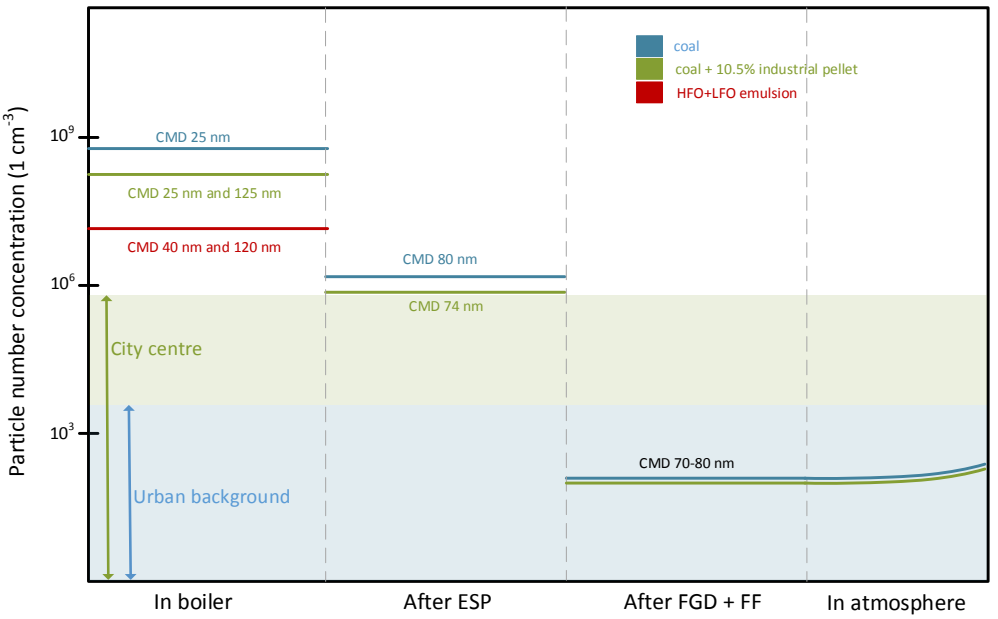

Figure 5.1: Overview of results regarding particle number concentrations (y-axis), particle mean diameters and their changes from boiler to atmosphere (x-axis). The results are presented for coal combustion in the CHP plant (blue), for the combustion of coal+10.5% industrial pellets in CHP plant (green) and for combustion of HFO+LFO emulsion (red) in a peak-load heating plant. For the latter two, a bimodal particle number size distribution is indicated by two different values for count mean diameter (CMD). Particle number concentrations of the power plant are compared to the urban background concentration (Pirjola et al., 2012) and city centre concentration (Lähde et al., 2014). Results from **papers I, II, III and IV**.

both of the flue-gas cleaning situations using measurements taken close to the stack. The atmospheric measurements were made upwind and downwind of the diluting flue-gas plume. The flue gas then diluted to the atmospheric concentrations some hundreds of seconds, after which the particle number concentration started to slowly increase. This increase in the particle number concentration was interpreted as new particle formation in the atmosphere. The increase was observed during two days, with three wind directions and with four flue-gas compositions.

The particle number size distribution from the HFO and HFO emulsion combustion was unimodal with a count median diameter of 47 nm. The addition of the LFO to the HFO emulsion caused the formation of a second mode to the particle number size distribution. The count median diameter of the second mode was around 100 nm. The particles from the oil-mixture combustion were treated with the TD to remove volatile components from the particle surfaces. The fine particles that originated from the oil-mixture combustion were not highly volatile only the second mode from the combustion of HFO mixed with LFO emulsion had some volatile components coating the particles. The hygroscopicity of the volatile and non-volatile particles from oil-mixture combustion was studied based on the hygroscopic growth factor. The growth factors altered from 0.9 to almost 1.4. The smallest studied dry particles (20 nm in diameter) had the highest growth factors, and

the larger the dry diameter was, the smaller the growth factor. Growth factor plotted as a function of particle diameter had a decreasing linear trend, and the slope of the graph got steeper when the fuel sulphur concentration was decreased. The oil-combustion particles had the potential to grow larger in the atmosphere at relative humidity over 85%.

Power plants' fuel choices have an effect on the particle formation in oil-fired and coal-fired combustion (**papers I and IV**). The combustion process could be optimised for the fuel based on the CO and O_2 concentrations and the temperatures in the boiler. Still, the optimised combustion does not guarantee the lowest particle number or mass concentrations. Here, the better-quality fuels (industrial pellet and LFO) decreased particle number concentrations in the boilers. On the other hand, the portion of 10.5% industrial pellet mixed with coal caused a second particle mode in the particle number size distribution. The second particle mode was within the size range of soot. Soot mode was also produced by the LFO addition in the oil-fired power plant, similarly to the industrial pellet addition in the coal-fired power plant. The LFO addition and the industrial pellet addition decreased the fuel sulphur and heavy metal concentrations. Previous studies have been reported that heavy metals could catalyse the combustion in engines (Anderson et al., 2015; Moldanová et al., 2013). Also, lower sulphur content in fuel has been found to correlate (Ntziachristos et al., 2016; Sippula et al., 2014) and uncorrelate (Anderson et al., 2015) with soot particles in marine engines designed for HFO combustion. The marine engine tests have shown that the fuel sulphur content affected the sulphate fraction in the particles (Lehtoranta et al., 2015). These results indicated that the fuel composition also drastically affected the emissions.

The effects of combustion originated particles on the atmosphere depended on the flue-gas cleaning technologies (**papers II and III**). Based on Table 5.1, the flue-gas cleaning could have affected the particle and gaseous emissions multiple ways. To make truthful conclusions about "generic" power plant emissions (high or low polluting), the emission source and the flue-gas cleaning devices inside the stack must be identified before publishing the results. Many different conclusions of particle formation could be made by assuming the emission-controlling techniques installed at the studied power plant. In addition, there is a small probability that substituting coal with wood pellets could be a trade-off between sulphate aerosol and BC (**paper III**). Fortunately, the trade-off can be controlled by applying flue-gas cleaning technologies. The ESP alone is not enough to remove the BC from wood pellet-combustion emissions; therefore, more versitile flue-gas cleaning might be needed.

Despite the flue-gas cleaning devices, new particle formation was observed in the flue-gas plume (**papers II and III**). The new particle formation was observed within two separate days and three wind directions and four precursor gas and condensation sink concentrations. The precursor gases and CS concentrations were defined by flue-gas cleaning. However, the fuel mixtures might have had an effect on the precursor gas concentrations (e.g. organics). High NO_x concentrations could hinder the OH^- formation in the atmosphere and slow the oxidation processes that can produce particle forming compounds. The new trend in power plants is to lower the NO_x concentrations. The NO_x reductions can change the oxidation process of VOC and the oxidant formation cycle, meaning that the particle formation potential can change.

Table 5.1: The most relevant emission-controlling techniques, discussed in this thesis applied in coal-fired power plants and the side effects of certain techniques for gaseous and particle emissions. The target implies the main purpose of the technique, and if the techniques has side effect they are shown in the table. The results from **papers I-III** are expressed in **bold**. The calculated decrease is marked with *. With the PN, the decrease can also mean that the PN fraction survives through the technique and appears to increase. The cleaning techniques have been organised by the installation order, and one technology (between each line) can be chosen by the power plant (except FF can not be used after wet-FGD).

flue-gas cleaning technique	target	side effect
wood pellets	SO_2, CO_2*, NO_x	decrease in **PM**;[1] **PN**; increase in BC
low-NO_x burners	NO_x	increase in BC and PM
SNCR[2]	NO_x	increase in NH_3
SCR[3]	NO_x	increase in NH_3 and SO_3 [4]
ESP	**PM, PN** [5]	
wFGD[6]	SO_2	increase in PM [7]and PN[7]
FGD	**SO_2**	decrease in **PM**[8]; increase in PN
FF	PM	decrease in **PN and SO_2**

[1] Increase in Nzihou and Stanmore (2015)
[2] Selective non-catalytic reduction
[3] Selective catalytic reduction
[4] Srivastava et al. (2004)
[5] Ylätalo and Hautanen (1998)
[6] Wet-FGD
[7] Ma et al. (2016)
[8] Córdoba et al. (2012)

5.1 Future outcomes

Future research questions could be related to potential aerosol mass produced from the emissions of a power plant or related to the volatility and hygroscopicity of the potential aerosol mass. These should be further studied to fully understand the atmospheric effets of the particles in terms of climate change and air quality. At the same time, it would be beneficial to study the gaseous precursors in more detail in the diluting flue-gas plume. The precursor gases seem to have a high impact on the particle number concentration in quite early stages in the atmosphere. A chemical-ionization atmospheric-pressure inlet time-of-flight mass spectrometer could be used to measure SO_3^-, H_2SO_4 and organics, but applicability, to atmospheric measurements to understand the cluster chemistry would be challenging. A simpler approach would be to use a Particle Size Magnifier and CPC to measure the particles below 3 nm in the flue-gas plume.

New particle formation in the flue gas clearly increased the particle concentrations in the atmosphere. These newly formed particles can grow larger due to coagulation, agglomeration and condensation. Larger particles can then further act as a cloud condensation nuclei. There is no information about the potential of a newly formed particles for cloud condensation nuclei activation.

Real-scale emission studies are still needed to understand what consequences real emissions have on particle formation and flue-gas cleaning devices. There is a lot of information on

the small-scale testing of different fuels. The results of gaseous emission measurements can be scaled to real-world applications. In comparison, no one knows if the particle concentrations measured in small-scale tests can be transferred to a real scale, because the aerosol processes depend on the gas phase composition, as well as the particle concentration and size. This scalability of particle emissions from laboratory to reality is one problem to solve using real-scale emission studies companied with small-scale studies.

A SNCR-system has been installed in Hanasaari because of the tightened NO_x emission limits (Ministry of the Environment, 2016). Nevertheless, the power plant has decided to shut down in 2024. However, on a global scale, coal will be still combusted, even though, coal combustion will end in Finland. I hope the results presented in the thesis will help people elsewhere to make decisions related to controlling power plant emissions. In addition, the fuel change can lower CO_2 emissions, but the change will not guarantee lower particle number emissions, and the fuel change can override the observed cooling radiative effect of particles (Frey et al., 2014).

Bibliography

BP Statistical Review of World Energy 2017, 1 St James's Square, London, SW1Y 4PD, 2017, registered in England and Wales, number 102498.

Abdul-Khalek, I., Kittelson, D., and Brear, F., "The influence of dilution conditions on diesel exhaust particle size distribution measurements," *SAE Technical Paper*, no. 1999-01-1142, 1999.

Aho, M., Gil, A., Taipale, R., Vainikka, P., and Vesala, H., "A pilot-scale fireside deposit study of co-firing cynara with two coals in a fluidised bed," *Fuel*, vol. 87, no. 1, pp. 58 – 69, 2008.

Alanen, J., Saukko, E., Lehtoranta, K., Murtonen, T., Timonen, H., Hillamo, R., Karjalainen, P., Kuuluvainen, H., Harra, J., Keskinen, J., and Rönkkö, T., "The formation and physical properties of the particle emissions from a natural gas engine," *Fuel*, vol. 162, pp. 155 – 161, 2015. [Online]. Available: http://dx.doi.org/10.1016/j.fuel.2015.09.003

Anderson, M., Salo, K., Hallquist, A. M., and Fridell, E., "Characterization of particles from a marine engine operating at low loads," *Atmospheric Environment*, vol. 101, pp. 65 – 71, 2015.

Boucher, O., Randall, D., Artaxo, P., Bretherton, C., Feingold, G., Forster, P., Kerminen, V.-M., Kondo, Y., Liao, H., Lohmann, U., Rasch, P., Satheesh, S., Sherwood, S., Stevens, B., and Zhang, X., *Clouds and Aerosols*. Cambridge, United Kingdom and New York, NY, USA: Cambridge University Press, 2013, book section 7, pp. 571 – 658. [Online]. Available: www.climatechange2013.org

Brock, C., Washenfelder, R., Trainer, M., Ryerson, T., Wilson, J., Reeves, J., Huey, L., Holloway, J., Parrish, D., Hübler, G., and Fehsenfeld, F., "Particle growth in the plumes of coal-fired power plants," *Journal of Geophysical Research D: Atmospheres*, vol. 107, no. 12, pp. AAC 9 – 1 – AAC 9 – 14, 2002.

Brock, C. A., Trainer, M., Ryerson, T. B., Neuman, J. A., Parrish, D. D., Holloway, J. S., Nicks, D. K., Frost, G. J., Hübler, G., Fehsenfeld, F. C., Wilson, J. C., Reeves, J. M., Lafleur, B. G., Hilbert, H., Atlas, E. L., Donnelly, S. G., Schauffler, S. M., Stroud, V. R., and Wiedinmyer, C., "Particle growth in urban and industrial plumes in Texas," *Journal of Geophysical Research: Atmospheres*, vol. 108, no. D3, pp. n/a – n/a, 2003. [Online]. Available: http://doi.wiley.com/10.1029/2002JD002746

Broström, M., Kassman, H., Helgesson, A., Berg, M., Andersson, C., Backman, R., and Nordin, A., "Sulfation of corrosive alkali chlorides by ammonium sulfate in a biomass fired CFB boiler," *Fuel Processing Technology*, vol. 88, no. 11-12, pp. 1171 – 1177, 2007.

Burtscher, H., Reis, A., and Schmidt-Ott, A., "Particle charge in combustion aerosols," *Journal of Aerosol Science*, vol. 17, no. 1, pp. 47–51, 1986.

Córdoba, P., Font, O., Izquierdo, M., Querol, X., Leiva, C., López-Antón, M. A., Díaz-Somoano, M., Ochoa-González, R., Rosa Martinez-Tarazona, M., and Gómez, P., "The retention capacity for trace elements by the flue gas desulphurisation system under operational conditions of a co-combustion power plant," *Fuel*, vol. 102, pp. 773–788, 2012. [Online]. Available: http://www.sciencedirect.com/science/article/pii/S0016236112004796

Damle, A. S., Ensor, D. S., and Ranade, M. B., "Coal Combustion Aerosol Formation Mechanisms: A Review," *Aerosol Science and Technology*, vol. 1, no. 1, pp. 119–133, 1981. [Online]. Available: http://dx.doi.org/10.1080/02786828208958582

Davidsson, K. O., Åmand, L. E., Leckner, B., Kovacevik, B., Svane, M., Hagström, M., Pettersson, J. B. C., Petterson, J., Asteman, H., Svensson, J. E., and Johansson, L. G., "Potassium, chlorine, and sulfur in ash, particles, deposits, and corrosion during wood combustion in a circulating fluidized-bed boiler," *Energy and Fuels*, vol. 21, no. 1, pp. 71–81, 2007.

Dittenhoefer, A. C. and De Pena, R. G., "A study of production and growth of sulfate particles in plumes from a coal-fired power plant," *Atmospheric Environment*, vol. 12, pp. 297–306, 1978.

Drinovec, L., Mocnik, G., Zotter, P., Prevot, A., Ruckstuhl, C., Coz, E., Rupakheti, M., Sciare, J., Müller, T., Wiedensohler, A., and Hansen, A. A., "The "dual-spot " Aethalometer : an improved measurement of aerosol black carbon with real-time loading compensation," *Atmospheric Measurement Techniques*, vol. 8, pp. 1965–1979, 2015.

Flagan, R. and Friedlander, S. K., "Particle formation in pulverized coal combustion-a review," in *Recent developments in aerosol science*, Shawn, D. T., Ed. Michigan: Wiley, 1978, ch. 2, pp. 25–59.

Frey, A., Saarnio, K., Lamberg, H., Mylläri, F., Karjalainen, P., Teinilä, K., Carbone, S., Tissari, J., Niemelä, V., Häyrinen, A., Rautiainen, J., Kytömäki, J., Artaxo, P., Virkkula, A., Pirjola, L., Rönkkö, T., Keskinen, J., Jokiniemi, J., and Hillamo, R., "Optical and chemical characterization of aerosols emitted from coal, heavy and light fuel oil, and small-scale wood combustion," *Environmental Science and Technology*, vol. 48, no. 1, 2014.

Giechaskiel, B., Ntziachristos, L., and Samaras, Z., "Calibration and modelling of ejector dilutors for automotive exhaust sampling," *Measurement Science and Technology*, vol. 15, no. 11, pp. 2199–2206, 2004.

Happonen, M., Heikkilä, J., Aakko-Saksa, P., Murtonen, T., Lehto, K., Rostedt, A., Sarjovaara, T., Larmi, M., Keskinen, J., and Virtanen, A., "Diesel exhaust emissions and particle hygroscopicity with HVO fuel-oxygenate blend," *Fuel*, vol. 103, pp. 380–386, 2013.

Heikkilä, J., Rönkkö, T., Lähde, T., Lemmetty, M., Arffman, A., Virtanen, A., Keskinen, J., Pirjola, L., and Rothe, D., "Effect of Open Channel Filter on Particle Emissions of Modern Diesel Engine," *Journal of the Air & Waste Management Association*, vol. 59:10, pp. 1148–1154, 2009.

Helble, J. J., "Model for the air emissions of trace metallic elements from coal combustors equipped with electrostatic precipitators," *Fuel processing technology*, vol. 63, no. 2, pp. 125–147, 2000.

Henning, S., Ziese, M., Kiselev, A., Saathoff, H., Möhler, O., Mentel, T. F., Buchholz, A., Spindler, C., Michaud, V., Monier, M., Sellegri, K., and Stratmann, F., "Hygroscopic growth and droplet activation of soot particles: Uncoated, succinic or sulfuric acid coated," *Atmospheric Chemistry and Physics*, vol. 12, no. 10, pp. 4525–4537, 2012.

Hinds, W., *Aerosol Technology*. John Wiley & Sons, 1982.

IPCC, *Summary for Policymakers*. Cambridge, United Kingdom and New York, NY, USA: Cambridge University Press, 2013, book section SPM, pp. 1–30. [Online]. Available: www.climatechange2013.org

Jamil, R., Ming, L., Jamil, I., and Jamil, R., "Application and development trend of flue gas desulfurization (FGD) process: A review," *International Journal of Innovation and Applied Studies*, vol. 3, no. 4, pp. 286–297, 2013.

Jiménez, S. and Ballester, J., "A Comparative Study of Different Methods for the Sampling of High Temperature Combustion Aerosols," *Aerosol Science and Technology*, vol. 39, no. 9, pp. 811–821, 2005.

Johnson, T., Caldow, R., Pöcher, A., Mirme, A., and Kittelson, D., "A new electrical mobility particle sizer spectrometer for engine exhaust particle measurements," in *SAE Technical Paper*. SAE International, 03 2004. [Online]. Available: https://doi.org/10.4271/2004-01-1341

Joutsensaari, J., Kauppinen, E. I., Ahonen, P., Lind, T. M., Ylätalo, S. I., Jokiniemi, J. K., Hautanen, J., and Kilpeläinen, M., "Aerosol formation in real scale pulverized coal combustion," *Journal of Aerosol Science*, vol. 23, pp. S241–S244, 1992.

Junkermann, W., Hagemann, R., and Vogel, B., "Nucleation in the Karlsruhe plume during the COPS/TRACKS-Lagrange experiment," *Quarterly Journal of the Royal Meteorological Society*, vol. 137, no. SUPPL. 1, pp. 267–274, 2011.

Junkermann, W., Vogel, B., and Sutton, M. A., "The climate penalty for clean fossil fuel combustion," *Atmospheric Chemistry and Physics*, vol. 11, no. 24, pp. 12 917–12 924, 2011.

Junninen, H., Lauri, A., Keronen, P., Aalto, P., Hiltunen, V., Hari, P., and Kulmala, M., "Smart-SMEAR: On-line data exploration and visualization tool for SMEAR stations," *Boreal Environment Research*, vol. 14, no. 4, pp. 447–457, 2009.

Kauppinen, E. I. and Pakkanen, T. A., "Coal Combustion Aerosol: A field study," *Environmental Science & Technology*, vol. 24, no. 12, pp. 1811–1818, 1994.

Keil, A., Wendisch, M., and Heintzenberg, J., "A case study on microphysical and radiative properties of power-plant-originated clouds," *Atmospheric Research*, vol. 63, pp. 291–301, 2002.

Keskinen, J., Pietarinen, V., and Lehtimäki, M., "Electrical Low Pressure Impactor," *Journal of Aerosol Science*, vol. 23, no. 4, pp. 353–360, 1992.

Klug, W., "A method for determining diffusion conditions from synoptic observations," *Staub-Reinhalt Luft*, vol. 29, pp. 14–20, 1969.

Korpela, T., Majanne, Y., Salminen, O., Laari, A., and Björkqvist, T., "Monitoring of spraying in semi-dry desulfurization processes in coal fired power plants," *IFAC-PapersOnLine*, vol. 48, no. 30, pp. 403–408, 2015. [Online]. Available: http://linkinghub.elsevier.com/retrieve/pii/S2405896315030542

Kuittinen, N., "Polttoaineen vaikutus laivamoottorin pienhiukkaspäästön fysikaalisiin ja kemiallisiin ominaisuuksiin," Master's thesis, Tampere University of Technology, 2016.

Kulmala, M., Lehtinen, K. E. J., and Laaksonen, A., "Cluster activation theory as an explanation of the linear dependence between formation rate of 3 nm particles and sulphuric acid concentration," *Atmospheric Chemistry and Physics*, vol. 6, no. 3, pp. 787–793, 2006. [Online]. Available: http://www.atmos-chem-phys.net/6/787/2006/

Kulmala, M., Kontkanen, J., Junninen, H., Lehtipalo, K., Manninen, H. E., Nieminen, T., Petäjä, T., Sipilä, M., Schobesberger, S., Rantala, P., Franchin, A., Jokinen, T., Järvinen, E., Äijälä, M., Kangasluoma, J., Hakala, J., Aalto, P. P., Paasonen, P., Mikkilä, J., Vanhanen, J., Aalto, J., Hakola, H., Makkonen, U., Ruuskanen, T., Mauldin, R. L., Duplissy, J., Vehkamäki, H., Bäck, J., Kortelainen, A., Riipinen, I., Kurtén, T., Johnston, M. V., Smith, J. N., Ehn, M., Mentel, T. F., Lehtinen, K. E. J., Laaksonen, A., Kerminen, V.-M., and Worsnop, D. R., "Direct Observations of Atmospheric Aerosol Nucleation," *Science*, vol. 339, no. 6122, pp. 943 LP – 946, Feb 2013. [Online]. Available: http://science.sciencemag.org/content/339/6122/943.abstract

Kuuluvainen, H., Karjalainen, P., Bajamundi, C. J. E., Maunula, J., Vainikka, P., Roppo, J., Keskinen, J., and Rönkkö, T., "Physical properties of aerosol particles measured from a bubbling fluidized bed boiler," *Fuel*, vol. 139, pp. 144–153, 2015. [Online]. Available: http://dx.doi.org/10.1016/j.fuel.2014.08.048

Lähde, T., Rönkkö, T., Virtanen, A., Schuck, T., Pirjola, L., Hämeri, K., Kulmala, M., Arnold, F., Rothe, D., and Keskinen, J., "Heavy duty diesel engine exhaust aerosol particle and ion measurements," *Environmental Science and Technology*, vol. 43, pp. 163–168, 2009.

Lähde, T., Niemi, J. V., Kousa, A., Rönkkö, T., Karjalainen, P., Keskinen, J., Frey, A., Hillamo, R., and Pirjola, L., "Mobile particle and NOx emission characterization at Helsinki Downtown: Comparison of different traffic flow areas," *Aerosol and Air Quality Research*, vol. 14, no. 5, pp. 1372–1382, 2014.

Lazaridis, M., Isukapalli, S. S., and Georgopoulos, P. G., "Modelling of aerosol processes in plumes," *Tellus, Series B: Chemical and Physical Meteorology*, vol. 53, no. 1, pp. 83–93, 2001.

Lehtinen, K. E. J., Dal Maso, M., Kulmala, M., and Kerminen, V. M., "Estimating nucleation rates from apparent particle formation rates and vice versa: Revised formulation of the Kerminen-Kulmala equation," *Journal of Aerosol Science*, vol. 38, no. 9, pp. 988–994, 2007.

Lehtoranta, K., Vesala, H., Koponen, P., and Korhonen, S., "Selective catalytic reduction operation with heavy fuel oil: NO_x, NH_3, and particle emissions," *Environmental Science & Technology*, vol. 49, no. 7, pp. 4735–4741, 2015.

Liebsch, E. and De Pena, R. G., "Sulfate aerosol production in coal-fired power plant plumes," *Atmospheric Environment (1967)*, vol. 16, no. 6, pp. 1323–1331, 1982.

Likens, G. E. and Bormann, F., "Acid rain: a serious regional environmental problem," *Science*, vol. 184, pp. 1176–1179, 1974.

Linak, W. P., Miller, C. a., and Wendt, J. O., "Comparison of particle size distributions and elemental partitioning from the combustion of pulverized coal and residual fuel oil." *Journal of the Air & Waste Management Association (1995)*, vol. 50, no. June 2015, pp. 1532–1544, 2000.

Liu, B. and Pui, D. Y., "On the performance of the electrical aerosol analyzer," *Journal of Aerosol Science*, vol. 6, pp. 249–264, 1975.

Lonsdale, C. R., Stevens, R. G., Brock, C. A., Makar, P. A., Knipping, E. M., and Pierce, J. R., "The effect of coal-fired power-plant SO_2 and NO_x control technologies on aerosol nucleation in the source plumes," *Atmospheric Chemistry and Physics*, vol. 12, no. 23, pp. 11 519–11 531, 2012.

Lyyränen, J., Jokiniemi, J., Kauppinen, E. I., Backman, U., and Vesala, H., "Comparison of Different Dilution Methods for Measuring Diesel Particle Emissions," *Aerosol Science and Technology*, vol. 38, no. 1, pp. 12–23, 2004. [Online]. Available: http://www.informaworld.com/10.1080/02786820490247579

Ma, Z., Li, Z., Jiang, J., Deng, J., Zhao, Y., Wang, S., and Duan, L., "PM2.5 Emission Reduction by Technical Improvement in a Typical Coal-Fired Power Plant in China," *Aerosol and Air Quality Research*, pp. 636–643, 2016. [Online]. Available: http://www.aaqr.org/Doi.php?id=AAQR-16-05-2015AAC-0200{_}proof

Maricq, M. M., "On the electrical charge of motor vehicle exhaust particles," *Journal of Aerosol Science*, vol. 37, no. 7, pp. 858–874, 2006.

Marjamäki, M., Ntziachristos, L., Virtanen, A., Ristimäki, J., Keskinen, J., Moisio, M., Palonen, M., and Lappi, M., "Electrical filter stage for the ELPI," *SAE 2002 World Congress*, vol. 2002-01-00, no. 724, 2002.

McElroy, M. W., Carr, R. C., Ensor, D. S., and Markowski, G. R., "Size distribution of fine particles from coal combustion," *Science*, vol. 215, no. 4528, pp. 13–18, 1982.

Meagher, J., Stockburger, L., Bonanno, R., Bailey, E., and Luria, M., "Atmospheric oxidation of flue gases from coal-fired power plants–A comparison between conventional and scrubbed plumes," *Atmospheric Environment (1967)*, vol. 15, no. 5, pp. 749–762, jan 1981. [Online]. Available: https://www.sciencedirect.com/science/article/pii/0004698181902791

Mikkanen, P. and Moisio, M., "Sampling Method for Particle Measurements of Vehicle Exhaust," *SAE Publication series*, no. 724, pp. 1–6, 2001.

Mikkonen, S., Romakkaniemi, S., Smith, J. N., Korhonen, H., Petäjä, T., Plass-Duelmer, C., Boy, M., McMurry, P. H., Lehtinen, K. E. J., Joutsensaari, J., Hamed, A., Mauldin, R. L., Birmili, W., Spindler, G., Arnold, F., Kulmala, M., and Laaksonen, A., "A statistical proxy for sulphuric acid concentration," *Atmospheric Chemistry and Physics*, vol. 11, no. 21, pp. 11 319–11 334, 2011.

Ministry of the Environment, "Valtioneuvoston asetus suurten polttolaitosten päästöjen rajoittamisesta no 936/2014," 2014, http://www.finlex.fi/fi/laki/smur/2014/20140936.

– – –, "Liite 6: Laitosten alustavatpäästöjen vähennystoimet (pdf)," 2016, http://www.ym.fi/fi-FI/Ymparisto/Lainsaadanto_ja_ohjeet/Ilmansuojelulainsaadanto.

Mirme, A., "Electric aerosol spectrometry," Ph. D. Thesis, Tartu University, 1994.

Moldanová, J., Fridell, E., Winnes, H., Holmin-Fridell, S., Boman, J., Jedynska, A., Tishkova, V., Demirdjian, B., Joulie, S., Bladt, H., Ivleva, N. P., and Niessner, R., "Physical and chemical characterisation of PM emissions from two ships operating in European Emission Control Areas," *Atmospheric Measurement Techniques*, vol. 6, no. 12, pp. 3577–3596, 2013. [Online]. Available: http://www.atmos-meas-tech.net/6/3577/2013/

Montgomery, M., Vilhelmsen, T., and Jensen, S. A., "Potential high temperature corrosion problems due to co-firing of biomass and fossil fuels," *Materials and Corrosion*, vol. 59, no. 10, pp. 783–793, 2008.

Nielsen, M. T., Livbjerg, H., Fogh, C. L., Jensen, J. N., Simonsen, P., Lund, C., Poulsen, K., and Sander, B., "Formation and emission of fine particles from two coal-fired power plants," *Combustion Science and Technology*, vol. 174, no. 2, pp. 79–113, 2002. [Online]. Available: http://www.tandfonline.com/doi/abs/10.1080/714922606

Ninomiya, Y., Zhang, L., Sato, A., and Dong, Z., "Influence of coal particle size on particulate matter emission and its chemical species produced during coal combustion," *Fuel Processing Technology*, vol. 85, no. 8-10, pp. 1065–1088, 2004.

Ntziachristos, L., Saukko, E., Lehtoranta, K., Rönkkö, T., Timonen, H., Simonen, P., Karjalainen, P., and Keskinen, J., "Particle emissions characterization from a medium-speed marine diesel engine with two fuels at different sampling conditions," *Fuel*, vol. 186, pp. 456 – 465, 2016.

Nzihou, A. and Stanmore, B. R., "The Formation of Aerosols During the Co-combustion of Coal and Biomass," *Waste and Biomass Valorization*, vol. 6, no. 6, pp. 947–957, 2015.

Ochi, K., "Latest Low-NO_x Combustion Technology for Pulverized-coal-fired Boilers," vol. 58, no. 5, pp. 187–193, 2009.

Olson, M. R., Garcia, M. V., Robinson, M., Van Rooy, P., Dietenberg, M., Bergin, M., and Schauer, J., "Investigation of black and brown carbon multiple-wavelength- dependent light absorption from biomass and fossil fuel combustion source emissions," *Journal of Geophysical Research: Atmospheres*, pp. 1–16, 2015.

Paasonen, P., Kupiainen, K., Klimont, Z., Visschedijk, A., Van Der Gon, H. A., and Amann, M., "Continental anthropogenic primary particle number emissions," *Atmospheric Chemistry and Physics*, vol. 16, no. 11, pp. 6823–6840, 2016.

Pagels, J., Khalizov, A. F., McMurry, P. H., and Zhang, R. Y., "Processing of Soot by Controlled Sulphuric Acid and Water Condensation–Mass and Mobility Relationship," *Aerosol Science and Technology*, vol. 43, no. 7, pp. 629–640, 2009. [Online]. Available: http://www.tandfonline.com/doi/abs/10.1080/02786820902810685

Pirjola, L., Lähde, T., Niemi, J., Kousa, A., Rönkkö, T., Karjalainen, P., Keskinen, J., Frey, A., and Hillamo, R., "Spatial and temporal characterization of traffic emissions in urban microenvironments with a mobile laboratory," *Atmospheric Environment*, vol. 63, no. Supplement C, pp. 156 – 167, 2012.

Pirjola, L., Pajunoja, A., Walden, J., Jalkanen, J. P., Rönkkö, T., Kousa, A., and Koskentalo, T., "Mobile measurements of ship emissions in two harbour areas in Finland," *Atmospheric Measurement Techniques*, vol. 7, no. 1, pp. 149–161, 2014.

Pirjola, L., Karl, M., Rönkkö, T., and Arnold, F., "Model studies of volatile diesel exhaust particle formation: are organic vapours involved in nucleation and growth?" *Atmospheric Chemistry and Physics*, vol. 15, no. 18, pp. 10 435–10 452, 2015. [Online]. Available: https://www.atmos-chem-phys.net/15/10435/2015/

Pisa, I. and Lazaroiu, G., "Influence of co-combustion of coal/biomass on the corrosion," *Fuel Processing Technology*, vol. 104, pp. 356–364, 2012.

Rönkkö, T., Lähde, T., Heikkilä, J., Pirjola, L., Bauschke, U., Arnold, F., Schlanger, H., Rothe, D., Yli-Ojanperä, J., and Keskinen, J., "Effects of Gaseous Sulphuric Acid on Diesel Exhaust Nanoparticle Formation and Characteristics," *Environmental Science & Technology*, vol. 47, pp. 11 882–11 899, 2013.

Saarnio, K., Frey, A., Niemi, J. V., Timonen, H., Rönkkö, T., Karjalainen, P., Vestenius, M., Teinilä, K.and Pirjola, L., Niemelä, V., Keskinen, J., Häyrinen, A., and Hillamo, R., "Chemical composition and size of particles in emissions of a coal-fired power plant with flue gas desulfurization," *Journal of Aerosol Science*, vol. 73, pp. 14–26, 2014.

Sarnela, N., Jokinen, T., Nieminen, T., Lehtipalo, K., Junninen, H., Kangasluoma, J., Hakala, J., Taipale, R., Schobesberger, S., Sipilä, M., Larnimaa, K., Westerholm, H., Heijari, J., Kerminen, V. M., Petäjä, T., and Kulmala, M., "Sulphuric acid and aerosol particle production in the vicinity of an oil refinery," *Atmospheric Environment*, vol. 119, pp. 156–166, 2015.

Schmidt, E. W., Gieseke, J. A., and Allen, J. M., "Size distribution of fine particulate emissions from a coal-fired power plant," *Atmospheric Environment*, vol. 10, pp. 1065–1069, 1976.

Sgro, L. A., D'Anna, A., and Minutolo, P., "Charge fraction distribution of nucleation mode particles: New insight on the particle formation mechanism," *Combustion and Flame*, vol. 158, no. 7, pp. 1418–1425, 2011. [Online]. Available: http://dx.doi.org/10.1016/j.combustflame.2010.11.010

Sippula, O., Koponen, T., and Jokiniemi, J., "Behavior of Alkali Metal Aerosol in a High-Temperature Porous Tube Sampling Probe," *Aerosol Science and Technology*, vol. 46, no. 10, pp. 1151–1162, 2012.

Sippula, O., Stengel, B., Sklorz, M., Streibel, T., Rabe, R., Orasche, J., Lintelmann, J., Michalke, B., Abbaszade, G., Radischat, C., Gröger, T., Schnelle-Kreis, J., Harndorf, H., and Zimmermann, R., "Particle emissions from a marine engine: Chemical composition and aromatic emission profiles under various operating conditions," *Environmental Science & Technology*, vol. 48, no. 19, pp. 11 721–11 729, 2014. [Online]. Available: http://dx.doi.org/10.1021/es502484z

Srivastava, R. K., Miller, C. A., Erickson, C., and Jambhekar, R., "Emissions of sulfur trioxide from coal-fired power plants." *Journal of the Air & Waste Management Association (1995)*, vol. 54, no. 6, pp. 750–762, 2004.

Stevens, R. G. and Pierce, J. R., "A parameterization of sub-grid particle formation in sulfur-rich plumes for global- and regional-scale models," *Atmospheric Chemistry and Physics*, vol. 13, no. 23, pp. 12 117–12 133, 2013.

———, "The contribution of plume-scale nucleation to global and regional aerosol and CCN concentrations: Evaluation and sensitivity to emissions changes," *Atmospheric Chemistry and Physics*, vol. 14, no. 24, pp. 13 661–13 679, 2014.

Stevens, R. G., Pierce, J. R., Brock, C. A., Reed, M. K., Crawford, J. H., Holloway, J. S., Ryerson, T. B., Huey, L. G., and Nowak, J. B., "Nucleation and growth of sulfate aerosol in coal-fired power plant plumes: Sensitivity to background aerosol and meteorology," *Atmospheric Chemistry and Physics*, vol. 12, no. 1, pp. 189–206, 2012.

Stockie, J. M., "The Mathematics of Atmospheric Dispersion Modeling," *SIAM Review*, vol. 53, no. 2, pp. 349–372, 2011.

Stolzenburg, M. R. and McMurry, P. H., "An Ultrafine Aerosol Condensation Nucleus Counter," *Aerosol Science and Technology*, vol. 14, no. October 2014, pp. 48–65, 1991.

Termuehlen, H. and Emsperger, W., "Evolutionary Development of Coal-Fired Power Plants," in *Clean and Efficient Coal-Fired Power Plants*, Termuehlen, H. and Emsperger, W., Eds. New York, NY: ASME, jun 2003. [Online]. Available: http://dx.doi.org/10.1115/1.801942.ch1

Thomas, D., "UK set for first full day without coal power," April 2017, [Online; posted 21-April-2017, accessed 5.9.2017]. [Online]. Available: http://www.bbc.com/news/business-39668889

Vesala, H., "Diluting sampler and a method for collecting and diluting a gaseous sample," Patent US 2010/0 186 523 A1, 1 12, 2007.

Wang, S. C. and Flagan, R. C., "Scanning Electrical Mobility Spectrometer," *Aerosol Science and Technology*, vol. 13, no. 2, pp. 230–240, 1990.

Wang, X., Jing, H., Dhungel, B., Wang, W.-n., Kumfer, B. M., Axelbaum, R. L., and Biswas, P., "Characterization of organic and black carbon aerosol formation during coal combustion : An experimental study in a 1 MW pilot scale coal combustor," *Fuel*, vol. 180, pp. 653–658, 2016. [Online]. Available: http://dx.doi.org/10.1016/j.fuel.2016.04.057

Wiedensohler, A., "An approximation of the bipolar charge distribution for particles in the submicron size range," *Journal of Aerosol Science*, vol. 19, no. 3, pp. 387–389, 1988.

Xu, M., Yu, D., Yao, H., Liu, X., and Qiao, Y., "Coal combustion-generated aerosols: Formation and properties," *Proceedings of the Combustion Institute*, vol. 33, no. 1, pp. 1681–1697, 2011. [Online]. Available: http://dx.doi.org/10.1016/j.proci.2010.09.014

Yi, H., Hao, J., Duan, L., Tang, X., Ning, P., and Li, X., "Fine particle and trace element emissions from an anthracite coal-fired power plant equipped with a bag-house in China," *Fuel*, vol. 87, no. 10-11, pp. 2050–2057, 2008.

Ylätalo, S. I. and Hautanen, J., "Electrostatic Precipitator Penetration Function for Pulverized Coal Combustion," *Aerosol Science and Technology*, vol. 29, no. 1, pp. 17–30, 1998. [Online]. Available: http://www.tandfonline.com/doi/abs/10.1080/02786829808965547

Yli-Ojanperä, J., Kannosto, J., Marjamäki, M., and Keskinen, J., "Improving the nanoparticle resolution of the ELPI," *Aerosol and Air Quality Research*, vol. 10, no. 4, pp. 360–366, 2010.

Ymparisto.fi, "Ilman epäpuhtauksien päästöt Suomessa: Pienhiukkaset (PM2.5)-päästöt vuodelle 2015 (t)," 2015, http://www.ymparisto.fi/fi-FI/Kartat_ja_tilastot/Ilman_epapuhtauksien_paastot.

Publications

Publication I

Mylläri, F., Karjalainen, P., Taipale, R., Aalto, P., Häyrinen, A., Rautiainen, J., Pirjola, L., Hillamo, R., Keskinen, J., Rönkkö, T. "Physical and chmical characteristics of flue-gas particles in large pulverized fuel-fired power plant boiler during co-combustion of coal and wood pellets", *Combustion and Flame*

Combustion and Flame 176 (2017) 554–566

Contents lists available at ScienceDirect

Combustion and Flame

journal homepage: www.elsevier.com/locate/combustflame

Physical and chemical characteristics of flue-gas particles in a large pulverized fuel-fired power plant boiler during co-combustion of coal and wood pellets

Fanni Mylläri[a], Panu Karjalainen[a], Raili Taipale[b], Pami Aalto[c], Anna Häyrinen[d], Jani Rautiainen[d], Liisa Pirjola[e], Risto Hillamo[f], Jorma Keskinen[a], Topi Rönkkö[a,*]

[a] Aerosol Physics Laboratory, Department of Physics, Tampere University of Technology, P.O. Box 692, FI-33101 Tampere, Finland
[b] VTT Technical Research Centre of Finland, P.O. Box 1603, FI-40101 Jyväskylä, Finland
[c] School of Management/Politics, University of Tampere, FI-33101 Tampere, Finland
[d] Helen Oy, Helen, FI-00090 Helsinki, Finland
[e] Department of Technology, Metropolia University of Applied Sciences, FI-00180 Helsinki, Finland
[f] Atmospheric Composition Research, Finnish Meteorological Institute, FI-00560 Helsinki, Finland

ARTICLE INFO

Article history:
Received 5 August 2016
Revised 13 September 2016
Accepted 29 October 2016

Keywords:
Biomass combustion
High temperature aerosol
Total particle number concentration
Particle number size distribution
Pulverized fuel
Coal

ABSTRACT

Fossil fuel combustion should be decreased in future years in order to lower the CO_2 emissions of energy production. The reduction can be achieved by increasing the amount of CO_2-neutral fuels in energy production. Here 6–13% of coal was substituted with industrial or roasted pellets in a pulverized fuel-fired power plant without making any changes to fuel grinding or low-NO_x burners. The effect of pellet addition for the flue gas particles was studied with direct sampling from the boiler super heater area. Based on primary dilution ratio tests, transmission electron microscope images, and the natural electric charge of the particles, it was observed that particles in the flue gas are spherical and have been formed in the boiler at high temperatures. The pellet addition lowered the total particle number concentrations with all of the studied pellet–coal mixtures in comparison to the coal combustion. The 10.5% industrial pellet addition caused a second mode in the particle number size distribution. In addition, based on the chemical analysis of the collected size-fractioned particle samples, results indicated that the pellet addition did not increase the corrosion risk of the boiler. However, the changes in the particle number size distribution and total particle number concentration can affect the operation of electrostatic precipitators and flue gas cleaning.

1. Introduction

Climate change has caused a global need to reduce CO_2 emissions. These emission reductions are driven mainly by local political decisions [1,2], but larger scale political actions also exist. In principle, smaller CO_2 emissions can be achieved by reducing the usage of fossil fuels in traffic, residential needs, and in power generation. This can take place by reducing the energy consumption or by substituting fossil fuels with renewable fuels (e.g., biofuels, solar and wind power). One likely cost effective possibility in these actions is to utilize existing coal-fired power plant infrastructures and substitute the coal used in those with biomass. However, decreased CO_2 emissions and the addition of biomass can change the emission of other harmful pollutants and also increase the corrosion risks for the power plant boilers. Biomass-based fuels have a different chemical composition than fossil fuels such as coal [3]. Biomass fuels typically contain more alkali metals and chlorides [3,4], which can, in the combustion process, be vaporized into the flue gas [5]. For instance, alkali chlorides are found to be harmful for the power plant boiler materials [6]. After the combustion process, corrosion-causing elements can exist in the vapour or particle phase [7], depending on the temperature and concentrations [8]. For instance, a change in the boiler temperature profile affects the deposition locations of the alkali chloride [8]. In principle, the amount of alkali chlorides in the particle phase can be determined when the particle size distribution and chemical composition of the particles are studied simultaneously.

In addition to the temperature profile existing in the boiler and the chemical composition of the fuel, the fuel grain size also has

* Corresponding author.
E-mail address: topi.ronkko@tut.fi (T. Rönkkö).

http://dx.doi.org/10.1016/j.combustflame.2016.10.027
0010-2180/

an effect on the combustion process and the slagging and fouling of the super heater surfaces. The fuel grain size affects the particle size distribution after combustion in the flue gas. Ninomiya et al. [9] have studied the effect of coal grain size in terms of particle mass (PM) emission. They discovered that <63 µm coal particles produce bimodal PM distribution, with mode means of 500 nm and 4 µm. They also found that there is a small mode around 130 nm, which consisted of alkali metals, heavy metals and their sulphate, chloride and phosphate salts. The flue gas is steered to flue gas ducts and released in to atmosphere with or without some flue gas cleaning. Particle properties such as size, chemical composition, and the electric charge carried by particles affect the flue gas cleaning efficiency [10,11].

In general, the flue-gas changes in large power plant boilers can affect, for example, the corrosion of the super heater area and other parts of the flue-gas system, the flue-gas cleaning systems and, finally, the emissions of power plants. These effects depend on the characteristics of aerosol generated in the combustion process. The emissions of particles from combustion plants and other sources are governed by the Convention on Long-Range Transboundary Air Pollution of the United Nations Economic Committee for Europe. The 2012 amendments to the Convention include national emission reduction commitments by 2020 and beyond. The limit values for SO_2, NO_x, ammonia, volatile organic compounds and particulate matter (i.e., with a diameter equal to or less than 10 µm), including black carbon, are separately defined for coal and biomass with no mention of co-combustion [12]. In addition to the EU Member States, Canada, the United States, Russia and several countries of Southern and Eastern Europe, the Caucasus and Central Asia are also expected to sign the amendments. In its related legislation, the European Union also separates the emissions from coal and biomass without any mention of prospects of co-combustion [13–15].

However, the partial substitution of coal by biomass and subsequent co-combustion is one of the pathways identified in the European Industrial Bioenergy Initiative (EIBI) of the European Commission and the EU Member States. The EIBI pays attention to local variation in the available biomass feedstock options and suggests "a pragmatic approach to select the most promising options, based on transparent criteria reflecting a set of key economic, environmental and social performances expected" [16]. The European Commission deems co-combustion of biomass and coal to be "the most cost-effective option for electricity production". Addition of biomass up to 10% share of total power output has been successfully demonstrated and the technology is commercially available. This technology makes use of existing plant infrastructure and requires only limited investments in biomass pre-treatment and feed-in systems [17]. However, "feeding, fouling and ash disposal pose technical challenges that reduce reliability and lifetime of coal plants. Higher co-firing mix will require more sophisticated boiler design, process control and fuel handling and control systems" [18]. The European Commission is hesitant towards to establish a specific policy for the co-combustion of biomass and coal. It notes that the incentives of the utilities running relevant combustion plants are national support schemes and/or the emission ceiling of the emissions trading scheme (ETS). Therefore setting a policy for co-combustion installations without similar measures for coal-combustion plants might lead to decreased use of biomass and hence, by implication, higher emissions [19].

In the United States, short tests of co-combustion have been conducted since the 1990s. The Energy Information Administration expects co-combustion to be up to 20 times more prevalent by 2024 than it was in 2010 [20]. Federal-level research into the heating qualities of different biomass contents and emissions continues [21]. The 2014 Clean Power Plan offered by President Obama and the Environmental Protection Agency mentions that, in co-combustion, the "use of some kinds of biomass has the potential to offer a wide range of environmental benefits, including carbon benefits", and that "[I]ncreasing renewable energy (RE) use will also continue to lower other air pollutants (e.g., fine particles, ground-level ozone, etc.)" [22]. While federal level regulation is debated, individual states can use renewable energy standards (RES) to incentivize power plant operators for co-combustion [20]. However, by 2012, only 3% RPS-motivated renewable energy capacity additions came from biomass [23]. With regard to co-combustion, plant operators hesitate over the costs of acquiring and transporting the biomass, as well as the long-term effects on process equipment [20].

In this article, flue-gas aerosol from a large scale pulverized coal-fired power plant boiler is investigated. The power plant combusted various mixtures of coal and two types of wood pellet. Special attention is paid to the particle number size distributions, total particle number concentration and chemical composition of particles in the diluted flue-gas sample taken from the boiler super heater area. In addition, the effects of wood pellets on the concentrations of gaseous species and particulate matter (PM) in the flue gas are shown. The aim is to understand the effect of co-combustion of wood pellets and coal on flue-gas aerosol formation and characteristics.

2. Experimental

2.1. Power plant

The power plant where the experiments of this study occurred is situated in Helsinki, Finland. In the power plant, there are two separate boilers, both equipped with flue gas cleaning systems that include electrostatic precipitators, semi-dry desulphurization, and fabric filters, in the given order after the boiler. Boilers (363 MW_{th}) are equipped with a reheater and utilizes the natural circulation of flue gas. Boilers are equipped with 12 low-NO_x technology burners (Tampella/Babcock-Hitachi HTNR low NO_x) that are at the front wall. The combustion air and at the same time the carrier air for the pulverized fuel is preheated up to 350 °C before the boiler and grinders. Main operation principle of low-NO_x burners is air staging with secondary and tertiary air, which lowers the combustion temperature to the level of around 1100 °C. Air staging decreases NO_x formation. The power plant boiler has originally been designed to combust pulverized coal that is fed to the boiler after being ground in ball ring grinders.

2.2. Fuel properties

In this study, some of the measurements were made with 100% Russian coal and some with mixtures of coal and pellets. In the latter case, coal was substituted with 6–13% (of the boiler thermal power) wood pellets; roasted pellets or industrial pellets (see experimental matrix in Table 1). Roasted pellet is torrefactioned wood pellet, also known as black pellet, steamed pellet, torrefactioned pellet and bio coal, manufactured from wood pellets by heat treatment at approximately 300 °C.

Industrial pellet (wood pellet of industrial quality) fulfils the standard EN 14961-1 requirements having lower quality than domestic quality wood pellets. Industrial pellet can include, for example, bark, which does not exist in higher quality wood pellets. Normally, wood for industrial pellets is gained by grinding stem wood or logs to powder and, after drying, by pressing the powder to pellets. Due to the preparation principle of industrial pellets, it is more brittle than domestic pellets and it contains more ash components.

Table 1
Experimental matrix. Coal was combusted during the nights and for that reason the "c" test took only 2 h. Note that there is a lower load in "c+rp7.6%" situation. The deviations we mainly caused by instability of the pellet feeding system.

Label	$Power_{coal}$	$Power_{pellet}$	Portion of pellet from fuel power (%)	DLPI sampling time	Duration of co-firing test
c+rp6.8%	301.6–322.2	5.2–33	1.6–9.9	2 h	3 h
c+rp7.6%	246.3–248.7	19.0–21.9	7.1–8.2	2 h 30 min	5 h
c+rp9.8%	294.7–320.3	15.7–44.1	4.7–13	2 h 10 min	5 h
c+rp13.1%	287.3–318.5	34.9–47.5	9.9–14.2	2 h	3 h
c+ip6.6%	299.2–312.9	12.8–31.8	3.9–9.6	2 h	5 h
c+ip10.5%	297.9–302.7	28.3–36.8	8.5–11.0	1 h 40 min	4 h
c	328.0–335.7	0	0	1 h 40 min	2 h

The coal is stored inside the power plant building in four intermediate storages, "day silos". From the intermediate storages the coal is divided to a belt conveyor which carries the coal to the grinders. Below each belt conveyor there is a grinder, which pulverizes the coal. The pellet is added to the grinder by a separate feeding system. The pulverization is performed with ball ring grinders (9 rolling balls). The pulverized fuel is blown into three burners together with the combustion air. Over each grinder there is a sieve which returns the largest particles back to the grinder. The fuel mixture was grinded simultaneously in two of the four grinders and thus in total 6 burners were combusting wood–pellet coal mixtures. When pulverizing coal the mean fuel particle size was 47–62 μm (58–69% was below 74 μm and 100% was <600 μm). For "c+rp" the mean fuel particle size was 56–90 μm (32–74% was below 74 μm and 87–100% was <600 μm), whereas for the "c+ip" the mean fuel particle size was 54–174 μm (28–59% was below 74 μm and 79–99% was <600 μm). These numbers show that the wood pellet substitution changes the pulverized fuel by increasing the fuel particle diameter.

Pellet and coal properties are listed in Table 2. Table 2 shows that the pellets had lower water and ash content in contrast to the coal. Also, the sulphur content and chloride contents were significantly lower in the pellets than the coal. Instead, the oxygen and volatile content were higher in the pellets than in the coal. It is notable, that the sum of alkali metals (K and Na) was higher in coal than in the pellets, which means that actually the pellet addition diluted the alkali concentration in the boiler. The heating value of coal was higher than the heating value of pellets.

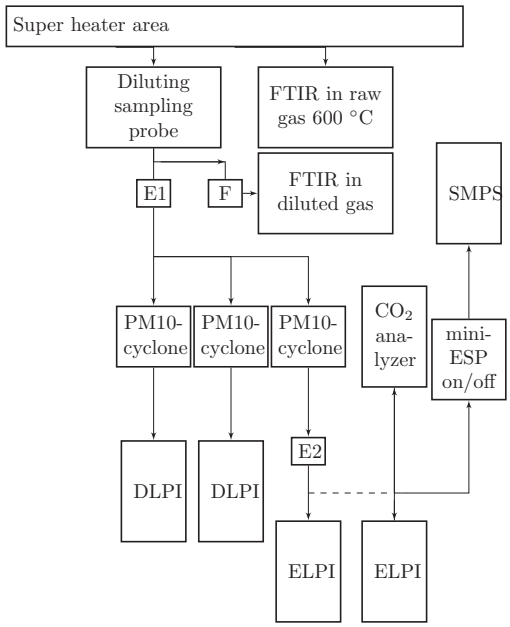

Fig. 1. Measurement setup. E is ejector type diluter, F is a particle filter, and PM10-cyclone is a cyclone with 10 μm cut–off diameter. The diluted sample was taken at 900–1000 °C temperature area and the raw flue gas sample at 600 °C temperature area of the boiler. The dashed line indicates the 11-m long sampling line.

2.3. Measurement setup and analytical methods

The measurement setup used is shown in Fig. 1. All the measurements with pure coal and coal–pellet mixtures were made from the same boiler unit. In these measurements, the flue-gas sample was taken from the boiler super heater area where the temperature ranges from 900 to 1000 °C. Due to the temperature variations and turbulence in the boiler, the flue-gas sampling was not designed to be isokinetic. This can affect representativeness of absolute concentration values measured for large particles, but not to the relative concentrations between the studied fuel-mixtures. Primary dilution of the sample was performed with a porous tube-type diluter using nitrogen (200 °C) as diluting gas, similar to the one in [24]. Due to the hot flue gas condition, the outer shell of the dilution probe was cooled with pressurized air flow, whereas the inner shell was heated to prevent the condensation of the gaseous components. Secondary dilution was performed with an ejector diluter (Dekati Ltd.), using nitrogen as a diluting gas, with a dilution ratio of 2.83. The primary dilution ratio was calculated based on CO_2 and H_2O measurements. In most of the measurements, the primary dilution ratios were between 6.0 and 8.3. The primary dilution ratio was chosen so that the sample cools enough in the primary diluter. Primary dilution ratio was changed in one of the experiments to see how sensitive the particle size distribution is to the variations in primary dilution conditions. Secondary dilution was used to lower the temperature of the sample even more to the room temperature. The sample temperature before the secondary diluter was approximately 200 °C.

After the secondary dilution the particles were collected with two parallel Dekati low pressure impactors (DLPI, Dekati Ltd.) in order to measure the mass size distribution and the chemical composition of the particles. A cyclone with cut-off diameter of 10 μm was applied before the DLPIs. The DLPI collection plates were greased polycarbonate films, whereas the smallest particle fraction was collected to a teflon filter. The particulate sample collected by one of the DLPI was used to analyse the water soluble fraction of the particles, and the other to analyse the acid-soluble particles. In this study, 13 size fractions of DLPI were combined afterwards into five different size categories <30 nm, ≥ 30 nm to

Table 2
Fuel properties.

		Industrial pellet	Roasted pellet	Coal
Moisture	%	6.7	6.0	11.0–11.3
Ash	%	0.8	3.3	10.5–11.4
Volatiles	%	78.1	64.6	32.8–33.1
Heating value	GJ/t	17.7	20.3	24.6–24.9
C	%	47.4	53.8	62.3–63.1
H	%	5.6	5.2	4.1–4.2
N	%	0.1	0.3	1.8–2
O	%	39.4	31.7	0
S	mg/kg dry	180	580	3100–4600
Cl	mg/kg dry	39	84.3	236
Ca	mg/kg dry	2300	6100	4300–4800
Mg	mg/kg dry	280	740	1700–1900
Na	mg/kg dry	69	240	1400–1600
K	mg/kg dry	760	3200	2500–2900
Fe	mg/kg dry	140	1100	4800–5700
Al	mg/kg dry	130	580	14200–15000
Ti	mg/kg dry	8.8	47	600–640
Ba	mg/kg dry	26	25	270–280
B	mg/kg dry	<40	<40	210–230
Ag	mg/kg dry	<0.5	<0.5	<0.5
As	mg/kg dry	<0.5	<0.5	4.9–14
Be	mg/kg dry	<0.5	<0.5	<0.5
Bi	mg/kg dry	<0.7	<0.7	<0.7
Cd	mg/kg dry	0.2	1.2	0.1
Co	mg/kg dry	<0.5	<0.5	1.4–2.1
Cr	mg/kg dry	1.2	13	9.7–11
Cu	mg/kg dry	1.6	5.9	7.8–8.5
Li	mg/kg dry	<0.5	1.1	9.3–10
Mn	mg/kg dry	140	140	38-66
Mo	mg/kg dry	<0.5	0.9	1.1–1.3
Ni	mg/kg dry	<0.5	2.3	4.1–6.6
Pb	mg/kg dry	<0.5	6.1	3.4–4.1
Rb	mg/kg dry	2.5	6.4	5.2–9.0
Sb	mg/kg dry	<0.5	<0.5	<0.5
Se	mg/kg dry	<0.7	<0.7	<0.7–1.1
Sr	mg/kg dry	5.5	19	150–170
Th	mg/kg dry	<0.5	<0.5	1.2–1.3
Tl	mg/kg dry	<0.5	<0.5	<0.5
U	mg/kg dry	<0.5	<0.5	<0.5–0.6
V	mg/kg dry	<0.5	1.3	13–15
Zn	mg/kg dry	30	120	11–18

<90 nm, ≥ 90 nm to <260 nm, ≥ 260 nm to <600 nm, ≥ 600 nm to <1.6 μm, and > 1.6 μm.

The water-soluble anion (SO_4^{2-}, Cl^-, F^-) concentrations were determined with ion chromatography (measurement was based on standard SFS-EN ISO 10304-1 and instrument that was used was Dionex ICS-2000 Ion Chromatography system). The analysed water-soluble elements were Ca^{2+}, K^+, Na^+, SO_4^{2-}, Cl^-, F^-, and Zn, whereas the acid-soluble fraction was analysed for 31 elements (Ag, Al, As, B, Ba, Be, Bi, Ca, Cd, Co, Cr, Cu, Fe, K, Li, Mg, Mn, Mo, Na, Ni, Pb, Rb, Sb, Se, Sr, Th, Ti, Tl, U, V, Zn, Cl and S). Elements (water-soluble cations and acid-soluble elements) were determined with an Induction Coupled Plasmonic – Mass Spectrometer (ICP-MS). Measurement was based on standard SFS-EN ISO 17294-2 and the instrument that was used was a Thermo Fisher Scientific iCAP Q ICP-MS. It has to be noted that Si, carbon, carbonates and oxides were not analysed from the samples. The water-soluble cations and anions were dissolved in 25 ml of ultra-pure Milli-Q water in closed plastic tubes at room temperature for 5 days. During the dissolution, the samples were shaken for 2 h and stored for 2 h in an ultrasound bath. The acid-soluble elements were dissolved in 2 ml of nitrous acid–hydrogenfluoride acid (3:1) solution and the sample was diluted with 10 ml of Milli-Q water.

After the secondary dilution, part of the sample was diluted further with dilution ratio of 12 and conducted to an Electrical low-pressure impactor (ELPI, Dekati Ltd., Keskinen et al. [25]). ELPI was used parallel with the DLPIs to monitor the loading of the collection plates of DLPIs. Further, part of the sample flow was led with an 11-m-long sampling line to a scanning mobility particle sizer (SMPS, Wang and Flagan [26]), another ELPI and a CO_2 analyser (SickMaihak, SIDOR). These instruments were installed inside an air-conditioned room. The SMPS consisted of DMA 3071 (TSI Ltd.) and CPC 3025 (TSI Ltd.) with 0.6/6.0 lpm flows a thus corresponding to particle size range from 9.8 nm to 414 nm. The charging state of the particles was studied by utilizing a self-made electrostatic precipitator (mini-ESP). The mini-ESP was used in part of the measurements to remove the electrically charged particle fraction before the SMPS size distribution measurement. A schematic of the measurement setup is presented in Fig. 1. The diffusional losses for particles in the 11-m sampling line were calculated (Hinds [27, Eqs. (7-31) and (7-32)]) to be for 10 nm, 20 nm, 40 nm and 100 nm particles in diameter 48%, 25%, 10%, and 4%, respectively. The particle size distributions below have been corrected by these values.

In addition to particle measurements, the concentrations of gaseous species were measured simultaneously after primary dilution from the same sampling line as the particles. Gaseous components were measured with an FTIR gas analyser (Gasmet DX-4000), in which the optical path was 5.0 m. The gaseous sam-

Table 3
Concentrations of gaseous compounds CO_2 (% red. dry 6% O_2, marked as % r.) and CO, NO, SO_2, HCl, HF (ppm reduced dry 6% O_2, marked as ppm r.), total particle number concentration (N_{tot}, calculated from particle number size distribution measured with SMPS) and PM10 in the wet flue gas boiler reheater area. The "c" corresponds to coal and "rp" to roasted pellet and "ip" to industrial pellet; the percentages are the amount of pellet thermal power of the total fuel power.

Fuel	CO_2 (% r.)	CO (ppm r.)	NO (ppm r.)	SO_2 (ppm r.)	HCl (ppm r.)	HF (ppm r.)	N_{tot} ($\cdot 10^8$ cm^{-3})	PM10 $mgNm^{-3}$
c	13± 0.2	19.5± 2.3	289± 8.4	204± 13	18± 1.3	33.2± 0.8	2.76	600
c+rp6.8%	13± 0.2	18.3± 3.1	276± 23.5	158± 17.3	9± 1.1	29.3± 1.5	2.03	690
c+rp7.6%	13± 0.2	13.6± 1.1	272± 9.6	156± 14.6	9± 0.5	32.3± 1.6	1.90	510
c+rp9.8%	13± 0.2	11.9± 2.3	273± 16.7	183± 10.4	8± 0.4	32.1± 0.8	1.67	720
c+rp13.1%	14± 0.3	12.7± 3.6	294± 27.6	144± 10.4	14± 1	29.7± 0.8	1.73	820
c+ip6.6%	14± 0.2	16.0± 0.9	295± 16.9	146± 5.6	11± 0.7	30.5± 0.7	1.89	640
c+ip10.5%	14± 0.2	18.5± 1.6	278± 11.8	201± 6.1	16± 0.4	30.9± 0.7	2.20	570

ple was kept at 180 °C temperature. The gaseous components were also measured after the reheater where the flue gas temperature was around 600 °C. The measurement place was chosen to be at the reheater area due to lack of viewports at the superheater area. FTIR gas analyser (Gasmet DX-4000) was also used here, with the optical path of 2.5 m. The gaseous sample was taken with sampling probe made by M&C. This FTIR included also a zirconium oxide sensor to measure the humid sample gas oxygen content. The measured gaseous components were H_2O, CO_2, CO, N_2, NO, NO_2, SO_2, HCl, and HF.

The flue gas particles of one coal–pellet mixture "c+ip10.5%" were collected with a flow-through-type sampler onto holey carbon grids for microscopy studies. These particle samples were studied later with a transmission electron microscope (TEM, Jeol JEM-2010) equipped with energy dispersive X-ray spectrometer (EDS, Noran Vantage with Si(Li) detector, Thermo Scientific).

3. Results

3.1. Gaseous compounds

Table 3 shows the gaseous compounds (CO_2, CO, NO, SO_2, HCl and HF) studied from the boiler reheater area. Within the accuracy of measurements, no significant differences in the CO_2 concentration was observed. Concentration of carbon monoxide was lower for pellet–coal mixtures than for coal. The lowest CO concentration was achieved with "c+rp9.8%" (11.9 ppm) and the highest with coal (19.5 ppm). There was hardly any NO_2 present at the flue gas (<2 ppm) and, thus, the NO_x consisted mainly of NO. It can be seen that the pellet addition also decreased the SO_2, HCl and, in some cases the NO concentrations when compared to coal combustion. In principle the reductions of SO_2 and HCl concentrations were presumable due to the chemical composition of the fuels; pellets contain less sulphur and chloride compared to coal. However, the decrease in SO_2 concentration can be affected by changes of combustion and flue-gas processes such as conversion of SO_2 to SO_3 that may promote the existence of sulphate in particle phase. Lower carbon monoxide concentrations with pellet–coal mixtures can be due to higher oxygen content of the fuel.

3.2. Particle mass size distribution and chemical composition

Particle mass on each DLPI stage was weighted in order to gain the particle mass size distribution which is shown in Fig. 2. The particulate mass (below 10 µm, PM10) was calculated from the size fractioned masses and the PM10 was averaged between the two parallel particle collections. The PM10 values were 600 $mgNm^{-3}$, 690 $mgNm^{-3}$, 510 $mgNm^{-3}$, 720 $mgNm^{-3}$, 820 $mgNm^{-3}$, 640 $mgNm^{-3}$ and 570 $mgNm^{-3}$, respectively for

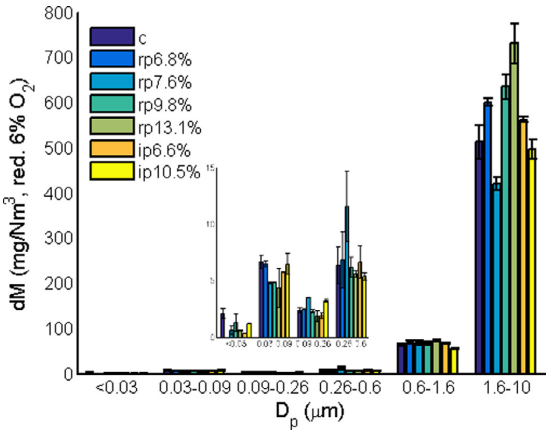

Fig. 2. Particle mass size distribution ($mgNm^{-3}$) calculated from the weighted particle samples that were collected with the parallel DLPIs. The bar shows the mean value of the mass on two different impactor stages and the standard deviation is calculated based on the same masses.

"c", "c+rp6.8%", "c+rp7.6%", "c+rp9.8%", "c+rp13.1%", "c+ip6.6%", and "c+ip10.5%" (with the legend in Fig. 2). The PM10 results indicate that the co-combustion of wood pellets and coal does not increase the PM10 in the boiler.

The chemical composition of the particles was determined from the particulate matter collected on the stages of DLPI. Based on the studied chemical components, a maximum of 50% of PM10 could be identified. This means that more than 50–80% of the particles consisted of unanalysed compounds (e.g., Si and black carbon). For instance, Frey et al. reported that, in the emissions of the same power plant, 80% of particle emission were other than water or acid-soluble fraction [28].

The results of size-fractioned ionic and elemental analysis are presented in Appendix C for each fuel mixture. The size fractions were determined based on the D50% diameters of the DLPI. The ionic composition of one size fraction was calculated in two steps: first, all analysed ion concentrations were added up in the specific size range; second, the ratio of the analysed mass of one ion to the whole analysed mass of ions in the specific size was calculated. Similar calculations were made from elemental analysis. The mass of some size fractions was not enough to determine the ionic or elemental composition. Thus, the composition of that kind of size fraction has been left blank in Fig. C.8 of Appendix C. In addition,

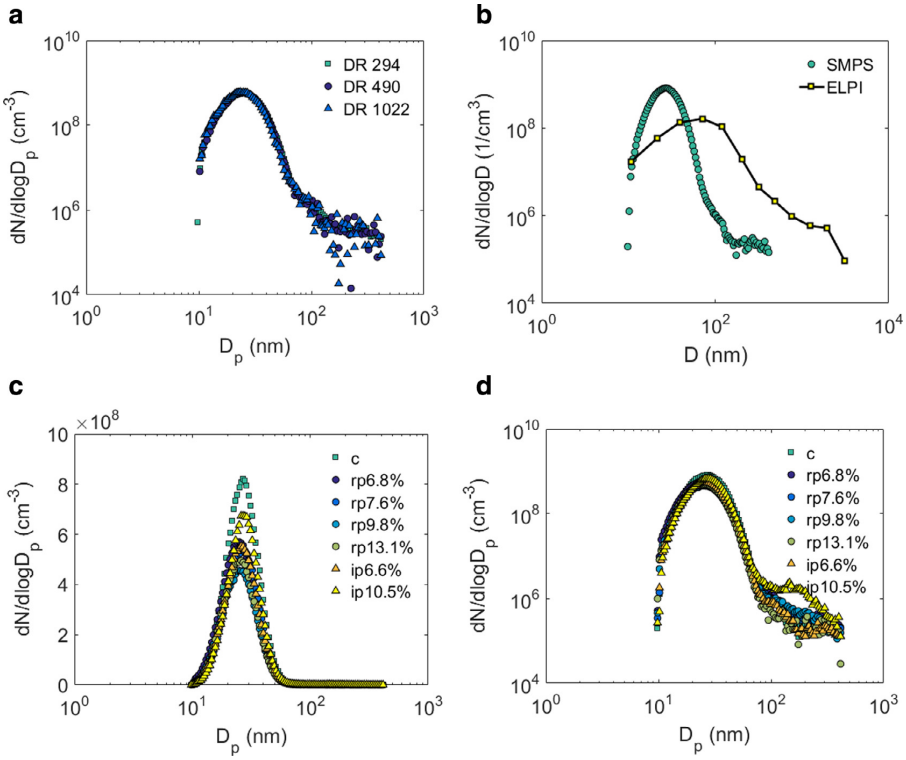

Fig. 3. (a) Effect of total dilution ratio on the measured particle number size distribution (c+rp7.6%). (b) Particle number size distribution measured with ELPI and SMPS (D indicates D_a and D_p in the figure, respectively) during coal combustion. (c, d) Particle number size distributions measured with SMPS. Concentrations have been corrected by the dilution ratio of the whole sampling system.

the missing composition can be due to undetectable concentration of the ions/elements in the sample.

The acid-soluble fraction was 20–50% of the PM10 and the water-soluble fraction was 2–3% of the PM10, specific percentages are shown in Appendix C over the graph. This means that the elemental composition of the particle is more important when studying the chemical composition. For all fuel mixtures, the most common measured elements in the particles were aluminium (Al), calcium (Ca), iron (Fe), magnesium (Mg), potassium (K) and sodium (Na). Aluminium was the main element in particles over 260 nm in diameter, whereas calcium and iron were the most common in particles that were 30–260 nm in diameter. The partition of elements is due to different volatilities of the elements in the fuel [29]. In addition, potassium existed mainly in the particles over 260 nm. The water-soluble fraction consisted mainly of Ca^{2+} and SO_4^{2-} ions in all size classes. In addition to Ca^{2+} and SO_4^{2-}, some K^+ and Na^+ was analysed in the samples. These results indicate that substituting coal with 6–13% of pellets does not have significant effect on the chemical composition of the particles.

3.3. Physical properties of particles

Figure 3a shows the number size distributions of particles (9.8–414 nm) sampled from the boiler super heater area where the temperature was in the range of 900–1000 °C "c+rp7.6%". The geometric-mean diameter (GMD) for the mode dominating the size distributions was around 25 nm. The variation in the dilution ratio did not affect the particle number size distribution corrected by the dilution ratio, which indicates that any of the studied dilution ratios can be used to achieve comparable results [30,31]. It should be noted that in addition to particle concentration, the mean particle size also did not change as a function of the dilution ratio. In other words, there were no significantly low-vapour pressure gaseous compounds that could have formed particles or condensed onto existing particles after the sampling, such as during dilution processes or in other parts of the sampling system. Thus, the results related to the insensitivity of the particle size distribution on the dilution ratio indicate that the particles were formed before the sampling process (i.e., they were present in particle phase already in high temperature conditions).

Figure 3b shows the particle size distribution for coal combustion with two different instruments, namely SMPS and ELPI. The measurement principle of these instruments differs from each other; while the SMPS classifies the particle in respect to their mobility size, the ELPI classifies the particles based on their aerodynamic diameter. The difference between measurement principles enables the evaluation of effective density of particles; see, for example, Ristimäki et al. [32] and Virtanen et al. [33]. Based on the ELPI and SMPS measurements and log-normal-distributions plotted to the size distributions, the particles had a mean mobility diameter of 25 nm and mean aerodynamic diameter of 55 nm. When the effective density is calculated using these particle sizes, its value is 2.05 gcm^{-3}. This is close to the bulk density of SiO_2 which is 2.196–2.648 g cm^{-3}, depending on the crystal form [34]. The effective density of the particles was the same with all studied fuel compositions.

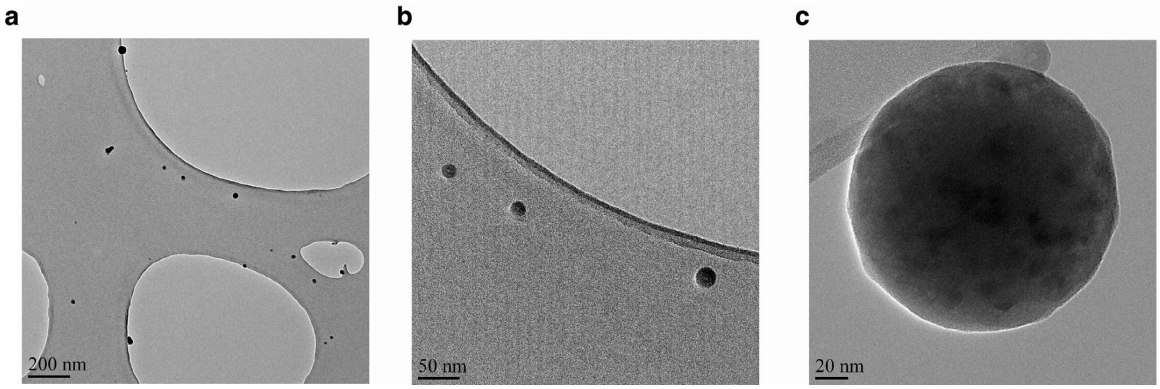

Fig. 4. Transmission electron microscope (TEM) images of particles collected from a flue gas sample. (a) General picture of the small particles, (b) particles having diameters of 10–25 nm and (c) example of larger particle with diameter of 120–130 nm.

Particle number size distribution was dominated by the particles in the range of 10–70 nm in diameter. Figure 3 c shows that the peak concentrations in the number size distribution were not the same with different fuels. The standard deviations for each studied wood pellet–coal mixture are shown in Appendix A. The total particle number concentrations (for particles in the size range of 9.8–414 nm) were calculated from the particle number size distributions and are listed in Table 3. The particle number size distributions were also used to calculate the volume size distribution of the particles (see Appendix B). The 100% coal has the highest peak concentration and, thus, indicates the highest total particle concentration in the boiler super heater area. The second highest peak concentration was observed with coal+ip10.5% case, whereas for the other coal–pellet mixtures total particle concentrations decreased with increasing pellet proportion. However, it seems that also "c+rp13.1%" had an increasing trend to the total particle number concentration (9.8–414 nm) compared with "c+rp9.8%". It can be concluded that the pellet substitution decreases the total particle number concentration in the boiler. The lowest total particle number concentration (9.8–414 nm) was achieved with combustion of roasted pellets and coal because all studied "c+rp"-mixtures, even over 10% substitution, decreased the total particle number concentration equally compared to coal combustion. It seems that over 10% substitution of industrial pellets can actually increase the total particle number concentration in the boiler compared to "c+rp"-mixtures.

Figure 3d shows that the particle number size distributions were mainly unimodal in size range of 9.8–414 nm with a mean electrical mobility diameter of 25 nm and a geometric standard deviation (GSD) of 1.4. However, when combusting "c+ip10.5%"-fuel, the other mode was also observed, in addition to the mode at 25 nm. The other particle mode had the GMD of around 120 nm (GSD 1.6), but the number concentration for this mode was about 3 orders of magnitude smaller than the number concentrations of mode at 25 nm. Thus, the combustion of other "c+rp"-mixtures decreased the total particle number concentration in the studied size range, but did not have an effect on the form of particle number size distribution, and the combustion of "c+ip10.5%" did cause a slightly higher total particle number concentrations and a bimodal particle size distribution. This can be a result of differences in some properties of the fuels, such as the grindability of the pellets. Roasted pellets are more similar to the coal and, thus, could be more easily ground with the coal compared to the industrial pellets which are less processed and look more like stemwood.

The particle sample for transmission electron microscope (TEM) analyses was collected during the combustion of "c+ip10.5%". Examples of the images of the particles are shown in Fig. 4. Based on the images, the typical particle sizes were determined to be 10–25 nm in diameter and 120–130 nm in diameter. Based on the TEM images, particles in both of these size ranges were spherical. The observed diameters correspond well with the particle size distribution measured with the SMPS. Qualitative chemical analysis of the smaller particles, conducted by the EDS method (in Fig. 4b), showed that the particles consisted of Si, Al, P, Fe, Ca and Ti. Similar analysis for larger particles (in Fig. 4c) showed that they consisted of Si, Al, P, Fe, Ca, Ti and Mg. Based on these qualitative analyses, the major difference in the chemical composition of particles was the existence of magnesium in larger particles.

The SMPS measurement for the aerosol sample (Fig. 3c and d) produced a number size distribution of all particles in the size range of the instrument. However, by using the mini-ESP upstream of the SMPS, the measurement produced the number size distribution of electrically neutral particles (i.e., electrically charged particles were removed from the sample before the size distribution measurement). The fraction of electrically charged particles was then calculated by subtracting the concentrations of electrically neutral particles from the concentrations of all particles. This was made for the particle size range of 20–80 nm in which range the particle concentrations were relatively high.

In addition to the results calculated from the measurements, the theoretical charging probabilities were calculated with two different charging probability functions: Boltzmann equilibrium charge distribution [35] and Wiedensohler parametrization [36]. Boltzmann equilibrium charge distribution was calculated in four different temperatures (293 K, 773 K, 1073 K and 1373 K), assuming 1–6 elemental charges of both polarities. The Boltzmann charging probabilities are shown in Fig. 5 with labels "B". Figure 5 also includes the charging probability from Wiedensohler parametrization at room temperature for one elemental charge with both polarities ("W1") and for two elemental charges with both polarities ("W1+W2").

In combustion studies, the amount of electric charge carried by particles have been used as an indicator of the formation temperature of the particles (Maricq [37], Filippo and Maricq [38], Lähde et al. [39], Alanen et al. [40]). In this study, it was observed that the fraction of electrically charged particles in the studied size range was strongly particle size dependent (see Fig. 5), being

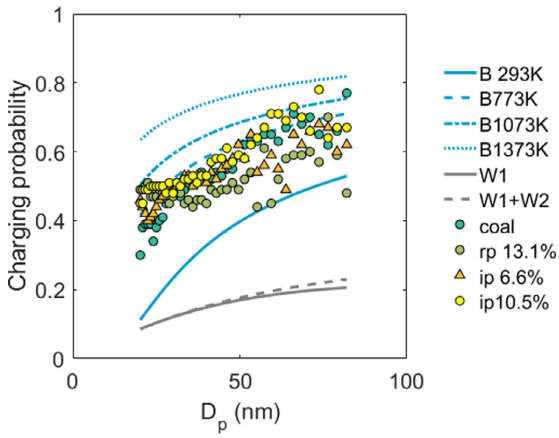

Fig. 5. Fraction of electrically charged particles in the boiler super heater area. Symbols are based on measurement and grey and blue lines denote the charging probability according to Wiedensohler and Boltzmann at different temperatures. (For interpretation of the references to colour in this figure legend, the reader is referred to the web version of this article.)

approximately 40% at 20 nm, 55% at 60 nm and 60% at 80 nm. Due to the mean particle size near 25 nm, for coal combustion, the fraction of electrically charged particles was, on average, 43%. Coal combustion originated particles 20–30 nm in diameter were slightly less charged than the same sized coal-pellet-combustion originated particles. In addition, particles in size range 30–80 nm from "c+rp13.1%" combustion are also less charged than particles from coal or "c+ip" combustion. The charging probability calculated based on particle size distribution measurements was higher than the charging probabilities calculated from Wiedensohler parametrization. This result is thought to be expected because the Wiedensohler parametrization is valid only at room temperatures. Actually, the comparison of measurement results with Wiedensohler parametrization indicates that the particles carried three to four times more electrical charge than the particles formed at room temperature.

When we took into account 1–4 elemental charges in one particle and calculated the Boltzmann charging probability, the charging probability at room temperature was similar to the Wiedensohler parametrization for the 20-nm particles in diameter, but closer the measurement results for the 80-nm particles in diameter. However, when the Boltzmann charging probability was calculated at elevated temperatures, the charging probability was approaching the charging probability that was calculated based on the measurements. The best fit between the Boltzmann charging probability and experimental results was gained at approximately 800 K. This similarity in charging probabilities at 800 K indicates that the particles have been formed at high temperatures. However, it has to be kept in mind that the Boltzmann temperature, at particle sizes below 50 nm in diameter, must be interpreted cautiously. It is also known from the measurements that the sample temperature after primary dilution was approximately 200 °C, which is less than the temperature predicted by the Boltzmann charging probability. This strongly supports the interpretation above (related to the insensitivity of particle size distribution on primary dilution ratio) that the particles were formed in the boiler before the primary dilution process of the sample.

4. Discussion

Fuel choices affect the aerosols released in combustion in power plants. The results of this study showed that coal–pellet mixture combustion reduces SO_2 concentrations in flue gas in comparison with pure coal combustion, which is reasonable based on the chemical composition on the fuels. In addition, coal–pellet mixture combustion reduced the concentrations of CO, and HCl concentrations so that the combustion was cleaner than the combustion of coal alone. Decrease of CO concentrations may be caused for example by the oxygen content of pellet fuels or changes of processes in combustion and flue gas. Additional reasons for the decrease in CO concentration could be the fuel particle size distribution, increased amount of volatile matter, but also using wood and, thus, improving the ignition of coal [41]. However, our data set does not offer unambiguous explanation for the decreased CO concentration. CO_2 concentrations of the flue gas did not change significantly because of fuel changes. It should be keep in mind that the combustion of pellet–coal mixture reduces indirectly also the CO_2 emissions of the power plant due to the carbon neutrality of the biomass pellets. In order to get information regarding the total benefits from CO_2 perspective e.g., the CO_2 emissions of fuel transportation should be taken into account.

In this study, the chemical composition of the particles sampled from the super heater area was very similar to all studied fuel combinations and, thus, it can be concluded that the 6–13% pellet substitution may not increase the corrosion risk of the boiler or super heaters. Nonetheless, the corrosion of boiler and super heater surfaces is a complicated process affected by both the initially gaseous and particulate compounds, as well as the temperature conditions in the boiler, and the detailed understanding of how the fuel changes affect those requires more detailed studies.

Combustion aerosol particles have been previously studied in power plants mostly by measurements for the flue gas in the stack or in duct before ESP. In this study, the particles were studied from the super heater area of the power plant. In general, the results are in line with previous studies made at the stack [42–45]. The results indicated that fuel changes have not had major effects on particle mass and the number size distributions of the flue gas. In addition, results show very clearly that, with all fuel mixtures studied here, the particle number size distributions (from 9.8 nm to 414 nm) were dominated by nanoparticles with a mean size of approximately 25 nm. From the emission point of view, this particle size is problematic because, in general, electrical charging of nanoparticles is not as efficient as the charging larger particles. For example, Ylätalo et al. [46] have shown that sub-100 nm particles penetrate through ESP. Thus, removal of these particles from the flue gas may require techniques other than electrostatic precipitators (ESP). Compared to the combustion of coal only, the combustion of coal–pellet mixtures was observed to decrease the number concentration of nanoparticles and, in addition, slightly increase the fraction of electrically charged nanoparticles. If the power plant is equipped with ESPs, both of these effects have the potential to decrease the particle emissions into the atmosphere. Thus, from the viewpoint of flue gas cleaning and particle emissions, the possible effects of co-combustion of coal and biomass pellets seems to be more positive than negative.

The particle number size distribution measurements supported by other measurements indicated that, for all fuel mixtures, the particles were solid, chemically stable and a significant part of them was electrically charged. For one fuel mixture (over 10% substitution of coal with industrial pellets), the particle number size distribution was observed to consist of two modes, and according to TEM analyses, both of these modes consisted of spherical particles. In general, although the particle measurements were made after diluting the flue gas sample and thus decreasing

its temperature into the room temperature, the results strongly indicate that the measured particles were formed at high temperature conditions before the sampling and dilution process. In addition to the chemical composition of the particles, this was also indicated by the insensitivity of the particle size distribution (number and size of particles) on the primary dilution ratio, as well as by the observation that the measured particles carried electric charge typical for high-temperature aerosol. Overall, the fraction of neutral/charged particles is at the same level as previously reported by Maricq [37] for particles originating from gasoline and diesel engines (data followed Boltzmann charge distributions at 800–1100 K). Thus, the measurement (sampling, dilution, instrumentation) setup used in this study is suitable to get information on particles existing in the high-temperature flue gas. On the other hand, results indicate indirectly that the flue gas from coal combustion and from the combustion of coal–pellet mixtures do not include a lot of such gaseous compounds that can directly condense on particle surfaces.

5. Conclusions

The transition from fossil fuel combustion to biomass combustion has been started, although relevant policies to support this transition are not yet in place. This study characterized how the substitution of coal with pellets changes the flue gas composition in the power plant super heater area. Gaseous components in the flue gas are directly affected by the fuel chemical composition; for example, the concentration of SO_2 and HCl were decreased in the flue gas by pellet substitution. The fuel oxygen content may improve the combustion which can be detected as lower CO concentration in the flue gas.

In addition to changes in the gaseous compounds of the flue gas, the particle chemical and physical properties might also be affected by the fuel changes. In this study, it was detected that the particle mass size distribution did not change significantly between the studied pellet–coal mixtures. However, the PM10 varied between 510 and 820 mg $N\,m^{-3}$. The particle samples gained from the determination of the particle mass size distribution were further analysed. The elemental and ionic analysis showed that the chemical composition of the particles was quite similar which indicates that the pellet–coal mixtures in 6–13% does not increase the corrosion risk. Even though the particle mass size distributions were similar with all of the fuels that were studied, the particle number size distributions have some differences, meaning that the fuel affects the fine particles in the flue gas. The primary dilution ratio did not have an effect on the particle size distribution, which indicates that the particles are formed before dilution in the boiler. The particle number size distributions have a mean diameter of 25 nm, but with “c+ip10.5%” there is also a second mode at 120 nm in diameter. Although, the second mode has 3 orders of magnitude lower particle number concentration compared to the 1st mode in 25 nm size. The bimodal particle number size distribution and, for “c+ip10.5%”, spherical shape of the particles could be also identified from the TEM images. There was also a difference in the particle number concentration (from 9.8 nm to 414 nm); the coal combustion caused the highest total particle number concentrations ($2.78 \cdot 10^8\ cm^{-3}$) and the “c+rp” the lowest ($1.67 \cdot 10^8\ cm^{-3}$), whereas the flue gas particle number concentrations for the coal–industrial pellet mixture were between these values ($1.89 \cdot 10^8\ cm^{-3}$–$2.20 \cdot 10^8\ cm^{-3}$).

Acknowledgments

The study was conducted in the MMEA WP 4.5.2. of Cleen Ltd., funded by Tekes (the Finnish Funding Agency for Technology and Innovation). Dr. Mari Honkanen is acknowledged for TEM imaging. F.M. acknowledges TUT Graduate School, KAUTE-foundation, TES-foundation for financial support. F.M., P.A. and T.R. acknowledges the financial support from the Academy of Finland (ELTRAN Grant 293437). Juho Kauppinen is acknowledged for performing the boiler sampling and the DLPI sample collections.

Appendix A. Standard deviation for the particle number size distributions

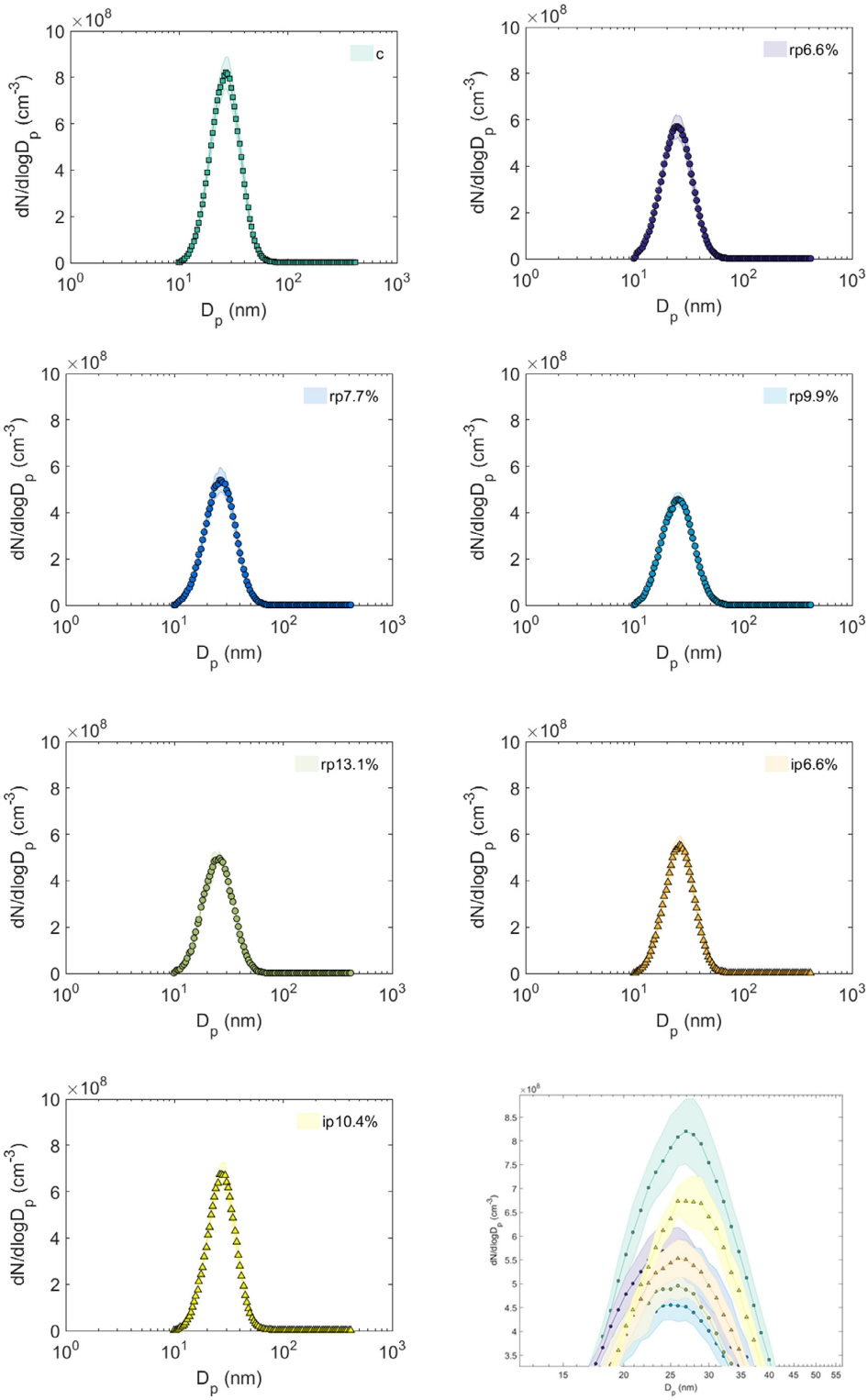

Fig. A.6. Standard deviations of the particle number size distributions measured with SMPS from the boiler super heater area.

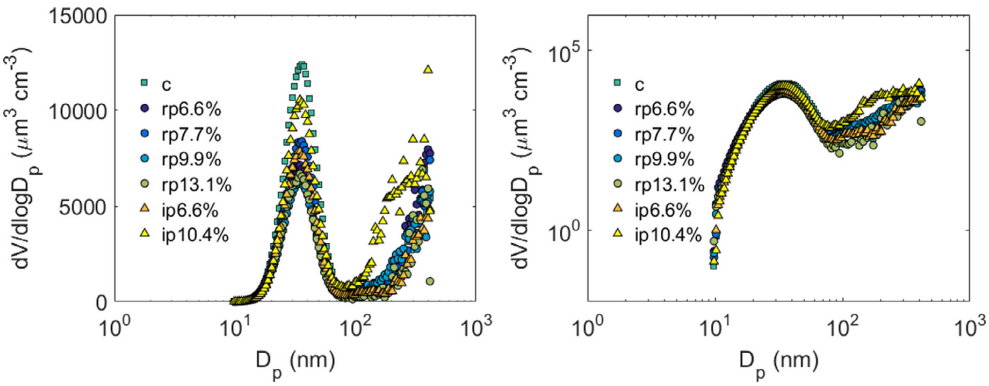

Fig. B.7. Particle volume size distribution calculated based on the assumption of spherical particles from the particle number size distribution measured with the SMPS.

Appendix B. Particle volume size distributions

The mode mean size was 35 nm and for "c+ip10.5%" the second mode mean was 300 nm. The mode mean size cannot be determined for other fuel-mixtures. However, the particle volume size distributions support the mass size distributions shown in Fig. 2.

Appendix C. Particle chemical composition

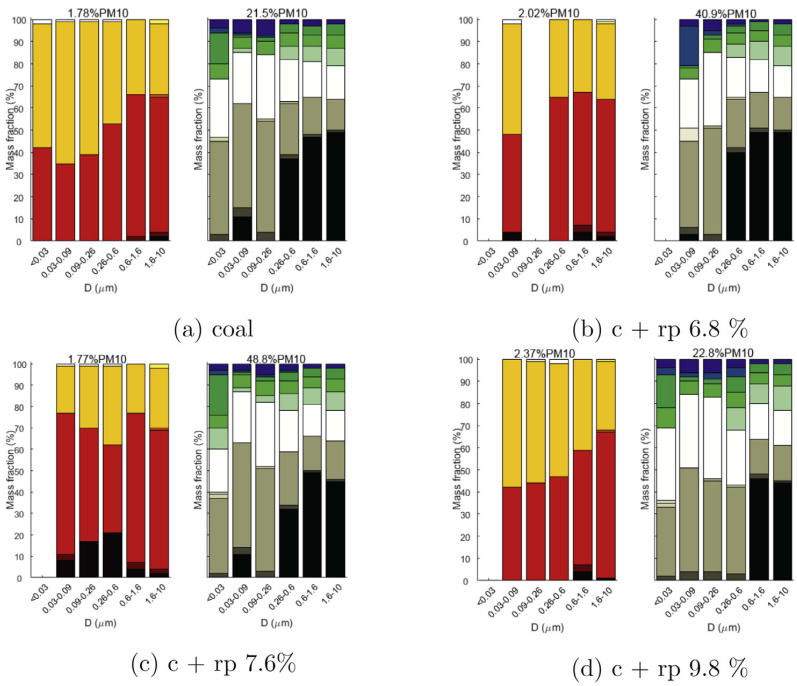

Fig. C.8. Particle chemical composition (ionic on the left and elemental on the right) with joint legend (bottom right) in different coal–pellet mixture cases. The mass ratios are calculated based on total identified mass and, thus some bars only show one chemical component. Studied PM10 mass fractions are presented above each subfigure.

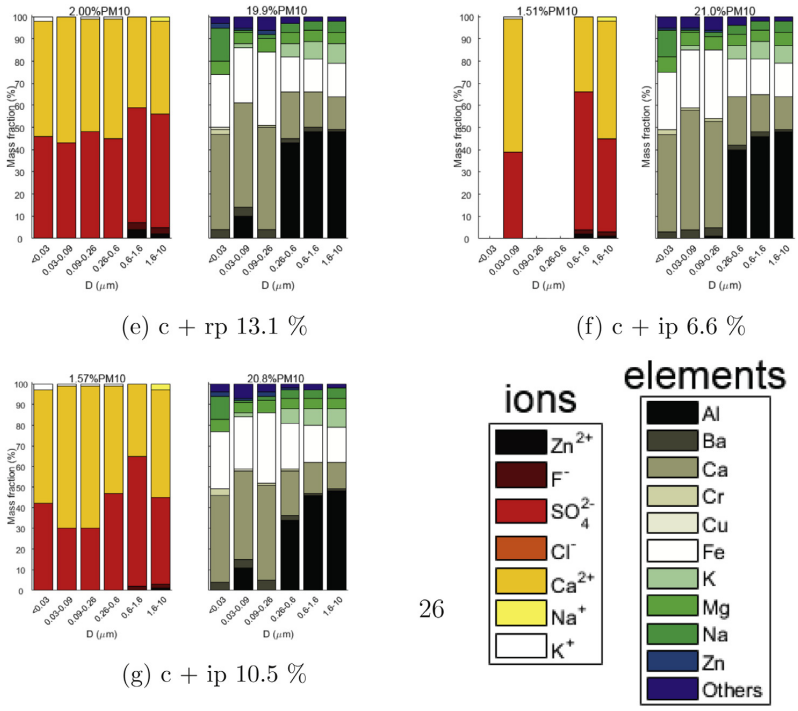

Fig. C.8. Continued

References

[1] U.S., The clean power plan, https://www.whitehouse.gov/climate-change, 2015(accessed 24.11.15).

[2] U.K., 2010 to 2015 government policy: greenhouse gas emissions, https://www.gov.uk/government/publications/2010-to-2015-government-policy-greenhouse-gas-emissions/2010-to-2015-government-policy-greenhouse-gas-emissions, 2015(accessed 24.11.15).

[3] K.V. Shah, M.K. Cieplik, C.I. Betrand, W.L. van de Kamp, H.B. Vuthaluru, Correlatind the effects of ash elements and their association in the fuel matrix with the ash release during pulverized fuel combustion, Fuel Process. Technol. 91 (2010) 531–545, doi:10.1016/j.fuproc.2009.12.016.

[4] B.M. Jenkins, L.L. Baxter, T.R. Miles Jr., T.R. Miles, Combustion properties of biomass, Fuel Process. Technol. 54 (1998) 17–46.

[5] T. Sorvajärvi, N. DeMartini, J. Rossi, J. Toivonen, In situ measurement technique for simultaneous detection of K, KCl, and KOH vapours released during combustion of solid biomass fuel in a single particle reactor, Appl. Spectrosc. 68 (2014) 179–184.

[6] H.P. Nielsen, F.J. Frandsen, K. Dam-Johansen, L.L. Baxter, The implications of chlorine-associated corrosion on the operation of biomass-fired boilers, Prog. Energy Combust. Sci. 26 (2000) 283–298.

[7] H. Kuuluvainen, P. Karjalainen, C.J.E. Bajamundi, J. Maunula, P. Vainikka, J. Roppo, J. Keskinen, T. Rönkkö, Physical properties of aerosol particles measured from a bubbling fluidized bed boiler, Fuel 139 (2015) 144–153.

[8] A. Leppänen, H. Tran, R. Taipale, E. Välimäki, A. Oksanen, Numerical modeling of fine particle and deposit formation in a recovery boiler, Fuel 129 (2014) 45–53, doi:10.1016/j.fuel.2014.03.046.

[9] Y. Ninomiya, L. Zhang, A. Sato, Z. Dong, Influence of coal particle size on particulate matter emission and its chemical species produced during coal combustion, Fuel Process. Technol. 85 (2004) 1065–1088, doi:10.1016/j.fuproc.2003.10.012.

[10] Y. Zhuang, Y.J. Kim, T.G. Lee, P. Biswas, Experimental and theorethical studies of ultra-fine particles behavior in electrostatic precipitators, J. Electrost. 48 (2000) 245–260.

[11] A. Suriyawong, C.J. Hogan, J. Jiang, P. Biswas, Charged fraction and electrostatic collection of ultrafine and submicrometer particles formed during O_2–CO_2 coal combustion, Fuel 87 (6) (2007) 673–682, doi:10.1016/j.fuel.2007.07.024.

[12] United Nations Economic Commission for Europe [UN-ECE], 1999 protocol to abate acidification, eutrophication and ground-level ozone to the convention on long-range transboundary air pollution, as amended on 4 May 2012, ECE/EB. AIR/114, United Nations Economic Commission for Europe [UN-ECE], 6 May 2013.

[13] The European Parliament and the European Council, On the limitation of emissions of certain pollutants into the air from large combustion plants, Directive 2001/80/EC, The European Parliament and the European Council, 23 October 2001.

[14] The European Parliament and the European Council, On industrial emissions (integrated pollution prevention and control) (Recast), Directive 2010/75/EU, The European Parliament and the European Council, 17 December 2010.

[15] The European Parliament and the European Council, On the limitation of emissions of certain pollutants into the air from medium combustion plants, Directive 2015/2193, The European Parliament and the European Council, 28 November 2015.

[16] The European Industrial Bioenergy Initiative, Boosting the contribution of Bioenergy to the EU climate and energy ambitions: implementationplan 2013–2017, Version of 24 January 2014, p. 3. https://setis.ec.europa.eu/system/files/Bioenergy%20EII%202013-2017%20IP.pdf

[17] The European Commission, State of play on the sustainability of solid and gaseous biomass used for electricity, heating and cooling in the EU, SWD(2014) 259 final, The European Commission, Brussels, 28 July 2014, p. 5.

[18] The European Commission, Technology assessment: accompanying the document energy technologies and innovation, COM(2013) 253 final, The European Commission, 2 May 2013, pp. 23, 25.

[19] The European Commission, Impact assessment: accompanying document to the report from the Commission to the Council and the European Parliament on sustainability requirements for the use of solid and gaseous biomass sources in electricity, heating and cooling, COM(2010) 11 final, The European Commission, Brussels, 25 February 2010, pp. 21, 42–43.

[20] National Energy Technology Laboratory, Role of alternative energy sources: pulverized coal and biomass co-firing technology assessment, DOE/NETL-2012/1537, National Energy Technology Laboratory, August 30, 2012, p. VII.

[21] Biomass R&D Board, "The Federal Activities Report on the Bioeconomy", 2016, pp. 34–35. http://www.biomassboard.gov/pdfs/farb_2_18_16.pdf

[22] Environmental Protection Agency, Carbon pollution emission guidelines for existing stationary sources: electric utility generating units; final rule, Fed. Regist. 80 (205) (2015) 64885, 64804(October 23, 2015, Friday).

[23] G. Barbose, Renewables portfolio standards in the united states: a status update, State-Federal RPS Collaborative National Summit on RPS, Washington, D.C., November 6 2013, Environmental Protection Agency (2013), p. 9. https://www.epa.gov/sites/production/files/2015-08/documents/cpp-final-rule.pdf.

[24] M. Aho, P. Vainikka, R. Taipale, P. Yrjas, Effective new chemicals to prevent corrosion due to chlorine in power plant superheaters, Fuel 87 (2008) 647–654. http://dx.doi.org/10.1016/j.fuel.2007.05.033

[25] J. Keskinen, K. Pietarinen, M. Lehtimäki, Electrical low pressure impactor, J. Aerosol Sci. 23 (1992) 353–360.
[26] S.C. Wang, R.C. Flagan, Scanning electrical mobility spectrometer, Aerosol Sci. Technol. 13 (1990) 230–240.
[27] W.C. Hinds, Aerosol technology properties, behavior, and measurement of airborne particles, 2nd ed., John Wiley & Sons, 1999. Eqs. (7-31) and (7-32))
[28] A.K. Frey, K. Saarnio, H. Lamberg, F. Mylläri, P. Karjalainen, K. Teinilä, S. Carbone, J. Tissari, V. Niemelä, A. Häyrinen, J. Rautiainen, J. Kytömäki, P. Artaxo, A. Virkkula, L. Pirjola, T. Rönkkö, J. Keskinen, J. Jokiniemi, R. Hillamo, Optical and chemical characterization if aerosols emitted from coal, heavy and light fuel oil, and small-scale wood combustion, Environ. Sci. Technol. 48 (2014) 827–836.
[29] E.I. Kauppinen, Aerosol formation in coal combustion processes, J. Aerosol Sci. 22 (1991) S451–S454. (Suppl. 1)
[30] U. Mathis, J. Ristimäki, M. Mohr, J. Keskinen, L. Ntziachristos, Z. Samaras, P. Mikkanen, Sampling conditions for the measurement of nucleation mode particles in the exhaust of a diesel vehicle, Aerosol Sci. Technol. 38 (12) (2004) 1149–1160, doi:10.1080/027868290891497.
[31] I. Abdul-Khalek, D. Kittelson, F. Brear, 1999, The influence of dilution conditions on diesel exhaust particle size distribution measurements, SAE Technical Paper 1999-01-1142, SAE, 10.4271/1999-01-1142.
[32] J. Ristimäki, A. Virtanen, M. Marjamäki, A. Rostedt, J. Keskinen, On-line measurement of size distribution and effective density of submicron aerosol particles, J. Aerosol Sci. 33 (11) (2004) 1541–1557.
[33] A. Virtanen, J. Ristimäki, J. Keskinen, Method for measuring effective density and fractal dimension of aerosol agglomerates, Aerosol Sci. Technol. 38 (5) (2004) 437–446.
[34] W.M. Haynes (Ed.), CRC Handbook of Chemistry and Physics, 96th Edition (Internet Version 2015-2016), CRC Press/Taylor & Francis, Boca Raton, FL, 2011, pp. 4–88.
[35] W.C. Hinds, Aerosol technology properties, Behavioir, and Measurement of Airborne Particles, 2nd ed., John Wiley & Sons (1999).
[36] A. Wiedensohler, An approximation of the bipolar charge distribution for particles in the submicron size range, J. Aerosol Sci. 19 (3) (1988) 387–389.
[37] M.M. Maricq, On the electrical charge of motor vehicle exhaust particles, Aerosol Sci. 37 (2006) 858–874.
[38] A.D. Filippo, M.M. Maricq, Diesel nucleation mode particles: semi-volatile or solid? Environ. Sci. Technol. 42 (2008) 7957–7962.
[39] T. Lähde, T. Rönkkö, A. Virtanen, T.J. Schuck, L. Pirjola, K. Hämeri, M. Kulmala, F. Arnold, D. Rothe, J. Keskinen, Heavy duty diesel engine exhaust aerosol particle and ion measurements, Environ. Sci. Technol. 43 (2009) 163–168.
[40] J. Alanen, E. Saukko, K. Lehtoranta, T. Murtonen, H. Timonen, R. Hillamo, P. Karjalainen, H. Kuuluvainen, J. Harra, J. Keskinen, T. Rönkkö, The formation and physical properties of the particle emissions from a natural gas engine, Fuel 162 (2015) 155–161.
[41] A. Gani, K. Morishita, K. Nishikawa, I. Naruse, Characteristics of co-combustion of low-rank coal with biomass, Energy Fuel 19 (2005) 1652–1659.
[42] J. Joutsensaari, E.I. Kauppinen, P. Ahonen, T.M. Lind, S.I. Ylätalo, J.K. Jokiniemi, J. Hautanen, M. Kilpeläinen, Aerosol formation in real scale pulverized coal combustion, J. Aerosol Sci. 23 (1992) S241–S244. (Suppl. 1)
[43] H. Yi, J. Hao, L. Duan, X. Tanf, P. Ning, X. Li, Fine particle and trace element emissions from an anthracite coal-fired power plant equipped with a bag–house in China, Fuel 87 (2008) 2050–2057.
[44] H. Wu, A.J. Pedersen, P. Glarborg, F.J. Frandsen, K. Dam-Johansen, B. Sander, Formation of fine particles in co-combustion of coal and solid recovered fuel in a pulverized coal-fired power station, Proc. Combust. Inst. 33 (2011) 2845–2852.
[45] F. Mylläri, E. Asmi, T. Anttila, E. Saukko, V. Vakkari, L. Pirjola, R. Hillamo, T. Laurila, A. Häyrinen, J. Rautiainen, H. Lihavainen, E. O'Connor, V. Niemelä, J. Keskinen, M.D. Maso, T. Rönkkö, New particle formation in the fresh flue-gas plume from a coal-fired power plant: effect of flue-gas cleaning, Atmos. Chem. Phys. 16 (2016) 1–12.
[46] S.I. Ylätalo, J. Hautanen, Electrostatic precipitator penetration function for pulverized coal combustion, Aerosol Sci. Technol. 29 (1) (1998) 17–30, doi:10.1080/02786829808965547.

Publication II

Mylläri, F., Asmi, E., Anttila, T., Saukko, E., Vakkari, V., Pirjola, L., Hillamo, R., Laurila, T., Häyrinen, A., Rautiainen, J., Lihavainen, H., O'Connor, E., Niemelä, V., Keskinen, J., Dal Maso, M., Rönkkö, T. "New particle formation in fresh flue-gas plume from a coal-fired power plant: effect of flue-gas cleaning" *Atmospheric Chemistry and Physics*

Atmos. Chem. Phys., 16, 7485–7496, 2016
www.atmos-chem-phys.net/16/7485/2016/
doi:10.5194/acp-16-7485-2016

Atmospheric Chemistry and Physics Open Access EGU

New particle formation in the fresh flue-gas plume from a coal-fired power plant: effect of flue-gas cleaning

Fanni Mylläri[1], Eija Asmi[2], Tatu Anttila[1], Erkka Saukko[1], Ville Vakkari[2], Liisa Pirjola[3], Risto Hillamo[2], Tuomas Laurila[2], Anna Häyrinen[4], Jani Rautiainen[4], Heikki Lihavainen[2], Ewan O'Connor[2], Ville Niemelä[5], Jorma Keskinen[1], Miikka Dal Maso[1], and Topi Rönkkö[1]

[1]Department of Physics, Tampere University of Technology, P.O. Box 692, 33101 Tampere, Finland
[2]Atmospheric Composition Research, Finnish Meteorological Institute, 00560, Helsinki, Finland
[3]Department of Technology, Metropolia University of Applied Sciences, 00180, Helsinki, Finland
[4]Helen Oy, 00090 Helen, Helsinki, Finland
[5]Dekati Ltd., Tykkitie 1, 36240 Kangasala, Finland

Correspondence to: Topi Rönkkö (topi.ronkko@tut.fi)

Received: 8 December 2015 – Published in Atmos. Chem. Phys. Discuss.: 5 February 2016
Revised: 24 May 2016 – Accepted: 30 May 2016 – Published: 15 June 2016

Abstract. Atmospheric emissions, including particle number and size distribution, from a 726 MW_{th} coal-fired power plant were studied experimentally from a power plant stack and flue-gas plume dispersing in the atmosphere. Experiments were conducted under two different flue-gas cleaning conditions. The results were utilized in a plume dispersion and dilution model taking into account particle formation precursor (H_2SO_4 resulted from the oxidation of emitted SO_2) and assessment related to nucleation rates. The experiments showed that the primary emissions of particles and SO_2 were effectively reduced by flue-gas desulfurization and fabric filters, especially the emissions of particles smaller than 200 nm in diameter. Primary pollutant concentrations reached background levels in 200–300 s. However, the atmospheric measurements indicated that new particles larger than 2.5 nm are formed in the flue-gas plume, even in the very early phases of atmospheric ageing. The effective number emission of nucleated particles were several orders of magnitude higher than the primary particle emission. Modelling studies indicate that regardless of continuing dilution of the flue gas, nucleation precursor (H_2SO_4 from SO_2 oxidation) concentrations remain relatively constant. In addition, results indicate that flue-gas nucleation is more efficient than predicted by atmospheric aerosol modelling. In particular, the observation of the new particle formation with rather low flue-gas SO_2 concentrations changes the current understanding of the air quality effects of coal combustion. The results can be used to evaluate optimal ways to achieve better air quality, particularly in polluted areas like India and China.

1 Introduction

On the global scale, nearly 40 % of annual production of electricity is covered by coal combustion (EU, 2014). In addition to CO_2 emissions, known to have climatic effects, coal combustion causes emissions of other harmful pollutants like NO_x, SO_2 and particulate matter, all decreasing the air quality and increasing health-related risks but also affecting climate directly and indirectly. For instance, SO_2 affects the climate indirectly because it tends to oxidize in atmosphere and form H_2SO_4, which affects particle formation. Coal-combustion-related air quality problems exist, especially in developing countries like China (Huang et al., 2014), where power production is not always equipped with efficient flue-gas cleaning systems. However, with proper combustion and flue-gas cleaning technologies the fine particle emissions of coal combustion can be decreased to a very low level and the emissions of gaseous pollutants other than CO_2 can also be decreased (Helble, 2000; Saarnio et al., 2014). Particle mass and number emission factors for the 300 MW coal-fired power plant with electrostatic precipitator (ESP) and flue-gas desulfurization unit (FGD) have been

reported by Frey et al. (2014): the emission for particle mass (PM_1) was 0.18 ± 0.06 mg MJ^{-1} and for fine particle number $2.3 \times 10^9 \pm 4.0 \times 10^9$ MJ^{-1}. However, it can be expected that particle emissions and characteristics such as particle size are highly dependent on technologies used in power production. Only a few studies have reported particle number size distributions and mean particle diameter for the coal combustion emissions. The mean particle diameters have been reported to be between 100 nm (Frey et al., 2014; Yi et al., 2008) and 1 µm (Yi et al., 2008; Lee et al., 2013). According to Saarnio et al. (2014), chemical composition of particles in the efficiently cleaned flue gas after the FGD is shifted towards desulfurization chemicals. Interestingly, sulfate particle emissions from coal combustion with proper cleaning technologies can restrain global warming due to a cooling effect of the particles (Frey et al., 2014; Charlson et al., 1992; Lelieveld and Heintzenberg, 1992).

Due to the emission limits of power plants, driven by the need for a healthier environment, emissions should be kept at minimum. This can be achieved by different technologies. Flue-gas NO_x emissions can be reduced in the power plant boiler by applying low-NO_x burners, whereas SO_2 emissions can be reduced by flue-gas desulfurization (FGD) (Srivastava and Jozewicz, 2001). Particle emissions can be reduced by electrostatic precipitators (ESP) and fabric filters (FF). Very low emission levels can be achieved by these techniques. For example, for particle emission, ESP typically removes 99 % (Helble, 2000) of fine particles. Further, Saarnio et al. (2014) showed that a desulfurization plant with fabric filters removes up to 97 % of fine particles. A combination of these techniques would then remove 99.97 % of fine particle emissions formed in combustion. However, particle emission as well as the effects of technologies can differ if the emissions are measured from the diluted flue gas in the atmosphere. In principle, particle number and even particle mass can increase in the atmosphere, for example, due to nucleation and condensation processes (Marris et al., 2012; Buonanno et al., 2012). However, there are very few observations of the processes in the diluting flue gas during the first few minutes after the stack.

Power plant plumes have been studied with aircraft by measuring long-distance crosswind profiles of gases and particles (Stevens et al., 2012; Brock et al., 2002; Lonsdale et al., 2012; Junkermann et al., 2011). Stevens et al. (2012) and Lonsdale et al. (2012) have compared these measurements to modelling results, which were based on emission inventory values. Modelling results indicated that secondary particle formation occurs in the plumes after emission from the stack and the measurement results show correlation with the model especially at distances of 10–20 km. Brock et al. (2002) argue that the secondary particle formation begins in a 2 h old plume. A study by Brock et al. (2002) has focused on 0 to 13 h old power plant plumes. However, Brock et al. (2002) do not report particle number concentrations for fresh flue gas. Crosswind profiles shown in the study of Stevens et al. (2012) were at distances from 5 km to a little over 50 km, and these results were also used in Lonsdale et al. (2012). On the contrary, Junkermann et al. (2011) followed the plume centre line based on the SO_2 concentrations and also made a few crosswind profiles of the studied plume.

The aim of this study was to characterize how the atmospheric emissions from a 726 MW coal-fired power plant depend on flue-gas cleaning, i.e. desulfurization plant and fabric filters (later referred to as "FGD + FF off" and "FGD + FF on"). In addition to the stack measurements for pollutants, the study aimed to show how the flue-gas cleaning affects real atmospheric concentrations of emitted CO_2, SO_2 and particles. The study included experiments conducted in the stack of the power plant, measurements conducted with a helicopter equipped with instruments for CO_2, SO_2 and particles and flue-gas plume dispersion and aerosol process modelling.

2 Experimentation

The studied power plant is a base-load station located near Helsinki city centre, Finland. The power plant consists of two 363 MW_{th} coal-fired boilers. The energy is produced by coal combustion in 12 low-NO_x technology burners (Tampella/Babcock-Hitachi HTNR low-NO_x), situated at the front wall of the boiler. The properties of coal used in this study are listed in Table S1 in the Supplement. Combustion releases flue gases that are cleaned in electrostatic precipitator (ESP), semi-dry desulfurization plant (FGD) and fabric filters (FF) before the stack. There are separate flue-gas ducts and flue-gas cleaning systems for each boiler.

The flue gas was studied in two different locations: the flue-gas plume and a reference point inside the stack. Measurements were made at both locations in two different flue-gas cleaning situations: FGD + FF off and, with all cleaning systems, FGD + FF on. The measurement location in the stack was at the height of +35 m above sea level. The flue-gas temperature inside the duct was 78 ± 2 °C in normal operation conditions and 130 ± 13 °C during FGD + FF off. The flue-gas plume concentrations were measured with a helicopter equipped with aerosol instruments. The flying altitude of the helicopter was 150 m above ground level or higher, which corresponds to the lidar (Halo Photonics Streamline Doppler lidar with full-hemispheric scanning capability, Pearson et al., 2009) (Fig. S2) results for plume altitude. It should be noted that only the flue gases from the boiler under investigation were steered to bypass FGD and FF. Thus, in the FGD + FF off situation, the flue-gas plume consisted of both the cleaned flue gas and the flue gas cleaned by ESP. This has to be kept in mind during the analysis of atmospheric measurements.

The measurements were made on 24 March 2014 in two separate 1 h periods (see specific times from Fig. S2, the black rectangles; the first illustrates FGD + FF on and the lat-

ter FGD + FF off). Weather conditions were stable during the study. The wind direction and speed were $216 \pm 5.51°$ (based on lidar data) and 6.5 m s^{-1} in FGD + FF off and $220 \pm 6.25°$ and 4 m s^{-1} in FGD + FF on. The marine boundary layer height was 246–258 m and the planetary boundary layer heights were 360–530 m. However the calculations were made within the marine boundary layer because the flue-gas plume did not rise above it. The background aerosol concentrations for each measured gaseous component were 403 ppm for CO_2 and less than 2–8 ppb for SO_2. The range of ambient temperature was 6.6–6.9 °C, the global radiation was 347–466 W m^{-2} and the visibility was 29 043–36 000 m (see standard deviations from Table S2).

The instrument installations in different locations are shown in Fig. S3. The sampling of flue gas in the stack was performed with a Fine Particle Sampler (FPS; Dekati Ltd., Mikkanen et al., 2001) with total dilution ratio (DR) of 27. Probe and dilution air temperatures were at 200 °C. The sample was analysed using the following instruments: Condensation Particle Counter (CPC3776; TSI Inc., Agarwal and Sem, 1980), Electrical Low Pressure Impactor (ELPI; Dekati Ltd., Keskinen et al., 1992), Scanning Mobility Particle Sizer (SMPS; Wang and Flagan, 1990) 0.6/6 standard L min^{-1} (DMA3071, CPC3775 TSI Inc.) and gas analysers for diluted CO_2 (model VA 3100, Horiba) and NO, NO_2 and NO_x (model APNA 360, Horiba). Measurement data were also received from a normal operation monitoring of the emissions, including raw flue-gas SO_2, NO_x, CO_2 concentrations and dust (SICK RM 230, calibrated based on SFS-EN 13284-1 standard). In contrast to stack sampling, the sample in the flue-gas plume dilutes naturally and can be sampled to equipment without additional dilution of aerosol sample. The sampling inlet position in the helicopter is shown in Fig. S3. Natural dilution causes rapid changes in concentrations, thus high measurement frequency equipment was used in the helicopter. CPC3776 (TSI Inc.) was installed to measure the total particle number concentration, whereas the Engine Exhaust Particle Sizer (EEPS, TSI Inc., Mirme, 1994) measured the particle number size distribution at 1 Hz sampling frequency from 5.6 to 560 nm. Gas concentrations for CO_2/CH_4/H_2O (Cavity spring-down spectrometry Picarro model G1301-m CO_2/CH_4/H_2O flight analyser) and SO_2 (Thermo Scientific Inc. model 43i SO_2 analyser, with 5 s response time) were measured continuously with 1 Hz frequency (see more details in Table S3).

Figure 1 shows the helicopter measurement routes for the FGD + FF on and FGD + FF off situations. The objective of flight routes was to follow the centre line of the flue-gas plume. The helicopter flew both up and down the plume; GPS data were used to separate these two flight situations to calculate the distance and the age of the plume separately.

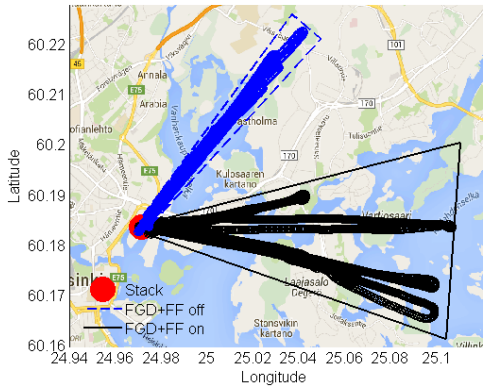

Figure 1. Helicopter flight routes. The wind blew at an angle of $216 \pm 5.51°$ (based on lidar data) and the flight direction was $213 \pm 4.14°$ (based on GPS data for helicopter) in FGD + FF off (blue circles). Corresponding angles for FGD + FF on (black circles) were $220 \pm 6.25°$ (wind direction based on lidar data) and $223 \pm 5.66°$ (flight direction based on GPS data for helicopter). The triangular shapes (black and blue lines) show the helicopter GPS coordinates that have been taken into account in the calculations.

2.1 Model description: Gaussian plume model

The Gaussian plume model is a solution to an advection–diffusion equation that describes the changes in the pollutant concentrations due to advection of wind and turbulent mixing with the surrounding air (Stockie, 2011). Accordingly, the concentration of a pollutant i, C_i, emitted from a point-like source, can be expressed as follows:

$$C_i(x,y,z) = \frac{Q_i}{2\pi U \sigma_y \sigma_z} \exp\left(-\frac{y^2}{\sigma_y^2}\right)\left[\exp\left(-\frac{(z-H)^2}{\sigma_z^2}\right) + \exp\left(-\frac{(z+H)^2}{\sigma_z^2}\right)\right]. \quad (1)$$

Here x, y and z are the spatial coordinates, aligned so that the x axis corresponds to the wind direction and H is the height at which i is emitted (stack height). Also, Q_i is the emission rate of i at the source, U is the mean wind speed and σ_z as well as σ_y are the so-called dispersion coefficients which reflect the spatial extent of the plume as a function of the downwind distance x. The dispersion coefficients were calculated using the parameterization of Klug (1969) and the atmospheric stability class, which is needed to calculate the dispersion coefficients. Atmospheric stability classes were estimated based on the measurements of the wind speed and solar radiative flux at the surface. Moreover, the pollutant concentrations were calculated along the centre line of the plume, the value of U was set to constant and was equal to the average wind speed during the flights. Finally the value of z was set equal to the stack height (150 m).

It is worth noting that the background concentration of i is zero according to Eq. (1): $C_i \to 0$ when $z \to \infty$ or $y \to \pm\infty$. However, the flue gas emitted from the stack was actually cleaner in terms of particle number concentration than the background air when the flue gas was cleaned properly. In order to account for such cases, the following equation was used instead of Eq. (1):

$$\hat{C} = C_\infty + \frac{C_0 - C_\infty}{C_0} \times C_i, \quad (2)$$

where C_∞ is the background concentration of i, and C_0 is its concentration at the source. It can be readily shown that Eq. (2) is a solution to the advection–diffusion equation underlying Eq. (1). Also, it is easily verified that $\hat{C} \to C_\infty$ when $z \to \infty$ or $y \to \pm\infty$. Finally, the value of Q_i in Eq. (1) was chosen so that $\hat{C} \to C_0$ when $z \to H$ and $x, y \to 0$.

An important output of the model is the dilution ratio of the flue-gas plume, DR, which is calculated based on Eq. (3).

$$\mathrm{DR}(t) = \frac{[\mathrm{CO_2}(t)] - [\mathrm{CO_{2,\infty}}]}{[\mathrm{CO_{2,stack}}] - [\mathrm{CO_{2,\infty}}]} \quad (3)$$

In Eq. (3) $[\mathrm{CO_2}(t)]$ and $[\mathrm{CO_{2,\infty}}]$ are the modelled CO_2 concentration at time t and the CO_2 concentration measured in the stack, respectively.

2.1.1 Model description: nucleation rate and particle formation calculations

The particle appearance (driven by nucleation and growth) rates for the particles 2.5 nm in diameter were calculated using the parameterization developed by Lehtinen et al. (2007) presented in Eq. (4). The key input parameters for the model are the nucleation rate (J_{nuc}), the particle growth rate (GR) and the coagulation sink, of which the coagulation sink describes clusters that are removed via coagulational scavenging (CoagS). The parameter J_{nuc} is calculated based on the estimated sulfuric acid concentrations as a function of plume age as detailed below, and the particle growth rates are calculated by assuming growth only via irreversible condensation of sulfuric acid. Also, CoagS is calculated from the condensation sink CS (which is calculated in a fashion described below) using the Eq. (8) in Lehtinen et al. (2007). Also, the initial size of the freshly nucleated clusters was varied, and the value of the shape factor (m in Eq. 6 in Lehtinen et al., 2007) was set equal to -1.6.

$$J_x = J_{\mathrm{nuc}} \times \exp\left(-\gamma \times d_1 \times \frac{\mathrm{CoagS}(d_1)}{\mathrm{CS}}\right) \quad (4)$$

The nucleation rates J_{nuc} in the studied plume were calculated using the parameterization developed by Kulmala et al. (2006), which has also been applied previously to model nucleation in plumes (Stevens et al., 2012; Stevens and Pierce, 2013).

$$J_{\mathrm{nuc}} = A \times [\mathrm{H_2SO_4}] \quad (5)$$

In Eq. (5) $A = 1\times10^{-7}\ \mathrm{s^{-1}}$ or $A = 1\times10^{-6}\ \mathrm{s^{-1}}$ and $[\mathrm{H_2SO_4}]$ ($\mathrm{cm^{-3}}$) is the sulfuric acid concentration. The value of $A = 1\times10^{-7}\ \mathrm{s^{-1}}$ was chosen according to the study by Stevens et al. (2012) and Stevens and Pierce (2013). The initial size of the nucleated particles was assumed to be of 1.5 nm.

Formation of $[\mathrm{H_2SO_4}]$ was calculated assuming that it is produced only via the $\mathrm{OH} + \mathrm{SO_2}$ reaction and the only loss pathway for H_2SO_4 is condensation onto the particle surfaces. When steady-state is assumed, the $[\mathrm{H_2SO_4}]$ can be calculated from Eq. (6).

$$[\mathrm{H_2SO_4}] = k_1 \times \frac{[\mathrm{SO_2}] \times [\mathrm{OH}]}{\mathrm{CS}} \quad (6)$$

In Eq. (6) k_1 is the reaction constant between OH and SO_2 (Table B.2 in Seinfeld and Pandis, 2006). The SO_2 concentrations were taken from the helicopter measurements, and the time development of CS and [OH] in the plume were modelled as follows. First, CS was calculated using the relation shown in Eq. (7).

$$\mathrm{CS} = \frac{\mathrm{CS_{stack}}}{\mathrm{DR}} + \mathrm{CS_\infty} \times \left(1 - \frac{1}{\mathrm{DR}}\right) \quad (7)$$

In Eq. (7) $\mathrm{CS_{stack}}$ is the condensation sink of aerosols measured in the stack, and $\mathrm{CS_\infty}$ is the condensation sink of the background aerosols. The value of the latter parameter was calculated from the size distributions measured at the SMEAR III station (Junninen et al., 2009), which is located around 2 km away from the power plant. Second, [OH] was calculated using the parameterization of Stevens et al. (2012), which has downward shortwave radiative flux at the surface and $[\mathrm{NO}_x]$ as main inputs. The value for the former parameter was taken from the measurements (using the value averaged over the measurement periods), and the NO_x concentrations were calculated from Eq. (8).

$$[\mathrm{NO}_x(t)] = \frac{[\mathrm{NO}_{x,\mathrm{stack}}]}{\mathrm{DR}(t)} \quad (8)$$

In Eq. (8) $[\mathrm{NO}_{x,\mathrm{stack}}]$ is the NO_x concentration measured in the stack. It should be noted here that in the calculations the background concentration of NO_x is assumed to be of minor importance when compared to NO_x emitted by power plants. To support this, the study of Pirjola et al. (2014) indicates that in the harbour area close to the power plant studied, the NO_x concentration level is typically clearly lower than 100 ppb.

3 Results

3.1 Primary emissions of the coal-fired power plant

The SO_2 and particle emissions of the power plant were strongly dependent on the flue-gas cleaning system. This can be seen in Table 1, which shows flue-gas concentrations for CO_2, SO_2, NO_x, O_2, particle number (N_{tot}), dust as well as

Table 1. Flue-gas concentrations of CO_2, SO_2, NO_x, O_2, total particle number (N_{tot}), dust and flue-gas flow rate in the stack. Mean values (and standard deviation) are presented for both flue-gas cleaning conditions (FGD + FF on and FGD + FF off).

	FGD + FF off	FGD + FF on
CO_2 (%)	9.92 ± 2.2	10.3 ± 0.96
SO_2 (ppbv)	$243\,000 \pm 71\,300$	$55\,200 \pm 14\,600$
NO_x (ppmv)	252 ± 74	258 ± 65
O_2 (%)	6.16 ± 0.11	6.11 ± 0.10
N_{tot} (cm^{-3})	$(1.8 \pm 0.2) \times 10^6$	420 ± 640
Dust ($mg\,Nm^{-3}$)	188 ± 82	4 ± 1
Flow ($Nm^3\,h^{-1}$)	$(4.86 \pm 0.20) \times 10^5$	$(4.65 \pm 0.064) \times 10^5$

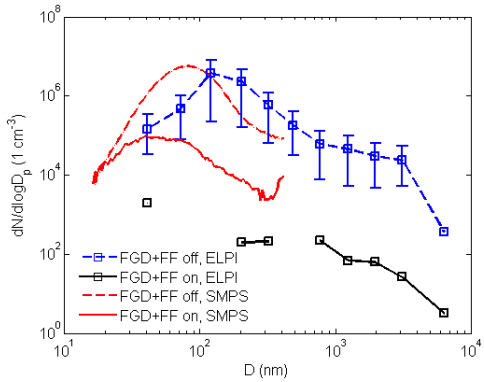

Figure 2. Particle size distributions measured with ELPI and SMPS from the flue gas in the stack. ELPI and SMPS data are shown in operation conditions, FGD + FF on and FGD + FF off. The x axis is aerodynamic diameter for ELPI data and electrical mobility diameter for SMPS data.

flow rate in the duct in both flue-gas cleaning conditions. In the shift from FGD + FF off to FGD + FF on, the SO_2 concentration decreased to nearly a fifth, the concentration of dust decreased by a factor of 50 and the N_{tot} decreased by a factor of 4000. For other parameters the effect of FGD + FF was insignificant.

Figure 2 shows the particle number size distributions of flue gas in the stack in both cleaning conditions. These were measured using an electrical low pressure impactor (ELPI) and a scanning mobility particle sizer (SMPS) in both FGD + FF on/off cases. In the FGD + FF on case, the SMPS measurement is a median value over a few hours of operation due to low particle number concentrations in the stack. Based on the SMPS measurement the particle geometric mean electrical mobility equivalent diameter was 80 nm and the width of particle number size distribution (geometric standard deviation, GSD) was 1.45 for FGD + FF off. In comparison, the geometric mean electrical mobility equivalent diameter was 31 nm for FGD + FF on and the width of particle number size distribution was 2.15. Based on the measurements using the ELPI geometric mean aerodynamic equivalent diameter was 141 nm and GSD was 1.41 for FGD + FF off. The difference in mean diameter measured using the ELPI and the SMPS comes from the difference in size classification principles of these instruments and enables the determination of effective density of measured particles. The effective density calculation is based on the relation between the electrical mobility equivalent diameter and the aerodynamic equivalent diameter of the particle (see Ristimäki et al., 2002). In this study case the difference in equivalent diameter indicates effective density larger than unit density for emitted particles (approximately $3.1\,g\,cm^{-3}$). In comparison, Saarnio et al. (2014) used an effective density of $2.5\,g\,cm^{-3}$ to convert the electrical mobility diameter measured using a SMPS to an aerodynamic diameter. When studying FGD + FF on, the particle concentrations were so low and thus accurate determination of mean particle size was not possible from the particle size distribution measured by the ELPI.

Flue-gas samples from the stack were diluted with hot dilution air before the particle instruments and thus the particle number concentrations (Table 1) and particle size distributions (Fig. 2) are for non-volatile particles. In combustion studies the hot dilution air is typically used to prevent the formation of liquid nucleation particles and to minimize the effects of condensation of semi-volatile compounds on particles. However, to ensure the measured particles were non-volatile and not affected by the dilution method itself, a thermodenuder (Rönkkö et al., 2011) was used periodically after the sampling and dilution. The thermodenuder did not affect the particle number size distribution, which confirms the non-volatile nature of the measured particles. Due to this non-volatility of the particles, the lifetime of the primarily emitted particles in the atmosphere can be longer than that of volatile particles, e.g. nucleation mode particles observed in vehicle exhaust (Lähde et al., 2009).

3.2 Atmospheric measurements

Figure 3 shows the measured flue-gas plume concentrations as a function of plume age. Diffusion losses for the particles in the sampling lines were calculated based on the measurement set-up (see Fig. S4). The data were recorded based on GPS coordinates, which were used to calculate distances from the stack, and the distances were changed to correspond plume age using wind speeds of 6.5 and $4.0\,m\,s^{-1}$ (lidar, Fig. S2). The calculation showed that nearly 70 % of the 2.5 nm particles in diameter was lost in the sampling lines and thus the total concentration shown in Fig. 3 can be higher than shown here. The vertical lines denote the 2 km distance from the stack. Figure 3 shows the dilution timescale of the flue gas in terms of CO_2 and SO_2 in both operation conditions. The same trend in SO_2 and N_{tot} concentrations as observed in Table 1 was measured by instruments installed in

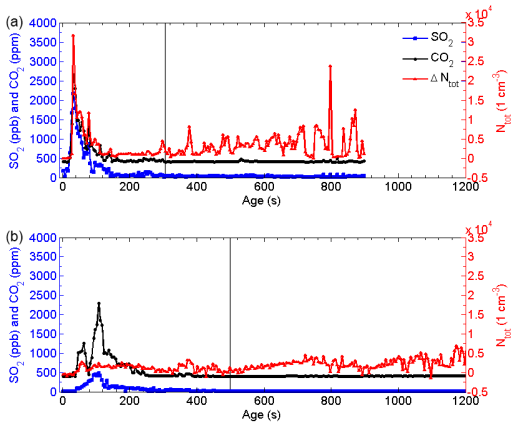

Figure 3. Concentrations of power plant flue-gas components measured by instruments installed in the helicopter as a function of plume age; FGD + FF off in the top panel and FGD + FF on in the bottom panel. SO_2 (ppb, blue line) and CO_2 (ppm, black line) concentrations on the left axes and total particle number concentration ΔN_{tot} (1 cm^{-3}, red line, from CPC) on the right axes. The ΔN_{tot} is calculated using the background value calculated from the upwind side of the stack ($CO_{2,bg}$ was 403 ppm and $SO_{2,bg}$ 2–8 ppb). The grey vertical lines denote 2 km distance from the stack in FGD + FF on/off. The presented results are 5 s median values.

the helicopter; in FGD + FF off the particle and SO_2 concentrations were higher than the FGD + FF on situation. It should be kept in mind that in FGD + FF off only one of the two flue-gas cleaning systems was bypassed.

Plume dilution can be evaluated by the CO_2 concentrations (in Fig. 3a and b), which show that the FGD + FF off case dilutes to approximately background levels in 200 s (0.74 km) and the FGD + FF on case in 300 s (1.5 km). The peak values for CO_2, SO_2 and N_{tot} were 3195 ppm, 2193 ppb, 3.3×10^4 cm^{-3} in the FGD + FF off and 3254 ppm, 585 ppb, 0.4×10^4 cm^{-3} for the FGD + FF on. However, dilution decreases the CO_2, SO_2 and N_{tot} concentrations in the atmosphere to 422 ppm, 52 ppb in FGD + FF off, and 473 ppm, 89 ppb in FGD + FF on. The N_{tot} reached near background concentrations after 200 s and 300 s. The background gaseous concentrations for each measured gaseous component were 403 ppm and 2–8 ppb for CO_2 and SO_2, respectively. The boundary layer mixing started during the FGD + FF on measurements and thus the background values measured from the upwind side flight loops from the stack were averaged and subtracted from both FGD + FF on/off. It can be noted that very near (first 10–50 s) the stack the helicopter was not in the plume. This can be seen from CO_2 and SO_2 concentration values presented in Fig. 3a and b when approaching plume age zero. Thus, the dilution process is discussed below, mainly from the maximum concentrations onward.

An increase in total particle concentration can be seen in Fig. 3 after 400 s aged the flue-gas plume. This tendency can be seen in both flue-gas cleaning situations. Based on Fig. 3a, for the FGD + FF off situation, the background particle concentration was 1430 cm^{-3}, after 200 s the concentration was at the background level and after 400 s it increased significantly, even up to an average level of 5000 cm^{-3}. Based on CO_2 measurements, the dilution of flue gas was practically complete at 200 s. Similarly, in the FGD + FF on situation after 500 s the particle concentration was slightly above background, after which it increased even up to 5000 cm^{-3} after 700 s. Thus, the concentrations in the diluted and aged flue-gas plume were higher than the background and significantly higher than could be expected based on the primary particle concentrations and observed dilution profiles. In general, taking into account the fact that there is no comprehensive measurement of the primary precursor matrix (only [SO_2] is measured), the primary precursor matrix might include low-volatile organics and SO_3, which can increase the probability of new particle formation. Due to the increasing trend in particle concentration, some estimation about formation rates can be calculated. Depending on the plume age, the mean formation rates calculated from the data shown in Fig. 3 depended on the plume age being for FGD + FF off 0–81 cm^{-3} s^{-1} and for FGD + FF on, 0 to 18 cm^{-3} s^{-1} (mean slope of increasing total particle number concentration at 400–482 and 500–692 s).

Particle size distributions, shown in Fig. S5, were calculated from the EEPS data measured from the helicopter in both FGD + FF on/off situations as a 10 s moving median method. The particle size distribution in the FGD + FF off case had a mode around 80 nm, which refers to the solid particle median diameter measured with the SMPS from the flue gas in the stack. The particle size distribution measurement made using the EEPS (Fig. S5) supports the results for total particle number measurement made by the CPC (Fig. 3), i.e. in terms of particles the flue gas dilutes in 0–300 s in FGD + FF off. In addition, the particle size distributions measured by the EEPS indicates a slight increase of nanoparticle concentrations during the dilution and dispersion of the flue gas in the atmosphere. Although EEPS total particle number concentration cannot be compared to total concentration of CPC because Levin et al. (2015) showed that EEPS total particle number concentration is not comparable with a CPC. Further, Fig. S5 shows that the EEPS particle size distribution data are noisy and, based on Awasthi et al. (2013), can show maximum of 67 % error compared to SMPS.

3.3 Model calculations: modelled vs. measured CO_2 concentrations

The validity of the Gaussian plume model was tested against CO_2 measurements from the plume. Median CO_2 concentrations were calculated using the measurement data at a 5 s

Table 2. Comparison between modelled CO_2 concentration and measured CO_2 concentration, and comparison between SO_2 measured from the atmosphere and Gaussian-model-diluted SO_2. Mean relative error (MRE) and correlation coefficients (R^2) were calculated between measured and modelled concentrations.

		CO_2		SO_2	
case	stab. class	MRE (%)	R^2	MRE (%)	R^2
FGD + FF off	c	5	0.97	131	0.95
	d	25	0.97	322	0.96
FGD + FF on	b	29	0.87	291	0.84
	c	40	0.87	413	0.85

interval separately for the FGD + FF on/off cases and the locations of the peak CO_2 concentration (t_{max}, $[CO_{2,max}]$) were identified from the resulting time series. The value C_0 was chosen for Eq. (2) so that the modelled CO_2 concentration, $\hat{C}_{CO_2}$, was around $[CO_{2,max}]$ when $t = t_{max}$. The choice of C_0 was made in this manner rather than initializing the model to use the stack concentrations due to the following two reasons. First, the Gaussian plume model does not yield reliable results close to the source, i.e. within a few tens of metres (Arya, 1995). Second, the comparison of the results near (first 10–50 s) the source is problematic because the helicopter was not located at the plume centre line during the initial stages of the measurements.

Comparison of the measured and modelled CO_2 concentrations is shown in Fig. 4 and in Table 2. The chosen stability classes were b and c for FGD + FF on and c and d for FGD + FF off, corresponding to the stability conditions ranging from unstable to neutral (Pasquill, 1961). As can be seen, the model reproduces the observed trends rather well, in particular for FGD + FF off, while the model tends to slightly overestimate the observed concentrations for FGD + FF on. The modelled and measured concentrations were within one standard deviation in general. Mean relative error (MRE) and correlation coefficients (R^2) were calculated between the measured and modelled concentrations for CO_2. In order to further investigate the performance of the model, a comparison was made between measured SO_2 and Gaussian-model-diluted SO_2 concentrations, shown in Fig. S6 and Table 2. The results showed that the model consistently overestimates the SO_2 concentration in the plume, typically by a factor between 3 and 4, compared to the measured values. This difference could be partly explained by the oxidation of SO_2 because it is not taken into account by the model. However, this discrepancy between MREs and R^2 does not affect the model performance as the measured SO_2 concentrations, instead of being modelled, were used in the plume model simulations.

3.4 Model calculations: nucleation and new particle formation

Modelled and measured CO_2 concentrations showed that the model reproduced the observed dispersion of the plume relatively accurately. Thus the model was applied to calculate $[NO_x]$, [OH] and $[H_2SO_4]$, which were needed to investigate the possibility of new particle formation in the plume. These results are summarized in Fig. 5. It is seen that sulfuric acid concentrations exponentially increase during the initial stages of the simulation and then reach constant concentration around 1×10^6 and 1×10^7 cm^{-3}, a range which is also comparable to the atmospheric observations of $[H_2SO_4]$ (Mikkonen et al., 2011) formation. Mikkonen et al. (2011) reported that H_2SO_4 concentrations varied between 1.86×10^5–2.94×10^6 molec cm^{-3} and Sarnela et al. (2015) reported $[H_2SO_4]$ concentrations 4.4×10^6–11.5×10^6 molec cm^{-3} for Finnish industrial and non-industrial area. More H_2SO_4 is formed in the FGD + FF off case because of higher primary SO_2 emission compared to the FGD + FF on case.

Initially, OH concentrations are lowered by large concentrations of NO_x which subsequently decrease during plume ageing. NO_x reduction leads to increases in [OH] and $[H_2SO_4]$. While the [OH] increased consistently during

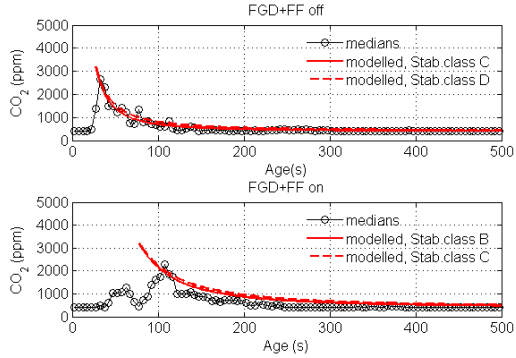

Figure 4. Comparison of measured and modelled CO_2 concentrations. Median of measured values are shown with black (circle) symbols along with the standard deviations. Dashed and dotted red lines correspond to model results for stability classes b and c (top panel) and c and d (bottom panel), respectively. The correlation coefficients between the model and the measurements are shown in Table 2.

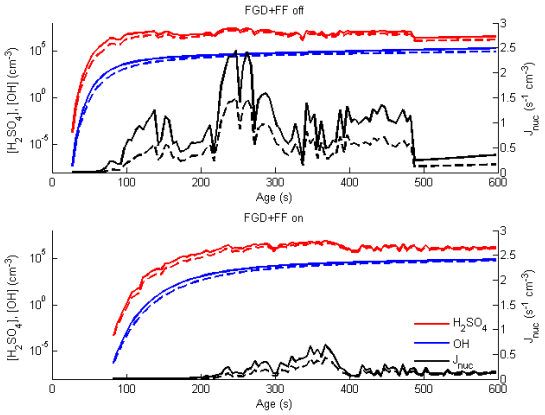

Figure 5. Time development of $[H_2SO_4]$ (red lines), nucleation rate (black lines), [OH] (blue lines) (cm^{-3}). Dashed and dotted red lines correspond to model results for stability classes c and d (top panel) and b and c (bottom panel), respectively.

the simulations, $[SO_2]$ decreased because of dilution. Due to these opposed trends, the production term for the sulfuric acid in Eq. (6), did not change greatly during the later stages of the simulations. Moreover, the condensation sink (CS) diluted rapidly to its background value, which was around $1 \times 10^{-2}\ s^{-1}$. These facts explain why the modelled sulfuric acid concentrations, calculated with Eq. (6), did not change notably after the initial rapid increase.

The modelled nucleation rate J_{nuc} is directly proportional to the sulfuric acid concentration and hence the trends in $[H_2SO_4]$ are directly reflected in J_{nuc} (Fig. 5). Furthermore, in our measurements the particles were detected at the lowest CPC detection limit which was 2.5 nm, $J_{2.5}$. According to the scheme applied here (see Eqs. 4 and 5), the fraction of freshly nucleated particles that survive into detectable sizes depends mainly on their growth rate (GR) and condensation sink (CS). The average given by the model GRs were 0.34 or 0.19 $nm\,h^{-1}$ in the FGD + FF off case, and 0.07 or 0.04 $nm\,h^{-1}$ in the FGD + FF on case for the two stability class scenarios. These values are clearly smaller than atmospheric GR observations in urban areas (e.g. Stoltzenburg et al., 2005). As a lower GR leads to a lower surviving fraction, we conclude that the modelling results do not explain the observed particle formation in the flue-gas plume.

A series of additional calculations were performed in order to investigate the sensitivity of the results to the values of the key input parameters. First, J_{nuc} is proportional to the constant A, the exact value of which is not accurately known, and this uncertainly translates directly into the calculated nucleation rates. A sensitivity analysis was made for the nucleation model in order to evaluate the sensitivity of nucleation rates to the value of A (shown in Table 3). In these calculations, a value of 1×10^{-6} was chosen for A, which is an order of magnitude higher than in base case simulations. The choice of the value was based on the study of Sihto et al. (2006) who investigated NPF (new particle formation) events occurring in boreal forest. As can be seen, an increased value of A alone is not sufficient to explain observed new particle formation. A second source of uncertainty is the sulfuric acid concentration, which was calculated using a rather simple scheme (see Sect. 2.1.1). Increases in $[H_2SO_4]$ leads to both increased J_{nuc} and GR and ultimately to larger $J_{2.5}$. Results displayed in Table 3 show that $J_{2.5}$ is more consistent with observations when $[H_2SO_4]$ is increased 5 or 10-fold and when A is set equal to 1×10^{-6} like in Sihto et al. (2006). Therefore, underestimation of $[H_2SO_4]$ may explain the discrepancy between the observations and base case model results. This might be caused by underestimation of [OH] or overestimation of CS. Regarding the modelled OH concentrations, it can be noted that they are relatively low, reaching values of around $1 \times 10^5\ cm^{-3}$ by the end of the flights. In comparison, concentrations of around $1 \times 10^6\ cm^{-3}$ have been reported during the daytime around noon in various atmospheric environments (Hofzumahaus et al., 2009; Petäjä et al., 2009), 0.26×10^6 molec cm^{-3} in Mace Head (Berresheim et al., 2002), and 1×10^6–2×10^7 molec cm^{-3} in Atlanta (Kuang et al., 2008). Relatively low modelled OH concentrations can be explained by high NO_x concentrations which were calculated to decrease consistently from several tens of ppm down to around 200 ppb during the flights (not illustrated here). Such high concentrations of NO_x are consistent with low [OH] (see Fig. 1 in Lonsdale et al., 2012). It could thus be speculated that the model underestimates $[H_2SO_4]$ and consequently the rate of new particle formation due to overestimation of $[NO_x]$. Moreover, it should be noted that neither SO_3 nor low-volatile organic vapours that might have been present in the measured flue gas were not accounted for in the modelling study. Previous studies suggest that these exhaust compounds may also increase the formation rate of nucleation particles (Pirjola et al., 2015; Ehn et al., 2012; Arnold et al., 2012), which may explain the discrepancy between measurements and model calculations. Regarding the estimation of the value of CS, it should be noted that its values were taken from the field site measurements located nearby rather than from in situ measurements. Therefore it can be speculated that actual CS values were lower than those used as input to the model, which causes additional uncertainties.

3.5 Discussion

Each power plant (over 50 MW) in the EU has emission limits for SO_2, NO_2 and particle mass concentrations. For the studied power plant the limits are 600 mg Nm^{-3} (210 ppm), 600 mg Nm^{-3} (290 ppm) and 50 mg Nm^{-3}. A comparison of the results in Table 1 with these emission limits shows that the emissions were clearly below these limits when the power plant operation was normal (FGD + FF on). It was observed that these low emissions can be achieved through properly

Table 3. Sensitivity analysis made for number of particles formed with diameters above 2.5 nm during the flight ($1\,cm^{-3}\,s^{-1}$) in the atmosphere with different values of A and $[H_2SO_4]$. The $[H_2SO_4]$ is calculated based on the measurement results and scaled up to test faster nucleation rates for both FGD + FF on and FGD + FF off cases and stability classes (sc).

$A = 1 \times 10^{-7}\,s^{-1}$							
	sc	$1 \times [H_2SO_4]$	$1.25 \times [H_2SO_4]$	$1.5 \times [H_2SO_4]$	$2 \times [H_2SO_4]$	$5 \times [H_2SO_4]$	$10 \times [H_2SO_4]$
FGD + FF off	b	1.00×10^{-4}	5.36×10^{-4}	1.73×10^{-3}	8.29×10^{-3}	0.289	1.74
	c	0	0	0	4.32×10^{-4}	4.78×10^{-2}	0.44
FGD + FF on	c	0	0	0	0	4.27×10^{-4}	1.85×10^{-2}
	d	0	0	0	0	0	1.73×10^{-3}
$A = 1 \times 10^{-6}\,s^{-1}$							
	sc	$1 \times [H_2SO_4]$	$1.25 \times [H_2SO_4]$	$1.5 \times [H_2SO_4]$	$2 \times [H_2SO_4]$	$5 \times [H_2SO_4]$	$10 \times [H_2SO_4]$
FGD + FF off	b	1.00×10^{-3}	5.36×10^{-3}	1.73×10^{-2}	8.29×10^{-2}	2.89	17.4
	c	0	0	4.47×10^{-4}	4.32×10^{-3}	0.48	4.43
FGD + FF on	c	0	0	0	0	4.27×10^{-3}	0.19
	d	0	0	0	0	0	0.017

working flue-gas cleaning systems. In addition to primary emissions, flue-gas cleaning systems also seemingly affect the compounds, which can act as precursors for new particles, e.g. SO_2 tends to oxidize in the atmosphere to form SO_3 and further forms H_2SO_4, which can nucleate or condensate to particle phase. This study clearly shows the importance of flue-gas cleaning technologies and underlines the proper usage of the technologies when the atmospheric pollution is discussed in terms of coal combustion. For example, according to Huang et al. (2014) in Xi'an and Beijing 37 % of the sulfate in atmospheric particles is emitted from coal burning.

In this study the power plant plume diluted to background levels in 2 km (200–400 s), which is faster than in other in-flight measurements (Stevens et al., 2012; Junkermann et al., 2011). This difference may be because the dilution of plume and other processes are affected by source strength, background concentrations and meteorology (Stevens et al., 2012). We observed that while SO_2 and CO_2 were already diluted to background levels, the effect of the source to aerosol concentration was still clearly distinguishable after 2 km. In our study, we collected high time-resolution data close to the power plant stack, which enabled us to model the plume dilution on a detailed scale. From this, we were able to observe that while SO_2 and CO_2 were already diluted to background levels at a distance of 2 km – in agreement with the dilution modelling – the effect of the source on the aerosol number concentration was distinguished at distances > 2 km. We attribute this to nucleation taking place in the ageing plume.

According to the modelling results from Stevens et al. (2012), atmospheric new particle formation via nucleation of sulfuric acid begins in the flue-gas plume at 1 km distance from the coal-fired power plant, whereas the sulfuric acid formation begins right after emission. Our study therefore supports this previous modelling work by showing that nucleation may take place in the aged plume and is most effective after 400 s, corresponding to a distance of approximately 2 km from the emission source in the atmosphere.

In light of the new results authors would like to distinguish the primary particle emission from the newly formed particle emission because those particles have different effects on the atmosphere and different formation mechanisms. By comparing primary particle emission with newly formed particle emission, the effects of different particles in the atmosphere could be taken into account more precisely in aerosol models or air quality assessments.

For instance, rough estimates for particle number emission factors can be calculated by comparing the measured particle number concentration with the simultaneously measured CO_2 concentration of the flue-gas plume (see e.g. Saari et al., 2016). By utilizing this method for particles existing in the flue-gas plume between the ages of 25–55 s, the emission factor with respect to CO_2 was $2.0 \times 10^{10}\,(g\,CO_2)^{-1}$, as well as from ages over 400 s $8 \times 10^{10}\,(g\,CO_2)^{-1}$ in the FGD + FF off case. Similarly, in the FGD + FF on case, the emission factors were $4 \times 10^{9}\,(g\,CO_2)^{-1}$ (for aerosol dispersed 55–85 s in the atmosphere) and $3.74 \times 10^{10}\,(g\,CO_2)^{-1}$ (for aerosol dispersed more than 500 s in the atmosphere). In comparison, the primary emissions were $1.75 \times 10^{10}\,(g\,CO_2)^{-1}$ for FGD + FF off and $8.0 \times 10^{6}\,(g\,CO_2)^{-1}$ for FGD + FF on. Thus, new particle formation can increase the real atmospheric particle number emissions even by several orders of magnitude. It should be noted that particle formation depends strongly on the plume age $[SO_2]$ and primary particle concentrations, and it is possible that there are some low-volatile organics or SO_3 present in the plume, affecting the nucleation.

Our observations show that the number of secondary particles formed in the flue-gas plume can be several orders of

magnitude higher than the primary particles directly emitted from the flue-gas duct. The formation can already be observed at a distance of ca. 2 km from the stack; this distance is significantly lower than the grid size used in many atmospheric models, which demonstrates the need for subgrid parameterizations for power-plant-originating secondary particles. Such a parameterization does already exist (Stevens and Pierce, 2013), but it does not account for different types of sulfur removal technologies such as semi-dry desulfurization and wet desulfurization. Determining the effect of different removal technologies on power plant secondary aerosol production would increase the accuracy of particle-loading predictions for regional air quality and global models.

4 Conclusions

Emissions of a coal-fired power plant into the atmosphere were studied comprehensively for the first time, by combining direct atmospheric measurements, measurements conducted in the power plant stack, and modelling studies for atmospheric processes of flue-gas plume. The stack measurements were made to estimate the effectiveness of flue-gas cleaning technologies, such as filtering and desulfurization. It was shown that the flue-gas cleaning technologies had a great effect on the SO_2 and total particle number concentrations in the primary emission. SO_2 concentration was reduced to fifth of FGD + FF off compared to FGD + FF on and the total non-volatile particle number concentration was reduced by several orders of magnitude. A similar trend in primary emission reduction was detected in the atmospheric measurements. In addition, the reduction in primary emissions directly affects the concentrations of gaseous precursors (SO_2) for secondary particle formation in the atmosphere.

It was observed that the flue gas dilutes to background concentrations in 200–300 s. This dilution timescale is faster than reported in previous studies. However, the concentration profiles also showed an increase in particle number concentration in an aged flue gas, dilution and dispersion processes. To validate the dilution timescale, a Gaussian model was used to calculate the dilution in the atmosphere, taking into account the primary emission and weather conditions. The Gaussian model confirms the dilution timescale, and the dilution ratio could be used to calculate the theoretical maximum values for different components in the flue-gas plume. Weather conditions and theoretical maximum value for [NO_x] were used to calculate the [OH] formation rate and further [H_2SO_4] formation rate. These were calculated because the measurement results showed an increase in particle number concentrations in the flue-gas plume during the dilution process. The modelling results for [H_2SO_4] formation rate support the hypothesis of sulfuric acid formation, but the sulfuric acid formation itself does not totally explain the increase in the total particle number concentration, therefore, e.g. low-volatile organics may exist on the flue-gas plume. The sensitivity analysis of the [H_2SO_4] formation showed that the atmospheric parameterization is not enough to explain the processes in the flue-gas plume.

Comparison between the primary particles and newly formed particles show that in the flue-gas plume of coal-fired power plant, the concentration of newly formed atmospheric particles can be several orders of magnitude higher than the primary particles from the flue-gas duct; therefore they should be considered when discussing emissions of power production. Including the effect of varying flue-gas cleaning technologies in parameterizations of power-plant-originating secondary particles is a necessary step in understanding their importance.

The Supplement related to this article is available online at doi:10.5194/acp-16-7485-2016-supplement.

Acknowledgements. The study was conducted in the MMEA WP 4.5.2. of Cleen Ltd., funded by Tekes (the Finnish Funding Agency for Technology and Innovation). Authors would like to acknowledge Anna Kuusala and Joni Heikkilä for programming Matlab, Aleksi Malinen for measurement help. Fanni Mylläri acknowledges TUT Graduate School, KAUTE-foundation, TES-foundation for financial support. Eija Asmi and Ewan O'Connor acknowledge the support of the Academy of Finland Centre of Excellence program (project number 272041). Ville Vakkari acknowledges the financial support of the Nessling foundation (grant 201500326) and the Academy of Finland Finnish Center of Excellence program (grant 1118615). Fanni Mylläri and Topi Rönkkö acknowledge the financial support from the Academy of Finland ELTRAN (grant 293437).

Edited by: F. Khosrawi

References

Agarwal, J. K. and Sem, G. J.: Continuous Flow, Single-particle Counting Condensation Nucleus Counter, J. Aerosol Sci., 11, 343–357, 1980.

Arnold, F., Pirjola, L., Rönkkö, T., Reichl, U., Schlager, H., Lähde, T., Heikkilä, J., and Keskinen, J.: First online measurements of sulfuric acid gas in modern heavy-duty diesel engine exhaust: Implications for nanoparticle formation, Environ. Sci. Technol., 46, 11227–11234, 2012.

Arya, S. P.: Modeling and parameterization of near-source diffusion in weak winds, J. Appl. Meteorol., 34, 1112–1122, 1995.

Awasthi, A., Wu, B.-S., Liu, C.-N., Chen, C.-W., Uang, S.-N., and Tsai, C.-J.: The effect of nanoparticle morphology on the measurement accuracy of mobility particle sizers, MAPAN-J. Metrol. Soc. I., 28, 205–215, 2013.

Berresheim, H., Elste, T., Tremmel, H. G., Allen, A. G., Hansson, H.-C., Rosman, K., Dal Maso, M., Mäkelä, J. M., and Kulmala,

M.: Gas-Aerosol relationships of H_2SO_4, MSA, and OH: Observations in the coastal marine boundary layer at Mace Head, Ireland, J. Geophys. Res., 107, 8100, doi:10.1029/2000JD000229, 2002.

Brock, C. A., Washenfelder, R. A., Trainer, M., Ryerson, T. B., Wilson, J. C., Reeves, J. M., Huey, L. G., Holloway, J. S., Parrish, D. D., Hübler, G., and Fehsenfeld, F. C.: Particle growth in the plumes of coal-fired power plants, J. Geophys. Res., 107, 4155, doi:10.1029/2001JD001062, 2002.

Buonanno, G., Anastasi, P., DiIorio, F., and Viola, A.: Ultrafine particle apportionment and exposure assessment in respect of linear and point sources, Atmospheric Pollution Research, 1, 36–43, 2012.

Charlson, R. J., Schwartz, S. E., Hales, J. M., Cess, R. D., Coakley Jr., J. A., Hansen, J. E., and Hofmann, D. J.: Climate Forcing by Anthropogenic Aerosols, Science New Series, 255, 423–430, 1992.

Ehn, M., Kleist, E., Junninen, H., Petäjä, T., Lönn, G., Schobesberger, S., Dal Maso, M., Trimborn, A., Kulmala, M., Worsnop, D. R., Wahner, A., Wildt, J., and Mentel, Th. F.: Gas phase formation of extremely oxidized pinene reaction products in chamber and ambient air, Atmos. Chem. Phys., 12, 5113–5127, doi:10.5194/acp-12-5113-2012, 2012.

EU: The EU Emissions Trading System (EU ETS), available at: http://ec.europa.eu/clima/policies/ets/index_en.htm, last access 15 December 2014.

Frey, A. K., Saarnio, K., Lamberg, H., Mylläri, F., Karjalainen, P., Teinilä, K., Carbone, S., Tissari, J., Niemelä, V., Häyrinen, A., Rautiainen, J., Kytömäki, J., Artaxo, P., Virkkula, A., Pirjola, L., Rönkkö, T., Keskinen, J., Jokiniemi, J., and Hillamo, R.: Optical and Chemical Characterization if Aerosols Emitted from Coal, Heavy and Light Fuel Oil, and Small-Scale Wood Combustion, Environ. Sci. Technol., 48, 827–836, 2014.

Helble, J. J.: A model for the air emissions of trace metallic elements from coal combustors equipped with electrostatic precipitators, Fuel Process. Technol., 63, 125–147, 2000.

Hofzumahaus, A., Rohrer, F., Lu, K., Bohn, B., Brauers, T., Chang, C.-C., Fuchs, H., Holland, F., Kita, K., and Kondo, Y.: Amplified trace gas removal in the troposphere, Science, 324, 1702–1704, 2009.

Huang, R.-J., Zhang, Y., Bozzetti, C., Ho, K.-F., Cao, J.-J., Han, Y., Daellenbach, K. R., Slowik, J. G., Platt, S. M., Ganonaco, F., Zotter, P., Wolf, R., Pieber, S. M., Bruns, E. A., Grippa, M., Ciarelli, G., Piazzalunga, A., Schwikowsko, M., Abbaszade, G., Schnelle-Kreis, J., Zimmerman, R., An, Z., Szidat, S., Baltenspergerm, U., El Haddad, I., and Prévôt, A. S. H.: High secondary aerosol contribution to particulate pollution during haze event in China, Nature, 514, 218–222, 2014.

Junkermann, W., Hagemann, R., and Vogel, B.: Nucleation in the Karlsruhe plume during the COPS/TRACKS-Lagrange experiment, Q. J. Roy. Meteor. Soc., 137, 267–274, 2011.

Junninen, H., Lauri, A., Keronen, P., Aalto, P., Hiltunen, V., Hari, P., and Kulmala, M.: Smart-SMEAR: on-line data exploration and visualization tool for SMEAR stations, Boreal. Environ. Res., 14, 447–457, 2009.

Keskinen, J., Pietarinen, K., and Lehtimäki, M.: Electrical Low Pressure Impactor, J. Aerosol Sci., 23, 353–360, 1992.

Klug, W.: A method for determining diffusion conditions from synoptic observations, Staub-Reinhalt. Luft, 29, 14–20, 1969.

Kuang, C., McMurry, P. H., McCormick, A. V., and Eisele, F. L.: Dependence of nucleation rates on sulphuric acid vapor concentration in diverse atmospheric locations, J. Geophys. Res., 113, D10209, doi:10.1029/2007JD009253, 2008.

Kulmala, M., Lehtinen, K. E. J., and Laaksonen, A.: Cluster activation theory as an explanation of the linear dependence between formation rate of 3 nm particles and sulphuric acid concentration, Atmos. Chem. Phys., 6, 787–793, doi:10.5194/acp-6-787-2006, 2006.

Lähde, T., Rönkkö, T., Virtanen, A., Schuck, T. J., Pirjola, L., Hämeri, K., Kulmala, M., Arnold, F., Rothe, D., and Keskinen, J.: Heavy duty diesel engine exhaust aerosol particle and ion measurements, Environ. Sci. Technol., 43, 163–168, 2009.

Lee, S. W., Herage, T., Dureau, R., and Young, B.: Measurement of $PM_{2.5}$ and ultra-fine particulate emissions from coal-fired utility boilers, Fuel, 108, 60–66, 2013.

Lehtinen, K. E. J., Dal Maso, M., Kulmala, M., and Kerminen, V.-M.: Estimating nucleation rates from apparent particle formation rates and vice versa: Revised formulation of the Kerminen-Kulmala equation, J. Aerosol Sci., 38, 988–994, 2007.

Lelieveld, J. and Heintzenberg, J.: Sulfate Cooling Effect on Climate Through In-Cloud Oxidation of Anthropogenic SO_2, Science New Series, 258, 117–120, 1992.

Levin, M., Gudmundsson, A., Pagels, J. H., Fiers, M., Mølhave, K., Löndahl, J., Jensen, K. A., and Koponen, I. K.: Limitations in the Use of Unipolar charging for Electrical Mobility Sizing Instruments: A Study of the Fast Mobility Particle Sizer, Aerosol Sci. Tech., 49, 556–565, 2015.

Lonsdale, C. R., Stevens, R. G., Brock, C. A., Makar, P. A., Knipping, E. M., and Pierce, J. R.: The effect of coal-fired powerplant SO_2 and NO_x control technologies on aerosol nucleation in the source plumes, Atmos. Chem. Phys., 12, 11519–11531, doi:10.5194/acp-12-11519-2012, 2012.

Marris, H., Deboudt, K., Augustin, P., Flament, P., Blond, F., Fiani, E., Fourmentin, M., and Delbarre, H.: Fast changes in chemical composition and size distribution of fine particles during the near-field transport of industrial plumes, Sci. Total Environ., 427–428, 126–138, 2012.

Mikkanen, P., Moisio, M., Keskinen, J., Ristimäki, J., and Marjamäki, M.: Sampling method for particle measurements of vehicle exhaust, SAE 2001 World Congress, 5–8 March 2001, Detroit, Michigan, USA, SAE Technical Paper Series, 2001-01-0219, 2001.

Mikkonen, S., Romakkaniemi, S., Smith, J. N., Korhonen, H., Petäjä, T., Plass-Duelmer, C., Boy, M., McMurry, P. H., Lehtinen, K. E. J., Joutsensaari, J., Hamed, A., Mauldin III, R. L., Birmili, W., Spindler, G., Arnold, F., Kulmala, M., and Laaksonen, A.: A statistical proxy for sulphuric acid concentration, Atmos. Chem. Phys., 11, 11319–11334, doi:10.5194/acp-11-11319-2011, 2011.

Mirme, A.: Electric aerosol spectrometry, PhD Thesis, Tartu University, Tartu, Estonia, 1994.

Pasquill, F.: The estimation of the dispersion of windborne material, The Meteorological Magazine, 90 , 33–49, 1961.

Pearson, G., Davies, F., and Collier, C.: An analysis of the Performance of the UFAM Pulsed Doppler Lidar for observing the Boundary Layer, J. Atmos. Ocean. Tech., 26, 240–250, doi:10.1175/2008JTECHA1128.1, 2009.

Petäjä, T., Mauldin, III, R. L., Kosciuch, E., McGrath, J., Nieminen, T., Paasonen, P., Boy, M., Adamov, A., Kotiaho, T., and

Kulmala, M.: Sulfuric acid and OH concentrations in a boreal forest site, Atmos. Chem. Phys., 9, 7435–7448, doi:10.5194/acp-9-7435-2009, 2009.

Pirjola, L., Pajunoja, A., Walden, J., Jalkanen, J.-P., Rönkkö, T., Kousa, A., and Koskentalo, T.: Mobile measurements of ship emissions in two harbour areas in Finland, Atmos. Meas. Tech., 7, 149–161, doi:10.5194/amt-7-149-2014, 2014.

Pirjola, L., Karl, M., Rönkkö, T., and Arnold, F.: Model studies of volatile diesel exhaust particle formation: are organic vapours involved in nucleation and growth?, Atmos. Chem. Phys., 15, 10435–10452, doi:10.5194/acp-15-10435-2015, 2015.

Ristimäki, J., Virtanen, A., Marjamäki, M., Rostedt, A., and Keskinen, J.: On-line measurement of size distribution and effective density of submicron aerosol particles, J. Aerosol Sci., 33, 1541–1557, 2002.

Rönkkö, T., Arffman, A., Karjalainen, P., Lähde, T., Heikkilä, J., Pirjola, L., Rothe, D., and Keskinen, J.: Diesel exhaust nanoparticle volatility studies by a new thermodenuder with low solid nanoparticle losses, 15th ETH Conference on Combustion Generated Nanoparticles, Zürich ETH Zentrum, 26–29 June 2011, Zurich, Switzerland, 2011.

Saari, S., Karjalainen, P., Ntziachristos, L., Pirjola, L., Matilainen, P., Keskinen, J., and Rönkkö, T.: Exhaust particle and NO_x emission performance of an SCR heavy duty truck operating in real-world conditions, Atmos. Environ., 126, 136–144, doi:10.1016/j.atmosenv.2015.11.047, 2016.

Saarnio, K., Frey, A., Niemi, J. V., Timonen, H., Rönkkö, T., Karjalainen, P., Vestenius, M., Teinilä, K., Pirjola, L., Niemelä, V., Keskinen, J., Häyrinen, A., and Hillamo, R.: Chemical composition and size of particles in emissions of coal-fired power plant with flue gas desulphurization, J. Aerosol Sci., 73, 14–26, 2014.

Sarnela, N., Jokinen, T., Nieminen, T., Lehtipalo, K., Junninen, H., Kangasluoma, J., Hakala, J., Taipale, R., Schobesberger, S., Sipilä, M., Larnimaa, K., Westerholm, H., Heijari, J., Kerminen, V.-M., Petäjä, T., and Kulmala, M.: Sulphuric acid and aerosol particle production in the vicinity of an oil refinery, Atmos. Environ., 119, 156–166, 2015.

Seinfeld, J. H. and Pandis, S. N.: Atmospheric chemistry and physics: from air pollution to climate change, second edition, John Wiley & Sons Inc., New York, USA, 2006.

Sihto, S.-L., Kulmala, M., Kerminen, V.-M., Dal Maso, M., Petäjä, T., Riipinen, I., Korhonen, H., Arnold, F., Janson, R., Boy, M., Laaksonen, A., and Lehtinen, K. E. J.: Atmospheric sulphuric acid and aerosol formation: implications from atmospheric measurements for nucleation and early growth mechanisms, Atmos. Chem. Phys., 6, 4079–4091, doi:10.5194/acp-6-4079-2006, 2006.

Srivastava, R. K. and Jozewicz, W.: Flue Gas Desulfurization: The State of the Art, J. Air Waste Manage., 51, 1676–1688, 2001.

Stevens, R. G. and Pierce, J. R.: A parameterization of subgrid particle formation in sulfur-rich plumes for global- and regional-scale models, Atmos. Chem. Phys., 13, 12117–12133, doi:10.5194/acp-13-12117-2013, 2013.

Stevens, R. G., Pierce, J. R., Brock, C. A., Reed, M. K., Crawford, J. H., Holloway, J. S., Ryerson, T. B., Huey, L. G., and Nowak, J. B.: Nucleation and growth of sulfate aerosol in coal-fired power plant plumes: sensitivity to background aerosol and meteorology, Atmos. Chem. Phys., 12, 189–206, doi:10.5194/acp-12-189-2012, 2012.

Stockie, J. M.: The Mathematics of Atmospheric Dispersion Modeling, SIAM Review, 53, 349–372, 2011.

Stolzenburg, M. R., McMurry, P. H., Sakurai, H., Smith, J. N., Mauldin III, R. L., Eisele, F. L., and Clement, C. F.: Growth rates of freshly nucleated atmospheric particles in Atlanta, J. Geophys. Res., 110, D22S05, doi:10.1029/2005JD005935, 2005.

Wang, S. C. and Flagan, R. C.: Scanning Electrical Mobility Spectrometer, Aerosol Sci. Tech., 13, 230–240, 1990.

Yi, H., Hao, J., Duan, L., Tang, X., Ning, P., and Li, X.: Fine particle and trace element emissions from an anthracite coal-fired power equipped with bag-house in China, Fuel, 2008, 87, 2050–2057, 2008.

Publication III

Mylläri, F., Pirjola, L., Lihavainen, H., Asmi, E., Saukko, E., Laurila, T., Vakkari, V., O'Connor, E., Rautiainen, J., Häyrinen, A., Niemelä, V., Maunula, J., Hillamo, R., Keskinen, J., Rönkkö, T. "Characteristics of particle emissions and their atmospheric dilution during co-combustion of coal and wood pellets in large combined heat and power plant" *Accepted to Journal of the Air & Waste Management Association*

Publication IV

Happonen, M., Mylläri, F., Karjalainen, P., Frey, A., Saarikoski, S., Carbone, S., Hillamo, R., Pirjola, L., Häyrinen, A., Kytömäki, J., Niemi, J. V., Keskinen, J., Rönkkö, T. "Size distribution, chemical composition, and hygroscopicity of fine particles emitted from an oil-fired heating plant" *Environmental Science & Technology*

Environmental Science & Technology

Article

pubs.acs.org/est

Size Distribution, Chemical Composition, and Hygroscopicity of Fine Particles Emitted from an Oil-Fired Heating Plant

Matti Happonen,[†] Fanni Mylläri,[†] Panu Karjalainen,[†] Anna Frey,[‡] Sanna Saarikoski,[‡] Samara Carbone,[‡] Risto Hillamo,[‡] Liisa Pirjola,[¶] Anna Häyrinen,[§] Jorma Kytömäki,[§] Jarkko V. Niemi,[∥] Jorma Keskinen,[†] and Topi Rönkkö*[,†]

[†]Aerosol Physics Laboratory, Department of Physics, Tampere University of Technology, P.O. Box 692, FI-33101 Tampere, Finland

[‡]Air Quality, Finnish Meteorological Institute, P.O. Box 503, FI-00101 Helsinki, Finland

[¶]Department of Technology, Metropolia University of Applied Sciences, P.O. Box 4000, FI-00180, Helsinki, Finland

[§]Helsingin Energia Plc, FI-00090 Helen, Helsinki, Finland

[∥]Helsinki Region Environmental Services Authority (HSY), P.O. Box 100, FI-00066 HSY, Finland

ABSTRACT: Heavy fuel oil (HFO) is a commonly used fuel in industrial heating and power generation and for large marine vessels. In this study, the fine particle emissions of a 47 MW oil-fired boiler were studied at 30 MW power and with three different fuels. The studied fuels were HFO, water emulsion of HFO, and water emulsion of HFO mixed with light fuel oil (LFO). With all the fuels, the boiler emitted considerable amounts of particles smaller than 200 nm in diameter. Further, these small particles were quite hygroscopic even as fresh and, in the case of HFO+LFO emulsion, the hygroscopic growth of the particles was dependent on particle size. The use of emulsions and the addition of LFO to the fuel had a reducing effect on the hygroscopic growth of particles. The use of emulsions lowered the sulfate content of the smallest particles but did not affect significantly the sulfate content of particles larger than 42 nm and, further, the addition of LFO considerably increased the black carbon content of particulate matter. The results indicate that even the fine particles emitted from HFO based combustion can have a significant effect on cloud formation, visibility, and air quality.

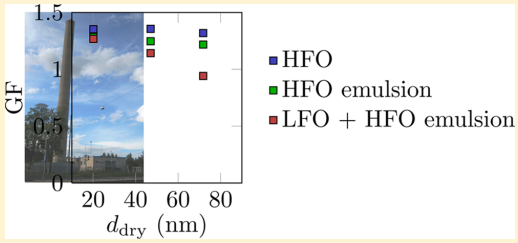

INTRODUCTION

Heavy fuel oil (HFO) is a petroleum product that is left when all distillates have been separated from crude oil. HFO includes much impurities such as sulfur, asphaltenes, and vanadium. The main uses of HFO are in industrial heating and power generation and in the transport sector, where it is used as fuel for large marine vessels. HFO is generally preheated before combustion to lower its viscosity. The combustion of HFO is known to produce considerable amounts of sulfur oxides (SO_x) and particulate matter (PM). Particulate matter emitted in HFO combustion has high metallic ash (Ni, V, Fe, Cr, Na)[1] and sulfur content. From these, the vanadium content has especially been of interest due to its adverse effects on human health.[2,3] Because of the high PM and sulfur emissions associated with HFO, meeting the emission legislation practically means either efficient exhaust after-treatment, influencing the fuel composition to achieve cleaner combustion, or both.

Techniques that can be used to modify the fuel in oil-fired burners are mixing a portion of light fuel oil (LFO) into HFO and creating water emulsions of the fuel oil. Mixing LFO into HFO mainly makes the fuel a higher grade of fuel oil, that is, the sulfur and ash contents of the resulting blend are lower than those of HFO. The advantage of using oil−water emulsion is the occurrence of the so-called microexplosions that take place in the emulsion prior to its combustion.[4,5] Microexplosions enable a secondary atomization of fuel droplets prior to the combustion. When the water−oil emulsion is sprayed into the combustion chamber, the small water droplets enclosed in oil droplets start to expand at a greater rate than the oil. The rapid evaporation of the water then results in disintegration of the oil droplets to smaller ones before the combustion of the oil.[6] The smaller droplets at the combustion then enable more efficient combustion of the fuel leading to a reduction in PM while the cooling effect of introducing water to the combustion reduces NO_x formation.[7] Size distribution of particles emitted in HFO combustion has typically been observed to be bimodal.[1,8] The larger particles (diameter typically >1 μm) consist of the char residues of oil droplets and particulates re-entrained to the exhaust from walls. The smaller particles (diameter <1 μm, mass median diameter typically 100−500 nm), on the other

Received: June 26, 2013
Revised: November 11, 2013
Accepted: November 18, 2013
Published: November 18, 2013

hand, consist mainly of soot, metallic ash, and sulfur compounds.[1,9,10]

Most fuel oil emission studies have concentrated on studying the larger particles due to their significance to the legislated particulate mass (PM10 or PM2.5) and due to the measuring equipment they have used. However, there are studies pointing out that, in fact, sufficiently small (<100 nm) particles may be the most harmful ones due to their ability to penetrate deep into lungs and even enter the bloodstream.[11] The adverse health effects associated with PM are not the sole reason to study combustion particles. The PM originating from combustion also affects the radiative properties of the atmosphere. Large amounts of black carbon in the atmosphere can increase the direct radiative forcing,[12] especially harmful to Arctic ice and snow,[13] whereas other types of particles, e.g., sulfuric acid particles, can reduce the radiative forcing via the indirect effect, i.e., cloud formation and resulting backscattering of solar radiation.[14] The key to understanding the consequences of emitting particles into the atmosphere is to determine their composition and properties. Moreover, depending on their hygroscopic properties, the fine particles may affect visibility and cloud formation and, thereby, also climate.

Not only has the previous research of fuel oil combustion been focused on the larger end of emitted particles, but also most of the studies have been performed on smaller boilers (rated below 1 MW).[7−9,15] In this paper, the particle emissions of an industrial scale boiler of a peak-load heating plant are studied focusing on the size distribution, hygroscopic properties, and chemistry of fine particles. Further, the impacts of using different fuels (HFO, HFO−water emulsion, and HFO +LFO−water emulsion) on the said properties are also studied. The aim of the research is to provide more detailed insight on the properties of emitted fine particles and on the effects of fuel alterations to the said properties.

EXPERIMENTAL SECTION

The studied boiler was an oil-fired water tube boiler of a peak-load heating plant having a rotary cup type burner. The nominal output of the boiler was 47 MW. The main fuel used in the boiler was natural gas but HFO or HFO+LFO blends could be used as auxiliary fuel. In this study, the boiler was operated at 30 MW power. The studied fuels were HFO, water emulsion of HFO, and water emulsion of HFO+LFO blend. The properties of the applied HFO and LFO can be found in Table 1. The HFO+LFO blend included 66 mol% of HFO and 34 mol% LFO. The resulting fuel sulfur content was 0.58 mol%.

Table 1. Properties of Studied HFO and LFO Fuels

analysis		method	HFO	LFO
Lower Heating Value (calculated)	[kWh/kg]	ISO 8217	11.381	12.043
Density	[g/cm^3]	ASTM D 4052	(at 60 °C) 0.9560	(at 20 °C) 0.8183
Viscocity	[mm^2/s]	ISO 3104	(at 60 °C) 99.52	(at 20 °C) 2.60
Water (Karl Fischer)	[mg/kg]	IEC 814	-	35
Water (by distillation)	[mol%]	ISO 3733	<0.05	-
Sulfur	[mol%]	ASTM D 1552	0.89	0.01
Carbon	[mol%]	ASTM D 5291	87.2	85

District heating water used in the convection part of the boiler was applied to produce the water emulsions. The district heating water is softened tap water where hydrazine has been added to bind residual oxygen and pyranine ($C_{16}H_7Na_3O_{10}S_3$) has been added as a colorant. The addition rate of water during emulsion tests was 3−4 L min^{-1}. The rates of fuel combustion for HFO, HFO emulsion, and HFO+LFO emulsion were 2.6, 2.2, and 2.5 t/h in total, respectively.

The particle measurement system applied in this study is presented in Figure 1. Particle sampling was performed with a Fine Particle Sampler (FPS, Dekati Inc.) from a smoke flue located inside the facility. The primary dilution air was heated to 39 °C and the nominal dilution ratio of the primary dilution was approximately 6. The dilution ratio of the downstream ejector diluter was approximately 10 during the tests. The particle sampling point was situated approximately 25 m from the boiler and approximately 10 m above the measurement instruments. Copper tubing was used to deliver the sample down to the level of the instruments. The sample was divided in a flow divider to provide the sample for the different branches of the measurement system. One branch led to a Nano-Micro-Orifice Uniform Deposit Impactor (nano-MOUDI model 125B, MSP Corporation, Shoreview, MN, USA) which obtained the particulate sample in the range of 0.01−10 μm for the elemental particle mass distribution analysis. The nano-MOUDI is a cascade impactor that separates the sampled particles into 13 stages. In addition, below the 0.01 μm stage there is a back-up stage to collect particles smaller than 0.01 μm. The model 125B rotates sampling stages during sampling leading to uniform samples. Total mass and chemical composition of particles <1 μm (aerodynamic diameter) was determined from the polytetrafluoroethylene (PTFE, Millipore, 3.0 μm, FSLW04700)-filter samples collected by filtration using a combination of five upper stages (7−11) of a Berner low pressure impactor (BLPI) and a filter cassette (Gelman Science) (flow rate 25 L min^{-1}).[16,17] The major ions (Na^+, NH_4^+, K^+, Mg^{2+}, Ca^{2+}, Cl^-, NO_3^-, SO_4^{2-}) were analyzed by a Dionex ICS-2000 ion chromatography (Dionex Corp., Sunnyvale, CA, USA)[18] from the section of PTFE and polycarbonate filters. Uncertainties in the ion chromatography (IC) analyses have been estimated to be around 10−15%).[19] The elemental components were analyzed by an Inductively Coupled Plasma Mass Spectrometer (ICP-MS; DRC II, Perkin-Elmer SCIEX, Concord, Ontario, Canada) and inductively coupled plasma optical emission spectrometry (ICP-OES; Vista Pro Radial, Varian Inc., Melbourne, Australia). The analyzed elements were aluminum (Al), arsenic (As), cadmium (Cd), cobalt (Co), chromium (Cr), copper (Cu), iron (Fe), manganese (Mn), nickel (Ni), lead (Pb), vanadium (V), zinc (Zn), barium (Ba), calcium (Ca), potassium (K), magnesium (Mg), and sodium (Na). The applied analyzing method is based on the standard SFS-EN 14902:2005 (Ambient air - Standard method for the measurement of Pb, Cd, As, and Ni in the PM10 fraction of suspended particulate matter) where hydrogen peroxide−nitric acid extraction is done for the samples. The yield for elements ranged between 54% and 104% and the results were corrected based on the yields of each element.

The second branch led to NO_x and CO_2 analyzers which, together with the gas analyzers measuring from the smoke flue, were used to calculate the dilution ratio of the FPS unit. The third branch consisted of two scanning mobility particle sizers (SMPS, TSI Inc.), an electrical low pressure impactor (ELPI,

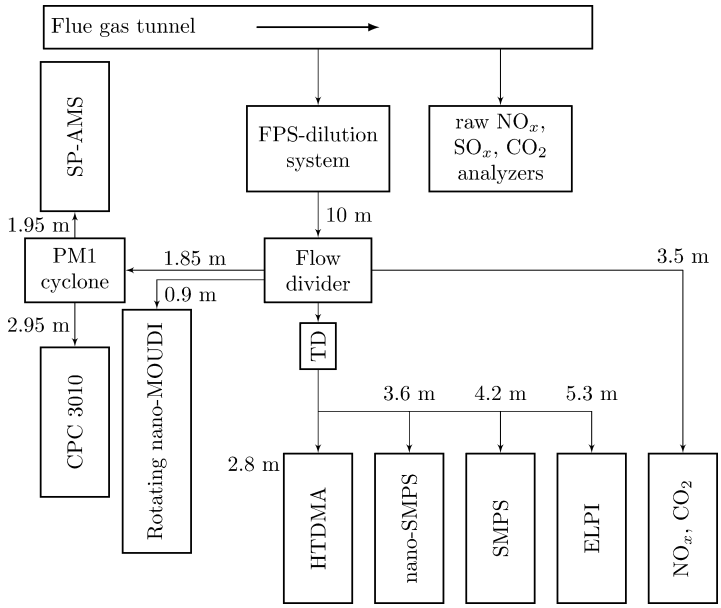

Figure 1. Measurement setup.

Dekati Inc.), and a hygroscopic tandem differential mobility analyzer (HTDMA). The third branch included a possibility to use a thermodenuder (TD) prior to the measurement instrumentation in order to remove semivolatile compounds from sampled particles. The duration of one measurement period with or without the thermodenuder was 10−15 min. The data measured after the thermodenuder treatment was corrected using particle losses reported by Heikkilä et al.[19] The residence time from the FPS dilution unit to the instruments was approximately 3.5 s when the thermodenuder was bypassed. The fourth branch had a Soot Particle Aerosol Mass Spectrometer (SP-AMS; Aerodyne Research Inc.) together with a CPC 3010 (TSI Inc.). The total flow of the SP-AMS and the CPC 3010 was 1.1 L min^{-1}. The SP-AMS was used to measure refractory black carbon (BC) with an intracavity laser vaporizer similar to Onasch et al.[17] It should be noted here that the SP-AMS has been calibrated separately for organics and BC, but due to the different collection efficiencies and relative ionization efficiencies, the carbon balance given by the SP-AMS has rather high uncertainty. Here, the concentration of organic carbon (OC) was obtained from the elemental analysis described by Aiken et al.[20]

One of the SMPSs was equipped with a DMA 3071 and a CPC C3775 and the other with a DMA 3085 and a CPC 3025 (TSI Inc.). Together the SMPSs provided particle number size distributions over the range of 3−400 nm, a wider range that was possible with either of the SMPSs alone. In the HTDMA, a single particle size is first chosen from the particle size distribution with the first differential mobility analyzer (DMA) after which this sampled particle size is subjected to chosen relative humidity. The second DMA and the following CPC then work as an SMPS and measure the particle size distribution after the humidity conditioning. Thus, the HTDMA measured the hygroscopic growth of emitted particles providing additional information about their behavior in the atmosphere. In fact, HTDMA measurements are rather commonly used to study the properties of atmospheric aerosols.[21] The HTDMA used in this study was the same as that used in Happonen et al.[22] However, during these measurements, the HTDMA had an additional 5-cm-thick layer of polyurethane insulation enclosing the humidifying part and the second DMA providing better thermal insulation. Further, a Peltier cooler was installed at the back of the insulated casing to provide active temperature control within the casing. The casing was set to operate at 20 °C temperature during the measurements by a PID controller. The ELPI was used to monitor the emission in real-time to ensure that the emission was stable during the actual measurements.

RESULTS AND DISCUSSION

Particle Number Size Distributions. Particle size distributions measured from the smoke flue with the SMPS using the DMA 3071 are presented in Figure 2. The distributions measured with the SMPS using the DMA 3085 are not presented here since they provided no additional information: no particle mode below 10 nm was observed with any of the fuels. The figure shows the distributions obtained using HFO, HFO emulsion, and HFO+LFO emulsion as fuel measured both through the thermodenuder (TD), to remove the volatile fraction from the sample, and bypassing the TD. In addition, the figure shows as dotted vertical lines the dry particle sizes that were chosen for hygroscopic growth measurements.

With all the studied fuels, the particle number size distributions were dominated by the particle mode having the GMD ca. 50 nm. In addition, it was observed that when the HFO+LFO emulsion was used the particle number size distribution was clearly different from the two other fuels; the

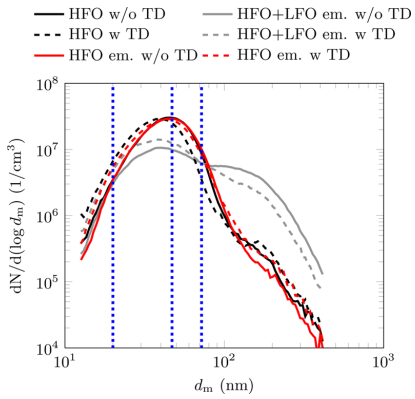

Figure 2. Particle number size distributions measured by the SMPS with ("w", solid lines) and without ("w/o", dashed lines) thermodenuder treatment with different fuels. The size distributions were corrected with dilution ratios and, when appropriate, with the particulate losses in the thermodenuder. The dotted vertical lines show the particle sizes which were chosen for the HTDMA measurements.

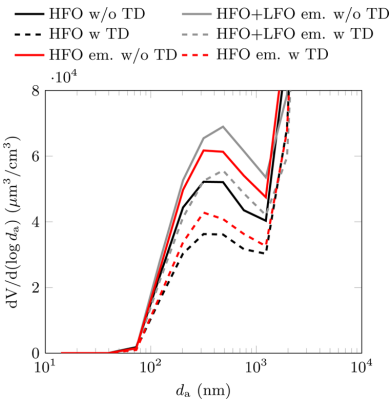

Figure 3. Volumetric size distributions as a function of aerodynamic diameter measured with an ELPI. The concentrations of particles larger than 1 μm are underestimated.

size distribution included another particle mode with the GMD ca. 120 nm, and the concentration of the smaller particles was considerably reduced. However, when the HFO+LFO emulsion was used, the total particle number concentration in the studied size range was over 25% lower compared to the situations with the other fuels. It was noted that HFO and LFO were not fully mixed prior to the combustion, which can at least partly explain the observations. In the case of HFO, applying the thermodenuder treatment slightly reduced the GMD of the emitted particles. This indicates that the particles were mostly nonvolatile but, anyway, they included an observable fraction of volatile compounds. When the HFO emulsion was used, the thermodenuder treatment barely affected the size distribution, which indicates that the particles were less volatile compared to the case of HFO. When the HFO+LFO emulsion was used, the thermodenuder treatment led to the shifting of particle number concentration from the larger mode to the smaller one. Nevertheless, a clear particle mode was still present at approximately 100 nm also after the thermodenuder treatment, only with lower concentration. Results indicate that the smaller particle mode with HFO+LFO emulsion consists essentially of nonvolatile particles and some of these particles have grown by absorbing volatile compounds into the particle sizes of the larger particle mode. In general, the thermodenuder treatment on the diluted flue gas sample shows that the particles emitted by the studied power plant consist mainly of nonvolatile compounds, indicating that at short time scales the evaporation characteristics do not limit the lifetime of particles in atmospheric conditions.

Most of the results presented in the literature about oil-fired boilers concentrate on particle mass and, therefore, the particle size distributions that are shown in the literature are mass, and in some cases, volumetric[9] size distributions. The mass distributions are generally measured by weighing the separate stages of cascade impactors.[23,24] To ease the comparison of size distribution data with the literature, Figure 3 presents volumetric particle size distributions measured in this study with an ELPI from the same situations as the numbers size distributions shown in Figure 2. The difference between volumetric and mass size distribution is particle density. The volumetric and mass distributions can be different in shape if particle density changes strongly with particle size. The presented volumetric size distributions underestimate the concentrations in the particle sizes larger than 1 μm. The reason is that the applied measurement setup for the ELPI induced notable losses for large particles in sampling, dilution, sample transfer lines, and in the thermodenuder, and these losses are not taken into account.

The volumetric distributions show one particle mode at the particle size of approximately 480 nm and larger particles having highest concentrations at the sizes above 2 μm. Thus, as can be expected, there is a shift to larger particle sizes in the size distribution when the point of view is changed from particle number to particle volume. The particle mode dominating the number size distributions is only barely observable at the lower size end of the volumetric distribution. It seems to be quite common that one particle mass/volume mode below 500 nm in aerodynamic diameter exists in the exhaust of HFO-fired boilers[8,9,25] and there can be a coarse mode in addition.[8,9] Using electrical mobility measurements Linak et al.[9] determined the location of the fine particle mode to be at approximately 100 nm in the volumetric particle distribution of a 59 kW laboratory scale refractory-lined combustor, but they found considerably lower concentrations of that mode when measuring from a 732 kW fire-tube package boiler. They interpreted the concentration of the ultrafine mode to be linked to the amount of metals vaporizing in the combustor. That is, the more metal is vaporized, the higher the ultrafine mode. Sippula et al. reported that the GMD of the ultrafine particle mode from 4 to 7 MW HFO boilers was approximately 100 nm (aerodynamic diameter) in the mass distribution and 49−61 nm in the number size distribution. Note that, with the exception of Hays et al.,[25] all the studies mentioned have been performed on quite small boilers compared to the boiler used in the current study (47 MW at maximum). Accessing the larger scale boilers with the measurement instruments in order to do research can be quite challenging, which may partly explain the limited amount of comprehensive studies about particulate emissions of such boilers. However, large oil-fired boilers are a reality in many countries and in large marine

vessels. Further, these boilers often lack flue gas after-treatment in developing countries.

Particle Composition. The composition of emitted particles was determined by analyzing the particle samples collected by the nano-MOUDI and the samples including the total PM1. From the nano-MOUDI, particle size segregated ion compositions were determined. These compositions are presented in Figure 4. The masses analyzed in the ion composition analysis were 45%, 47%, and 26% of the total weighed mass for HFO, HFO emulsion, and HFO+LFO emulsion, respectively.

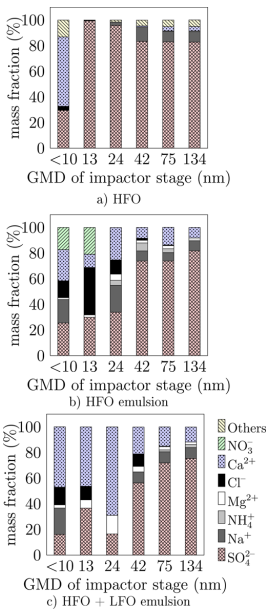

Figure 4. Size segregated ion composition of particles emitted from the heating plant using different fuels.

As shown in the figures, the sulfate fraction dominates the ion distributions of the particles in most fuel/size fraction combinations. Especially when HFO was used as the fuel (Figure 4a), the whole ion distribution was almost exclusively sulfate. Other than sulfate ions, only small fractions of sodium and calcium ions were observable mainly at particle sizes larger than 30 nm with the HFO fuel.

Compared to the case of HFO, the ion distribution was much more diverse when the HFO emulsion was used as fuel (Figure 4b). The ions of particles over 40 nm in diameter were still mainly sulfates but the particles also included larger fractions of calcium and magnesium compared to pure HFO fuel. On the size fraction below 40 nm, the fraction of sulfate ions of total ion concentration was below 50%. The rest of the ions were mainly chloride, calcium, nitrate (13 nm size fraction), and sodium (24 nm size fraction).

The particle size segregated ion distribution measured during the combustion of HFO+LFO emulsion (Figure 4c) was similar to the case of HFO emulsion in the respect that the contribution of sulfate ions was over 50% at aerodynamic particle sizes over 40 nm and less than 50% at smaller particle sizes. However, the fraction of calcium ions was higher when the LFO was involved. By taking into account that in the lowest particle sizes the low mass collected on filters (particle size below 13 nm) significantly increases the uncertainty of the results related the smallest particles, the addition of LFO does not seem to considerably change the ion distributions compared to HFO emulsion. Therefore, the calcium and chloride ions, which are present in much larger fractions in the particles emitted with emulsified fuels than with pure HFO, originate likely from the water used to produce the emulsions.

An elemental analysis of the particles was performed from a PM1 sample. The mass analyzed in the elemental analysis was 19%, 22%, and 10% of the total weighed mass for HFO, HFO emulsion, and HFO+LFO emulsion, respectively. The results of the ratios of each individual element to the total elemental mass are shown in Table 2. According to the analysis, the largest

Table 2. Relative Amounts of Mass of Elements from PM1 Samples with Different Fuels[a]

	mass fraction present in the elemental analysis (%)		
Element	HFO	HFO emulsion	HFO+LFO emulsion
Al	2.1	5.0	7.1
As	0.4	0.3	0.3
Co	0.8	0.8	0.8
Cr	0.4	0.1	0.0
Cu	0.2	0.1	0.1
Fe	23.2	21.0	20.7
Mn	0.2	0.1	0.1
Ni	19.8	18.4	18.4
Pb	0.2	0.1	0.1
V	23.6	27.4	27.3
Zn	0.6	0.5	0.4
Ba	0.4	0.8	0.8
K	21.6	14.7	13.2
Mg	6.4	10.7	10.7

[a]The analyzed mass for the elemental analysis was 19%, 22%, and 10% of the total weighed mass for HFO, HFO emulsion, and HFO+LFO emulsion, respectively. The black carbon content of the weighed mass was 7%, 6%, and 20%, respectively.

elemental fractions present in the samples were vanadium, iron, nickel, and potassium in this order. The black carbon content of the PM1 samples was 7%, 6%, and 20% of the PM1 mass for HFO, HFO emulsion, and HFO+LFO emulsion, respectively. Thus, the HFO+LFO emulsion increases the black carbon content in the PM emission. The mass closures of PM1 for the three fuels are shown in Figure 5. The results of the presented chemical analysis are rather well in line with the PM compositions reported earlier for HFO.[1,26]

Hygroscopic Growth. The hygroscopic growth of particles having mobility diameters of 20, 47, and 72 nm (see Figure 2) were studied using an HTDMA. The measurements were performed close to 90% relative humidity both through and bypassing the thermodenuder. The results of the obtained hygroscopic growth factors are presented in Figure 6. The hygroscopic growth results are the calculated averages of 2 to 7 separate HTDMA measurements with humidified air and of 4 to 7 separate HTDMA measurements with dry sheath air. The standard deviations of the hygroscopic growth factors in the figure are shown as error bars. The table above the figure shows the relative humidities at which each measurement was performed. The absolute error of the relative humidity values

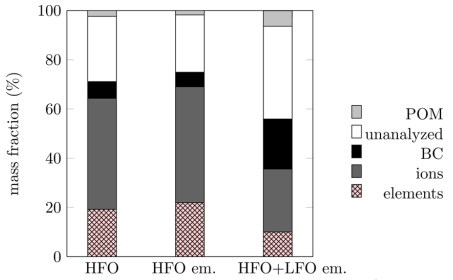

Figure 5. Mass closure for particles emitted from the heating plant using different fuels (HFO, HFO emul., and HFO+LFO emul.). Measured PM1 values were 14.5 mg m^{-3}, 14.6 mg m^{-3}, and 18.0 mg m^{-3}, respectively. POM factors for each fuel HFO, HFO emul., and HFO+LFO emul. are 1.9, 2.0, and 1.5 (Turpin, Barbara J. and Lim, Ho-Jin, "Species Contributions to PM2.5 Mass Concentrations: Revisiting Common Assumptions for Estimating Organic Mass", *Aerosol Sci. Technol.* 35 (1), 602−610).

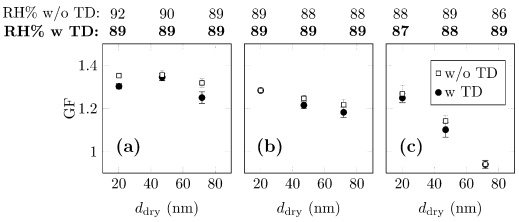

Figure 6. Growth factors as a function of dry particle size (GMD) for particles emitted using HFO (a), HFO emulsion (b), and HFO+LFO emulsion (c). Both the growth factors of particles measured through (circles) and bypassing (squares) the thermodenuder are presented. The relative humidities in which the growth factors were measured are presented above the figures. The standard deviations of the dry geometric mean diameters for 20, 47, and 72 nm particles are 0.1, 0.5, and 1.0 nm, respectively.

is approximately ±1.5%RH, but the repeatability of the RH values is under 1%RH. All the HTDMA measurements produced a narrow unimodal particle size distribution within the measurement range (<400 nm) indicating that all the given particle sizes were similar in their hygroscopic growth properties.

In general, it was observed that the measured hygroscopic growth factors were affected mostly by the fuel and the particle size. The highest growth factors (approximately 1.3−1.35, not significantly affected by thermodenuder treatment) were measured with dry particle sizes 20 and 47 nm when the boiler used HFO. In the case of 72 nm particles, the growth factors measured without the thermodenuder treatment were quite close to those observed for smaller particle sizes, but the use of the thermodenuder reduced the average growth factors for 72 nm particles to 1.25. This reduction may either mean that the volatile compounds in the particles increased particle hygroscopicity or the evaporation of the volatiles in the thermodenuder made the measured 72 nm particles more like agglomerates. For more agglomerate-like particles, the addition of water is less quickly seen as an increase in particle mobility diameter as the condensing water tends to first fill the cavities in the particles. The hygroscopic growth factors that were measured during the use of HFO emulsion were in general somewhat lower than those measured during the use of HFO. Further, the greater the particle diameter was, the lower the growth factor. This indicates that either particle chemistry or particle density/structure changes with particle diameter. The effect of the thermodenuder treatment was observed to be nearly negligible.

When the HFO+LFO emulsion was used, the growth factors of the measured particle sizes changed considerably with the particle size. The 20 nm particles had large growth factors (approximately 1.25) which were close to those measured without mixing the LFO into the HFO. Further, the thermodenuder treatment did not noticeably alter the growth factors of 20 nm particles. The 47 nm particles, on the other hand, had more moderate growth factors which were in the range of 1.1−1.15. The thermodenuder treatment lowered the growth factors of this particle size only very slightly. The largest (72 nm) particles, with and without the thermodenuder treatment, actually shrank in the carrier gas having high relative humidity. This behavior of growth factors in high relative humidities is similar to the case of fresh diesel soot particles.[22,27] The behavior indicates that 72 nm particles were agglomerates with low hygroscopicity. Pagels et al.[28] reported that the condensation of sulfuric acid or water on agglomerated soot initially results in shrinkage of mobility diameter due to the restructuring of the soot core. They report that a mass increase of 2−3 times the initial mass may be required for a transformation to spherical particles and only after that will the addition of condensate increase mobility diameter. It should be noted here that, based on the particle size distribution measurements, the 72 nm particles consist of particles from two different modes. Regardless, the HTDMA result of humidified particles shows one single particle mode. This indicates that either the two modes have similar chemical composition or the chemical composition is different but, nonetheless, the hygroscopic properties of the particle surface are similar.

In this study, the growth factors of the smallest (20 nm) and assumably the most compact particles were in the range of 1.25−1.35. These growth factors are quite close to those that Henning et al.[29] measured for sulfuric acid coated CAST soot particles having high organic carbon (OC) content (>80%) at 90%RH. The soot particles having lower OC content had also lower growth factors. They explained the phenomenon by claiming that sulfuric acid reacts with polyaromatic hydrocarbons (PAH) present in the OC fraction forming products with lower molecular weight than the initial PAHs. These products have higher solubility to water and, as a consequence, hygroscopic growth increases. Further, quite similar high growth factors as in the current study with HFO were also observed in the study of Khalizov et al. for sulfuric acid coated 30 and 50 nm propane soot particles at approximately 90% RH.[30] It was possible to obtain OC versus black carbon (BC) information from the emitted particles in this study with the SP-AMS. However, it should be noted that the size ranges of the HTDMA and the SP-AMS were not similar. The HTDMA measured 20, 47, and 72 nm particles separately, whereas the SP-AMS measured all the particles from 40 nm to approximately 1 μm without any size segregation. The OC/BC results are presented in Figure 7.

The figure shows that the OC/BC fraction of emitted particles remains practically the same between HFO and HFO emulsion, but the addition of LFO to the fuel resulted in a lower OC/BC ratio. The measured OC/BC ratios from HFO

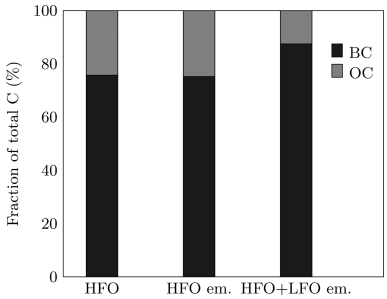

Figure 7. Fractions of organic and black carbon of the total emitted carbon with different fuels measured with the SP-AMS.

combustion are very similar to those reported by Sippula et al.[1] for a 4 MW HFO boiler. All in all, according to the OC/BC results, the reasoning of Henning et al.[29] on the significance of the OC content on hygroscopic growth factors is plausible also in the current study. However, it is equally possible that the reduction in the hygroscopicity of particles emitted with the emulsion of HFO+LFO compared to the HFO cases is explained by other differences in chemical composition. Particles emitted with HFO+LFO emulsion have, for example, much lower content of analyzed ion compounds and higher, quite insoluble, BC content. The HTDMA results show that the fine particles emitted from HFO combustion are quite hygroscopic even as fresh particles. However, by adding water to the combustion process and, further, by mixing HFO into LFO, the hygroscopic growth factors of emission particles decrease. Furthermore, it should be noted that particle mobility diameter growth factors depend very much on the size of the emitted particles. This is especially the case with the emulsion of a mix of HFO and LFO. Overall, it is probable that particles from HFO combustion will contribute to cloud formation, reduce visibility, and, furthermore, have a detrimental effect on the overall air quality especially in large cities. Recent studies have also shown that emissions of large ships that are primarily fueled by HFO could have a strong impact on the Earth's radiation budget by increasing local marine cloud albedo. Ship particles have been estimated to cause a change in the global radiative forcing of −0.11 W/m^2[31] and in the range of −0.27 to −0.58 W/m^2.[32] These estimates still include large uncertainties. The results of the current paper give some insight of particle properties, and thus might be utilized in global climate models.

AUTHOR INFORMATION

Corresponding Author

*E-mail: topi.ronkko@tut.fi.

Notes

The authors declare no competing financial interest.

ACKNOWLEDGMENTS

This work was supported by the Cluster for Energy and Environment (Cleen Ltd) Measurement, Monitoring and Environmental Assessment (MMEA) Work package 4.5.2.

REFERENCES

(1) Sippula, O.; Hokkinen, J.; Puustinen, H.; Yli-Pirilä, P.; Jokiniemi, J. Comparison of particle emissions from small heavy fuel oil and wood-fired boilers. *Atmos. Environ.* **2009**, *43*, 4855−4864.

(2) Carter, J. D.; Ghio, A. J.; Samet, J. M.; Devlin, R. B. Cytokine production by human airway epithelial cells after exposure to an air pollution particle is metal-dependent. *Toxicol. Appl. Pharmacol.* **1997**, *146*, 180−188.

(3) Osan, J.; Török, S.; Fekete, J. o.; Rindby, A. Case study of the emissions from a heavy-oil-fueled Hungarian power plant. *Energy Fuels* **2000**, *14*, 986−993.

(4) Fu, W. B.; Hou, L. Y.; Wang, L.; Ma, F. H. A unified model for the micro-explosion of emulsified droplets of oil and water. *Fuel Process. Technol.* **2002**, *79*, 107−119.

(5) Ocampo-Barrera, R.; Villasenor, R.; Diego-Marin, A. An experimental study of the effect of water content on combustion of heavy fuel oil/water emulsion droplets. *Combust. Flame* **2001**, *126*, 1845−1855.

(6) Kadota, T.; Yamasaki, H. Recent advances in the combustion of water fuel emulsion. *Prog. Energy Combust. Sci.* **2002**, *28*, 385−404.

(7) Ballester, J. M.; Fueyo, N.; Dopazo, C. Combustion characteristics of heavy oil-water emulsions. *Fuel* **1996**, *75*, 695−705.

(8) Miller, C. A.; Linak, W. P.; King, C.; Wendt, J. O. L. Fine particle emissions from heavy fuel oil combustion in a firetube package boiler. *Combust. Sci. Technol.* **1998**, *134*, 477−502.

(9) Linak, W. P.; Miller, C. A.; Wendt, J. O. L. Comparison of particle size distributions and elemental partitioning from the combustion of pulverized coal and residual fuel oil. *J. Air Waste Manage. Assoc.* **2000**, *50*, 1532−1544.

(10) Linak, W. P.; Andrew Miller, C.; Wendt, J. O. L. Fine particle emissions from residual fuel oil combustion: characterization and mechanisms of formation. *Proc. Combustion Inst.* **2000**, *28*, 2651−2658.

(11) Oberdörster, G.; Sharp, Z.; Atudorei, V.; Elder, A.; Gelein, R.; Kreyling, W.; Cox, C. Translocation of inhaled ultrafine particles to the brain. *Inhal. Toxicol.* **2004**, *16*, 437−445.

(12) Jacobson, M. Z. Strong radiative heating due to the mixing state of black carbon in atmospheric aerosols. *Nature* **2001**, *409*, 695−697.

(13) Corbett, J. J.; Lack, D. A.; Winebrake, J. J.; Harder, S.; Silberman, J. A.; Gold, M. Arctic shipping emissions inventories and future scenarios. *Atmos. Chem. Phys.* **2010**, *10*, 9689−9704.

(14) Forster, P.; Ramaswamy, V.; Artaxo, P.; Berntsen, T.; Betts, R.; Fahey, D. W.; Haywood, J.; Lean, J.; Lowe, D. C.; Myhre, G.; Nganga, J.; Prinn, R.; Raga, G.; Schultz, M.; Van Dorland, R. In *Climate Change 2007: The Physical Science Basis. Contribution fo Working Group I to the Fourth Assessment Report of the Intergovernmetal Panel on Climate Change*; Solomon, S., Quin, D., Manning, M., Chen, Z., Marquis, M., Averyt, K. B., Tignor, M., Miller, H. L., Eds.; Cambridge University Press: Cambridge, 2007.

(15) Huffman, G. P.; Huggins, F. E.; Shah, N.; Huggins, R.; Linak, W. P.; Miller, C. A.; Pugmire, R. J.; Meuzelaar, H. L. C.; Seehra, M. S.; Manivannan, A. Characterization of fine particulate matter produced by combustion of residual fuel oil. *J. Air Waste Manage. Assoc.* **2000**, *50*, 1106−1114.

(16) Berner, A.; Lürzer, C. Mass size distributions of traffic aerosols at Vienna. *J. Phys. Chem.* **1980**, *84*, 2079−2083.

(17) Saarikoski, S.; Timonen, H.; Saarnio, K.; Aurela, M.; Järvi, L.; Keronen, P.; Kerminen, V.-M.; Hillamo, R. Sources of organic carbon in fine particulate matter in northern European urban air. *Atmos. Chem. Phys.* **2008**, *8*, 6281−6295.

(18) Timonen, H.; Aurela, M.; Carbone, S.; Saarnio, K.; Saarikoski, S.; Mäkelä, T.; Kulmala, M.; Kerminen, V. M.; Worsnop, D. R.; Hillamo, R. High time-resolution chemical characterization of the water-soluble fraction of ambient aerosols with PILS-TOC-IC and AMS. *Atmos. Meas. Technol.* **2010**, *3*, 1063−1074.

(19) Heikkilä, J.; Rönkkö, T.; Lähde, T.; Lemmetty, M.; Arffman, A.; Virtanen, A.; Keskinen, J.; Pirjola, L.; Rothe, D. Effect of open channel filter on particle emissions of modern diesel engine. *J. Air Waste Manage. Assoc.* **2009**, *59:10*, 1148−1154.

(20) Aiken, A. C.; et al. O/C and OM/OC Ratios of Primary, Secondary, and Ambient Organic Aerosols with High Resolution Time-of-Flight Aerosol Mass Spectrometry. *Environ. Sci. Technol.* **2008**, *42*, 4478−4485.

(21) Swietlicki, E.; et al. Hygroscopic properties of submicrometer atmospheric aerosol particles measured with H-TDMA instruments in various environmentsÜ-A review. *Tellus B* **2008**, *60*, 432−469.
(22) Happonen, M.; Heikkilä, J.; Aakko-Saksa, P.; Murtonen, T.; Lehto, K.; Rostedt, A.; Sarjovaara, T.; Larmi, M.; Keskinen, J.; Virtanen, A. Diesel exhaust emissions and particle hygroscopicity with HVO fuel-oxygenate blend. *Fuel* **2013**, *103*, 380−386.
(23) Goldstein, H. L.; Siegmund, C. W. Influence of heavy fuel oil composition and boiler combustion conditions on particulate emissions. *Environ. Sci. Technol.* **1976**, *10*, 1109−1114.
(24) Allouis, C.; L'Insalata, A.; Fortunato, L.; Saponaro, A.; Beretta, F. Study of water-oil emulsion combustion in large pilot power plants for fine particle matter emission reduction. *Experimental Thermal and Fluid Science* **2007**, *31*, 421−426.
(25) Hays, M. D.; Beck, L.; Barfield, P.; Willis, R. D.; Landis, M. S.; Stevens, R. K.; Preston, W.; Dong, Y. Physical and chemical characterization of residual oil-fired power plant emissions. *Energy Fuels* **2009**, *23*, 2544−2551.
(26) Kaivosoja, T.; Jalava, P.; Lamberg, H.; Virén, A.; Tapanainen, M.; Torvela, T.; Tapper, U.; Sippula, O.; Tissari, J.; Hillamo, R.; M.-R., H.; Jokiniemi, J. Comparison of emissions and toxicological properties of fine particles from wood and oil boilers in small (20−25 kW) and medium (5−10 MW) scale. *Atmos. Environ.* **2013**, *77*, 193−201.
(27) Weingartner, E.; Burtscher, H.; Baltensperger, U. Hygroscopic properties of carbon and diesel soot particles. *Atmos. Environ.* **1997**, *31*, 2311−2327.
(28) Pagels, J.; Khalizov, F.; Alexei; McMurry, P. H.; Zhang, R. Y. Processing of soot by controlled sulphuric acid and water condensationÜmass and mobility relationship. *Aerosol Sci. Technol.* **2009**, *43*, 629−640.
(29) Henning, S.; Ziese, M.; Kiselev, A.; Saathoff, H.; Möhler, O.; Mentel, T. F.; Buchholz, A.; Spindler, C.; Michaud, V.; Monier, M.; Sellegri, K.; Stratmann, F. Hygroscopic growth and droplet activation of soot particles: uncoated, succinic or sulfuric acid coated. *Atmos. Chem. Phys* **2012**, *12*, 4525−4537.
(30) Khalizov, A. F.; Zhang, R.; Zhang, D.; Xue, H.; Pagels, J.; McMurry, P. H. Formation of highly hygroscopic soot aerosols upon internal mixing with sulfuric acid vapor. *J. Geophys. Res.* **2009**, *114*, D05208.
(31) Capaldo, K.; Corbett, J. J.; Kasibhatla, P.; Fischbeck, P.; Pandis, S. N. Effects of ship emissions on sulphur cycling and radiative climate forcing over the ocean. *Nature* **1999**, *400*, 743−746.
(32) Lauer, A.; Eyring, V.; Corbett, J. J.; Wang, C.; Winebrake, J. J. Assessment of near-future policy instruments for oceangoing shipping: Impact on atmospheric aerosol burdens and the Earth's radiation budget. *Environ. Sci. Technol.* **2009**, *43*, 5592−5598.

Tampereen teknillinen yliopisto
PL 527
33101 Tampere

Tampere University of Technology
P.O.B. 527
FI-33101 Tampere, Finland

ISBN 978-952-15-4193-3
ISSN 1459-2045